DAHLGREN DIVISION
NAVAL SURFACE WARFARE CENTER
Dahlgren, Virginia 22448-5100

NSWCDD/TR-98/122

HYBRID FENCE ALIGNMENT ANALYSIS

BY BRUCE R. HERMANN JACOB ROGINSKY

THEATER WARFARE SYSTEMS DEPARTMENT

JANUARY 1999

REPORT DOCUMENTATION PAGE

Form Approved
OMB No. 0704-0188

1. AGENCY USE ONLY (Leave blank)	2. REPORT DATE	3. REPORT TYPE AND DATES COVERED
	January 1999	Final

4. TITLE AND SUBTITLE

Hybrid Fence Alignment Analysis

5. FUNDING NUMBERS

6. AUTHOR(s)

Bruce R. Hermann Jacob Roginsky

7. PERFORMING ORGANIZATION NAME(S) AND ADDRESS(ES)

Commander
Naval Surface Warfare Center
Dahlgren Division (Code T12)
17320 Dahlgren Road
Dahlgren, VA 22448-5100

8. PERFORMING ORGANIZATION REPORT NUMBER

NSWCDD/TR-98/122

9. SPONSORING/MONITORING AGENCY NAME(S) AND ADDRESS(ES)

10. SPONSORING/MONITORING AGENCY REPORT NUMBER

11. SUPPLEMENTARY NOTES

12a. DISTRIBUTION/AVAILABILITY STATEMENT

Approved for public release; distribution is unlimited.

12b. DISTRIBUTION CODE

13. ABSTRACT (Maximum 200 words)

This report describes the methods used to quantify the geometrical properties of the Naval Space Command Naval Space Surveillance Radar Fence. The Space Surveillance system was designed and began operations soon after the launch of the first earth satellites. Its mission is to track and catalog objects passing through the plane of the radar beams. The fence comprises three transmitting sites and six receiving sites spread from Georgia to California, making it one of the largest multistatic radar systems ever conceived.

Because of the steady increase in the number of satellites launches and the associated orbiting debris from expendable launch vehicles, the number of objects in the catalog continues to grow. However, the catalog is not all inclusive and includes only a subset of all orbiting objects. At a time where the number of users of the catalog is increasing and the interest in a more complete and accurate description of the hazard is growing, improvements to the fence are being considered.

14. SUBJECT TERMS

Naval Space Command Naval Space Surveillance Radar Fence
multistatic radar system
satellites

15. NUMBER OF PAGES

90

16. PRICE CODE

17. SECURITY CLASSIFICATION OF REPORTS	18. SECURITY CLASSIFICATION OF THIS PAGE	19. SECURITY CLASSIFICATION OF ABSTRACT	20. LIMITATION OF ABSTRACT
UNCLASSIFIED	UNCLASSIFIED	UNCLASSIFIED	SAR

FOREWORD

Support for this work was provided by the Naval Space Surveillance Program of the Naval Space Command. Project oversight and direction was provided by Mr. Carroll C. Hayden, Program Manager and Mr. Alan C. Bauer, Technical Assistant. This work was performed between November 1997 and September 1998.

This final report has been reviewed by Dr. Jeffrey Blanton, Head, Space Systems Applications Branch, and Mr. James Sloop, Head, Space and Weapons Systems Analysis Division.

Approved by:

RICHARD T. LEE, Acting Head
Theater Warfare Systems Department

CONTENTS

ILLUSTRATIONS

ILLUSTRATIONS (Continued)

TABLES

1.0 INTRODUCTION

This report describes the methods employed to quantify the alignment of the Naval Space Command Naval Space Surveillance Radar Fence. The term *alignment* in this context implies that the relative positioning in space of the several linear arrays that constitute the fence be documented. The first task of this alignment analysis is to use the values from the surveyed points on the arrays to establish the vector direction of each array. From this information, the equation of the plane defined by the array and the perpendicular (normal) to it can be computed. The great circle of the array can be thought of as the *circle* defined by the intersection of the normal plane with the surface of the earth. Each array will have its unique normal plane, though by design these planes are expected to be approximately parallel and with zero separation.

All surveyed points are listed in the World Geodetic Coordinate System 1984 (WGS84) [1]. Among the constants that make up this geodetic system, the definition of the semimajor axis and the eccentricity of the reference ellipse lead to a mathematical surface from which ellipsoid heights are measured. These ellipsoid definitions were selected by some criteria to "best" fit the observed geoid. Since the geoid is a much more complex surface than a smooth ellipsoid, the two are rarely coincident. Thus, the respective normals to the two surfaces at any point will not coincide. This leads to the concept of geoid heights and deflections of the vertical. The geoid heights are defined by the vertical distance between the ellipsoid and the local geoid. The deflection of the vertical is the angle, usually written as north and east components, between the normals to the ellipsoid and the geoid at a given point.

For the linear antenna arrays that make up the Space Surveillance System to operate as a broadside array [2], they must be constructed so that all elements lie along a straight line. A broadside array implies that all elements are fed signals that are electrically in phase. In the far field, this results in the energy from all the elements interfering constructively (in phase) and forming an emission maximum in a plane perpendicular to the array. If the elements do not physically lie in a straight line and are not electrically compensated for any discrepancy that may exist, the result will be something less than peak efficiency.

In order to build the transmitter array at Lake Kickapoo, Texas, the straight line of the array had to be maintained for over 3.1 km. In fact, the Lake Kickapoo array was built in two segments. The south half was finished in mid 1961 and the north half in 1965. This probably is the reason for the apparent slight misalignment of the north half of the array, as described in a later section. At the latitude of Lake Kickapoo, a 3.1-km straight line in the north-south direction and tangent to the ellipsoid at its center would be about 19 cm above the ellipsoid at both ends.

2.0 GEOMETRICAL ANALYSIS

Ideally, the linear arrays that make up the radar fence should be positioned perpendicular to a single plane common to all. If the earth were a sphere, this plane would contain the earth's center as a point on the plane, and the plane would intersect the earth's surface along a curve that would be a great circle. In practice, the earth is not a simple geometrical shape. The WGS84 geodetic system models the earth as an ellipsoid of revolution about the axis of rotation. That is, the ellipsoid has a circular cross section as seen from a point above the poles, but an elliptical cross section as seen from a point above the equator.

The alignment analysis developed in this report will document the geometrical relationships needed to test each array and evaluate its conformity with the condition that all arrays must be perpendicular to the same plane. The accuracy of this analysis depends upon the site surveys performed by the Defense Mapping Agency (now the National Imagery and Mapping Agency, NIMA) in 1992 [3].

2.1 Planes and Lines

A plane is defined by the equation of a line normal to it. Therefore any equation of first degree represents a plane. The general form of a first-degree equation in Cartesian coordinates is given in Equation (1). For the purposes of this report, the coordinates x, y, and z represent the Earth-Centered Earth-Fixed (ECEF) 3-space defined by the WGS84 geodetic system. The x-axis pierces the ellipsoid at the intersection of the equator and the Greenwich meridian. The z-axis is coincident with the rotation axis, with the positive direction to the north. The y-axis completes the right-handed coordinate system. The coefficients A, B, C, are the *direction components*, and D is related to the distance of the plane from the origin.

$$Ax + By + Cz + D = 0 \tag{1}$$

The *direction cosines (l, m, n)* are defined in the manner shown in Equation (2). The direction cosines m and n are similar to Equation (2) with the numerator replaced by B and C, respectively.

$$l = \frac{A}{\sqrt{A^2 + B^2 + C^2}} \tag{2}$$

The perpendicular distance of a plane from a point is given by Equation (3), as described in Box 1.

Box 1—Distance of a Point to a Plane

Given the equation of a plane as in Equation (1), the perpendicular distance of the plane from the point (x_1, y_1, z_1), is d and can be found as follows. From Equation (2), the direction cosines l, m, n can be computed. Then, since Equation (1) represents a line normal to the plane, the normal line from the given point (x_1, y_1, z_1) to the plane can be represented as follows:

$$x = x_1 + lp$$
$$y = y_1 + mp$$
$$z = z_1 + np$$

Substitute these components into Equation (1) and solve for p. The result is given as Equation (3).

$$p = - \frac{Ax_1 + By_1 + Cz_1 + D}{\sqrt{A^2 + B^2 + C^2}} \tag{3}$$

The sense of p depends upon which side of the plane the point lies. The recipe in Box 1 moves from the point along the positive normal direction to reach the plane. If, instead, the point must move in the negative normal direction to reach the plane, then p has a negative sign. Stated another way, p is positive if movement in the negative normal direction is required to reach the point from the plane. If movement in the positive normal direction is required to reach the point, then p is negative. If the point in Equation (3) is the origin (0, 0, 0), then the distance of the plane from the origin is as expressed in Equation (4).

$$p_0 = - \frac{D}{\sqrt{A^2 + B^2 + C^2}} \tag{4}$$

A straight line is determined by two points. If the end points of an array are given by the pair of points like those listed in Equation (5), then the direction components for the line can be written by differencing these points as in Equation (6). With the direction components known, the direction cosines can be found from Equation (2).

$$\begin{matrix}(x_1, y_1, z_1) \\ (x_2, y_2, z_2)\end{matrix} \tag{5}$$

$$A = x_2 - x_1, \quad B = y_2 - y_1, \quad C = z_2 - z_1 \tag{6}$$

The computed midpoint of the array will be used as the point through which the perpendicular plane will pass. The midpoint of the line segment whose end points are those in Equation (5) is (x_m, y_m, z_m), as shown in Equation (7).

$$\begin{aligned} x_m &= \tfrac{1}{2}(x_1 + x_2) \\ y_m &= \tfrac{1}{2}(y_1 + y_2) \\ z_m &= \tfrac{1}{2}(z_1 + z_2) \end{aligned} \tag{7}$$

The plane perpendicular to the line segment and passing through the midpoint is given by Equation (8). This equation represents the plane in which the great circle, defined by the particular array whose end points are used, must lie. The justification for this form is presented in Box 2.

$$l(x - x_m) + m(y - y_m) + n(z - z_m) = 0 \tag{8}$$

Box 2—Equation for a Plane Through a Point

Given the plane

$$Ax + By + Cz + D = 0$$

and the point (x_1, y_1, z_1), if the plane is to pass through the point, the following must also hold:

$$Ax_1 + By_1 + Cz_1 + D = 0$$

Subtracting these two equations gives the following form:

$$A(x - x_1) + B(y - y_1) + C(z - z_1) = 0$$

It is desired that the system have its arrays constructed so that they all lie in the same plane. This is not likely to happen in practice, so it is of interest to compute the angle between the planes defined by each array. The small angle between two lines (*a and b*) in terms of their direction cosines is given by Equation (9). Since these lines are normal to their respective planes, this is also the angle between the planes.

$$\theta = Arccos\,(l_a l_b + m_a m_b + n_a n_b) \tag{9}$$

The minimum distance of each plane from the WGS84 origin can be found from Equation (8) by collecting the constant terms together, as shown in Equation (10). By comparison with Equation (4), it can be shown that the term in parentheses is the distance p.

$$lx + my + nz - (lx_m + my_m + nz_m) = 0 \tag{10}$$

The line from the WGS84 origin to the plane will be parallel with the array itself because they are both normal to the same plane. If this intersection of the plane is taken as the center of the great circle G, then its coordinates in the WGS84 system are given by Equation (11).

$$\begin{aligned} x_G &= -lp \\ y_G &= -mp \\ z_G &= -np \end{aligned} \tag{11}$$

2.2 Latitude of the Great Circle Given a Longitude

The plane defined by each array will intersect the WGS84 ellipsoid along a curve that may be oblique to the equator. Therefore the geodetic longitude of each intersecting point will have a unique latitude. The Cartesian coordinates of any point given in geodetic coordinates (λ, ϕ, h) can be found from Equation (12).

$$\begin{aligned} x &= (N + h)\cos\phi\cos\lambda \\ y &= (N + h)\cos\phi\sin\lambda \\ z &= (N(1 - \epsilon^2) + h)\sin\phi \end{aligned} \tag{12}$$

$$\text{where } N = \frac{a}{\sqrt{1 - \epsilon^2 \sin^2\phi}}.$$

If the longitude λ and ellipsoid height h are specified, then the value for latitude ϕ can be found using the relations given in Equation (12) and the equation for the plane, Equation (1), defined by a particular array baseline. Substitution of Equation (12) into Equation (1), with direction cosines used instead of direction components, results in a transcendental equation, Equation (13), which needs to be solved for ϕ.

$$(N + h)\cos\phi(l\cos\lambda + m\sin\lambda) + n(N(1 - \epsilon^2) + h)\sin\phi + d = 0 \qquad (13)$$

A solution to this equation can be found through the iterative use of Newton's method. A good initial guess for ϕ is 30 deg.

2.3 Deviation of an Array from a Straight Line

Each of the three transmitter arrays were surveyed at three points. These sites included points on the array representing the north and south end points plus the central point. From this information, it is possible to determine if the south-to-center line segment is parallel with the center-to-north line segment. Also, by using the north and south sites, the perpendicular distance between the central point and the midpoint of the south-to-north line can be calculated. This distance d_{OC}, shown schematically in Figure 1, can be used to establish how much the array may deviate from a straight line. The results obtained below for the transmitters are based on the site survey positions of the three points. The deviation derived for Lake Kickapoo is large enough to suggest that there may either be a height error in the survey, or the point surveyed is offset from the ground plane. The Lake Kickapoo coordinates should be verified before the consequences of this apparent deviation are accepted as truth.

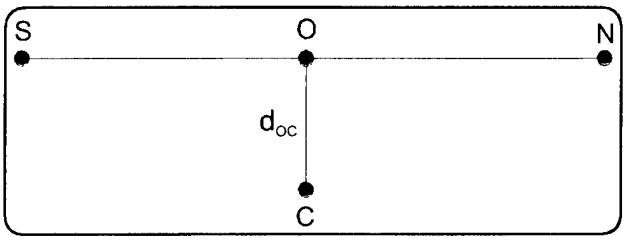

Figure 1—Perpendicular Distance Between South-to-North Line and Central Surveyed Point

The distance d_{OC} can be computed in the following way: using the properties of a line outlined above, the direction cosines can be computed from the difference between the north and south coordinates. The point **O** is on the line **SN**, so the segments **SN**, **SO**, and **ON** must have the same direction cosines. This result gives the three equations given in Equation (14).

$$\begin{aligned} x_O - \frac{d_{OS}(x_N - x_S)}{d_{SN}} &= x_S \\ y_O - \frac{d_{OS}(y_N - y_S)}{d_{SN}} &= y_S \\ z_O - \frac{d_{OS}(z_N - z_S)}{d_{SN}} &= z_S \end{aligned} \qquad (14)$$

The components of the south point, the north point, the central point, and the distance d_{SN} are known. A fourth equation, shown as Equation 15, can be written by invoking the requirement that the line **OC** must be perpendicular to **SN**. This additional equation allows for the point (x_O, y_O, z_O) and d_{OS} to be determined. With point **O** known, the distance d_{OC} can be computed.

$$(x_N - x_S)(x_C - x_O) + (y_N - y_S)(y_C - y_O) + (z_N - z_S)(z_C - z_O) = 0 \qquad (15)$$

The distances computed for the three transmitter arrays are listed in Table 1. Only Lake Kickapoo has a significant deviation from a straight line. The north and south sections of this array, which were constructed at two different times, apparently are tilted in the vertical plane, as illustrated schematically in Figure 2. Assuming that the south point is given, then Figure 2 indicates that either the north point is too high or the central point is too low. The results from the alignment analysis in the next section suggest that, compared to the other arrays, the north point at Lake Kickapoo is too high.

Table 1—Deviation From a Straight Line at the Three Transmitter Sites

Units = meters	Distance d_{oc}	Distance in height
Lake Kickapoo	1.6525	1.6522
Jordan Lake	0.0114	0.0094
Gila River	0.0309	0.0309

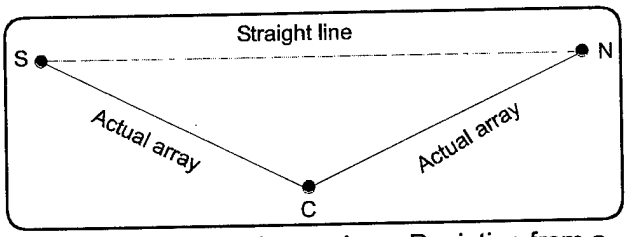

Figure 2—Lake Kickapoo Array Deviation from a Straight Line

Continuing with the analysis by assuming that the these three points are representative of the array elements in general, then the Lake Kickapoo array may act like two linear arrays pointed in slightly different directions. In the far field, the result of this may be the production of a two-lobed gain pattern. Each segment would be twice the expected beamwidth and have half the gain of the full array. A model of what the far-field pattern might look like is illustrated in Figure 3. The dashed line represents the ideal gain pattern for the full array, and the double-peaked solid line gives an indication of what the effect of the deviation from a straight line may have on performance. Also added to the far-field model (solid line) is the effect of a random 5-deg phase noise at each element.

2.4 Alignment

The alignment of the arrays can be illustrated by computing the intersection of the common plane with the WGS84 ellipsoid, as described in Section 2.2. Then, if that intersection is plotted as a function of longitude and latitude along with the central points from each site, the points should lie on the intersecting curve. This is illustrated in Figure 4 by using the south-to-north plane defined by the Lake Kickapoo transmitter as the reference plane intersecting the

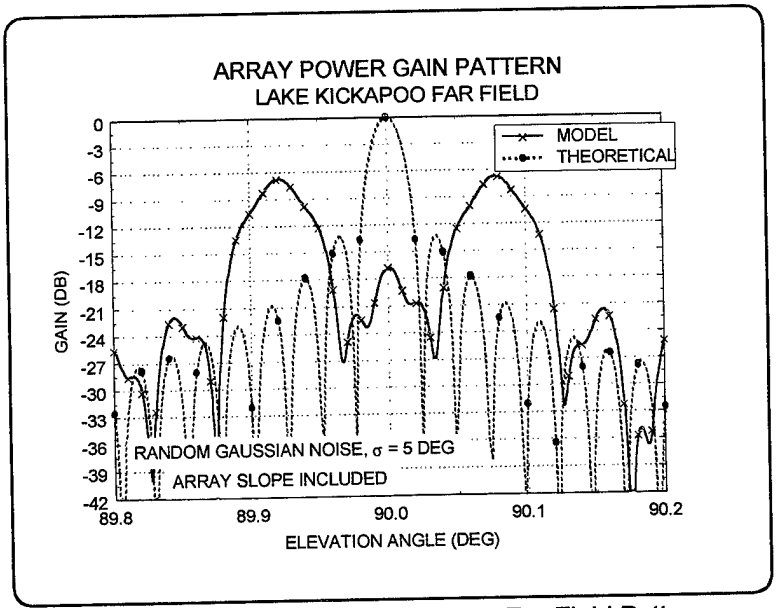

Figure 3—Model of Lake Kickapoo Far-Field Pattern

the reference plane intersecting the ellipsoid. As expected, the other sites are located at appropriate geodetic latitudes so that at their respective longitudes, they lie on the same plane.

Transmitters

The Lake Kickapoo, Texas, site is the main transmitter for the Naval Space Surveillance System. It has the longest array, stretching over 3.1 km. It is flanked by two smaller arrays at Gila River, Arizona, to the west and Jordan Lake, Alabama, to the east. The three surveyed points for each site in the WGS84 Geodetic System are listed in Table 2. The baseline components and lengths are listed in Table 3, and the direction cosines for each are given in Table 4. Also in Table 4 is the angle in degrees that each array line differs from the south-to-north line at Lake Kickapoo.

The intersections of the planes with the ellipsoid are defined by each baseline name in Table 2. The line of intersection with the ellipsoid is shown in Figure 5 at the longitude of Lake Kickapoo. Also in the figure are the three surveyed points listed in Table 2 for Lake Kickapoo. Since each plane was constructed to pass through the midpoint of the line joining the two surveyed points that define that plane, the lines in the figures representing the planes are seen to bisect the array and are normal to it. The planes intersecting the ellipsoid at the longitude of Jordan Lake and Gila River are shown in Figures 6 and 7, respectively.

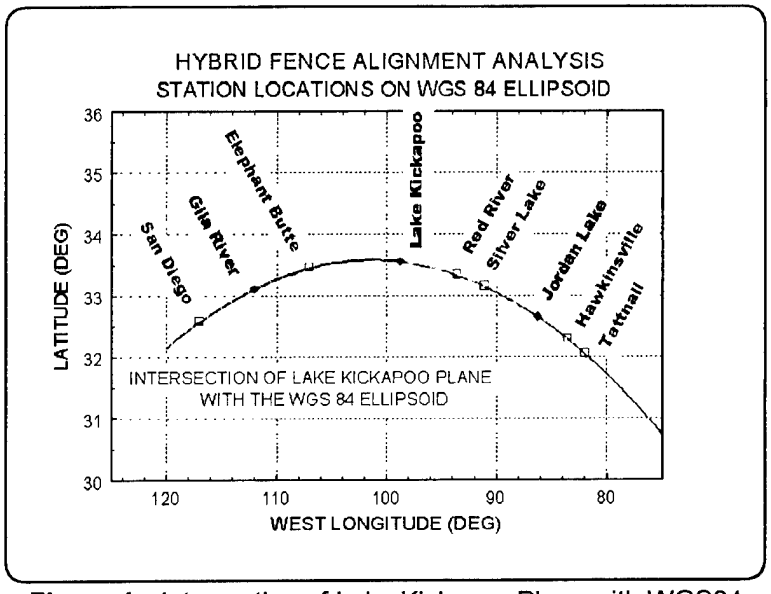

Figure 4—Intersection of Lake Kickapoo Plane with WGS84 Ellipsoid

Table 2—Transmitter Baselines and Length (meters)

LINE	ΔX	ΔY	ΔZ	L
Lake Kickapoo S-to-N	352.5085	1762.3724	2707.1539	3249.4462
Lake Kickapoo S-to-C	174.7397	873.7800	1339.2034	1608.5681
Lake Kickapoo C-to-N	177.7687	888.5924	1367.9504	1640.8798
Jordan Lake S-to-N	33.7900	169.2590	260.0570	312.1218
Jordan Lake S-to-C	16.9010	84.6390	130.0250	156.0638
Jordan Lake C-to-N	16.8890	84.6200	130.0320	156.0580
Gila River S-to-N	53.4740	267.1390	410.4390	492.6285
Gila River S-to-C	26.7460	133.5940	205.2030	246.3148
Gila River C-to-N	26.7280	133.5450	205.2360	246.3138

Table 3—Transmitter Surveyed Points: WGS84 (meters)

	X	Y	Z
Lake Kickapoo South	-810811.2334	-5259782.7972	3504157.2660
Lake Kickapoo Center	-810636.4936	-5258909.0172	3505496.4695
Lake Kickapoo North	-810458.7249	-5258020.4247	3506864.4199
Jordan Lake South	350263.4440	-5363720.7740	3422108.4690
Jordan Lake Center	350280.3450	-5363636.1350	3422238.4940
Jordan Lake North	350297.2340	-5363551.5150	3422368.5260
Gila River South	-2006039.5310	-4957535.5820	3464463.8590
Gila River Center	-2006012.7850	-4957401.9880	3464669.0620
Gila River North	-2005986.0570	-4957268.4430	3464874.2980

Table 4—Transmitter Direction Cosines and Angle with Respect to Lake Kickapoo S-to-N

LINE	l	m	n	cosine θ	Degrees
Lake Kickapoo S-to-N	0.10848263	0.54236085	0.83311237	1.00000000	0.00000000
Lake Kickapoo S-to-C	0.10863062	0.54320362	0.83254382	0.99999947	0.05898960
Lake Kickapoo C-to-N	0.10833745	0.54153412	0.83366887	0.99999949	0.05786590
Jordan Lake S-to-N	0.10825902	0.54228510	0.83319077	0.99999997	0.01447220
Jordan Lake S-to-C	0.10829546	0.54233595	0.83315294	0.99999998	0.01040830
Jordan Lake C-to-N	0.10822257	0.54223425	0.83322860	0.99999995	0.01786310
Gila River S-to-N	0.10854832	0.54227267	0.83316122	0.99999999	0.00724740
Gila River S-to-C	0.10858463	0.54237100	0.83309248	0.99999999	0.00724740
Gila River C-to-N	0.10851200	0.54217434	0.83322994	0.99999997	0.01447220

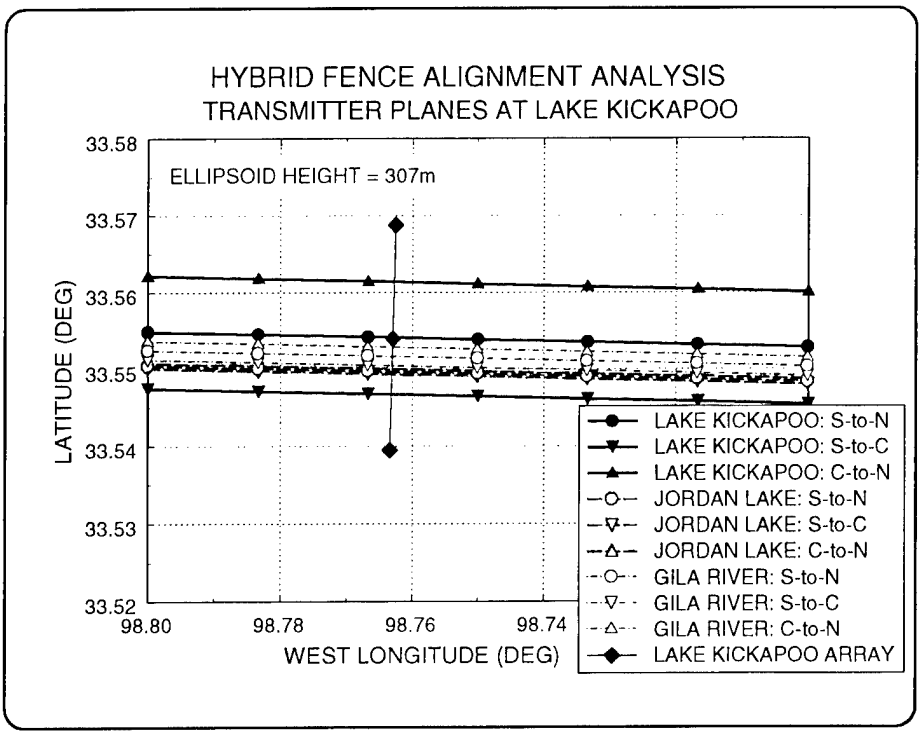

Figure 5—Intersection of Transmitter Planes with the Ellipsoid at Lake Kickapoo

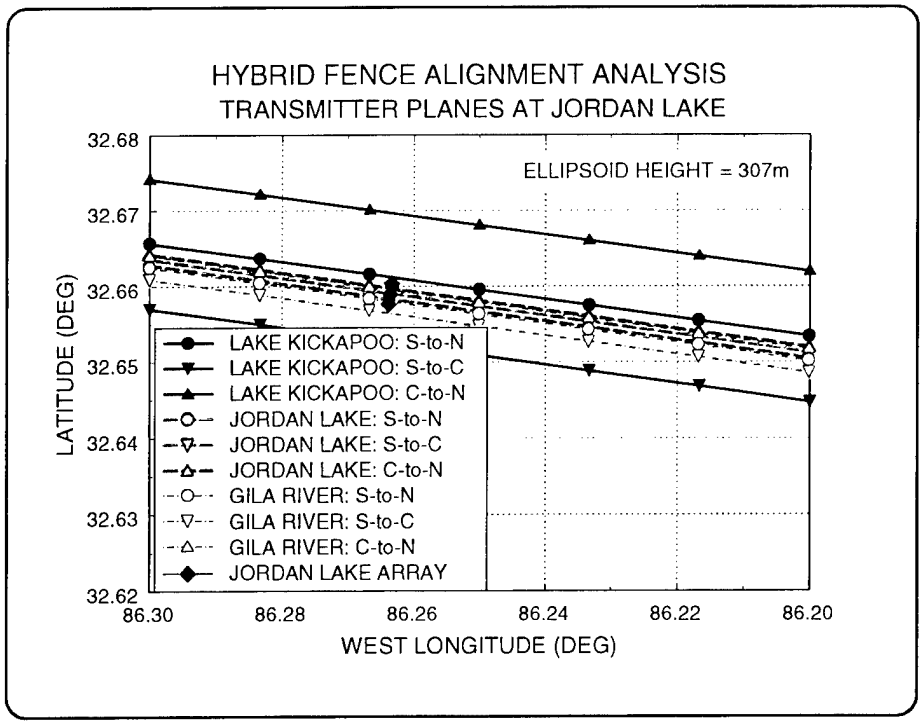

Figure 6—Intersection of the Transmitter Planes with the Ellipsoid at Jordan Lake

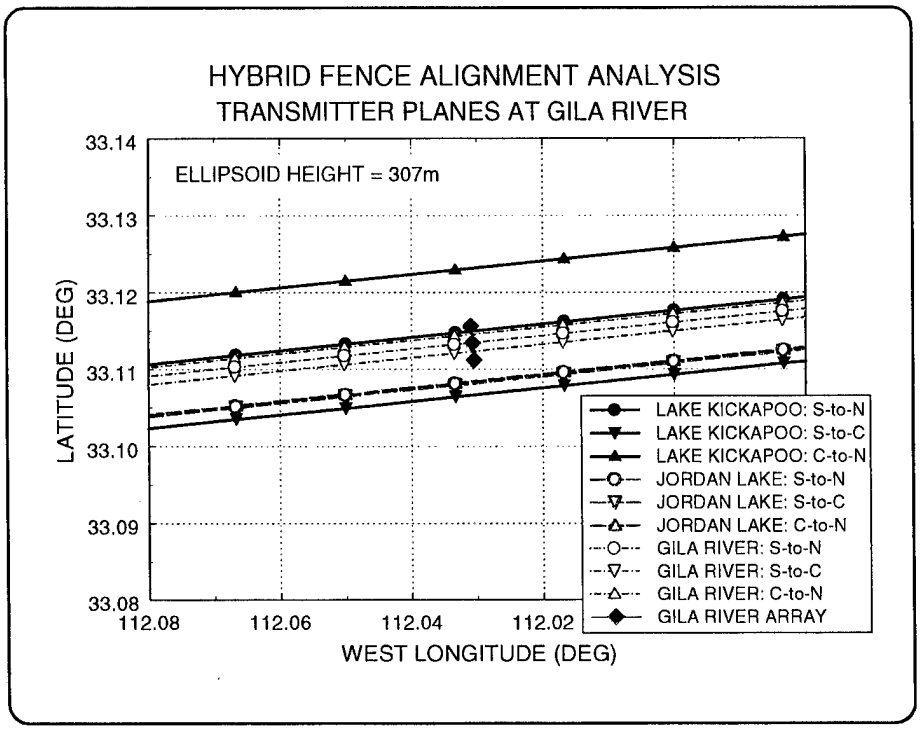

Figure 7—Intersection of the Transmitter Planes with the Ellipsoid at Gila River

Receivers

There are six receiving sites. They are located at Tattnall and Hawkinsville, Georgia; Silver Lake, Mississippi; Red River, Arkansas; Elephant Butte, New Mexico; and San Diego, California. These sites consist of several short arrays and one long (alert) array. The short arrays generally have survey points only at their center, and therefore it is not possible to define a plane for these. The long array is surveyed at its end points, with no central point. The coordinates of the two surveyed points for the long array at each receiver site are listed in Table 5. The baseline components and lengths are listed in Table 6, and the direction cosines for each line are given in Table 7. Also in Table 7 is the angle in degrees that each array line differs from the south-to-north array line at Lake Kickapoo.

Figures 8 through 13 show the positions of the Lake Kickapoo planes as they intersect the ellipsoid at the longitude of each of the receiver sites. Also in each figure is the plane defined by the alert array at that site and several symbols marking the position of the shorter arrays. A comparison of these figures show that the planes computed from all sites fall between the south-to-center and south-to-north planes defined by the Lake Kickapoo array. This amounts to an angular spread of about 0.01 deg. The only plane outside this range is the one defined by the center-to-north segment of the Lake Kickapoo array. This result suggests that the plane defined by the center-to-north array is inconsistent with the planes defined by the arrays at all the other sites.

2.5 Average Plane Computation

A plane can be determined from three or more points. Since there are nine sites and several arrays at each receiving site, there are more than enough points from which to compute an average plane. All points can be used, or some selected subset in a least-squares solution can be used. Also, each point

Table 5—Receiver Surveyed Points for Long Array: WGS84 (meters)

	X	Y	Z
Tattnall TAT4	759866.4772	-5357973.0121	3364442.3593
Tattnall TAT1	759906.1095	-5357774.5776	3364747.0702
Hawkinsville HAWK2	607726.7680	-5362947.7290	3387289.9840
Hawkinsville HAWK1	607766.4390	-5362749.4260	3387594.7280
Silver Lake SIL4	-95423.7870	-5344839.4470	3467465.5600
Silver Lake SIL1	-95384.1410	-5344641.1220	3467770.2710
Red River SW	-330517.4052	-5324297.1376	3484557.4828
Red River NW	-330477.7586	-5324098.8137	3484862.2415
Elephant Butte SW	-1557953.6717	-5095819.1259	3495960.5842
Elephant Butte NW	-1557913.9684	-5095620.7774	3496265.3240
San Diego A4S	-2440192.3340	-4794858.2120	3414447.8830
San Diego A1N	-2440139.4180	-4794593.8130	3414854.2450

Table 6—Receiver Baselines and Length (meters)

LINE	ΔX	ΔY	ΔZ	L
Tattnall	39.6323	198.4346	304.7108	365.7809
Hawkinsville	39.6710	198.3030	304.7440	365.7414
Silver Lake	39.6460	198.3250	304.7110	365.7231
Red River	39.6466	198.3239	304.7587	365.7623
Elephant Butte	39.7033	198.3485	304.7398	365.7661
San Diego	52.9160	264.3990	406.3620	487.6854

Table 7—Receiver Direction Cosines and Angle with Respect to Lake Kickapoo S-to-N

LINE	l	m	n	cosine θ	Degrees
Tattnall	0.10834996	0.54249565	0.83304187	0.99999998	0.01226180
Hawkinsville	0.10846735	0.54219456	0.83322259	0.99999997	0.01343710
Silver Lake	0.10840441	0.54228181	0.83317400	0.99999998	0.01226180
Red River	0.10839443	0.54222067	0.83321509	0.99999997	0.01343710
Elephant Butte	0.10854834	0.54228238	0.83315490	0.99999999	0.00724740
San Diego	0.10850439	0.54215078	0.83324626	0.99999997	0.01343710

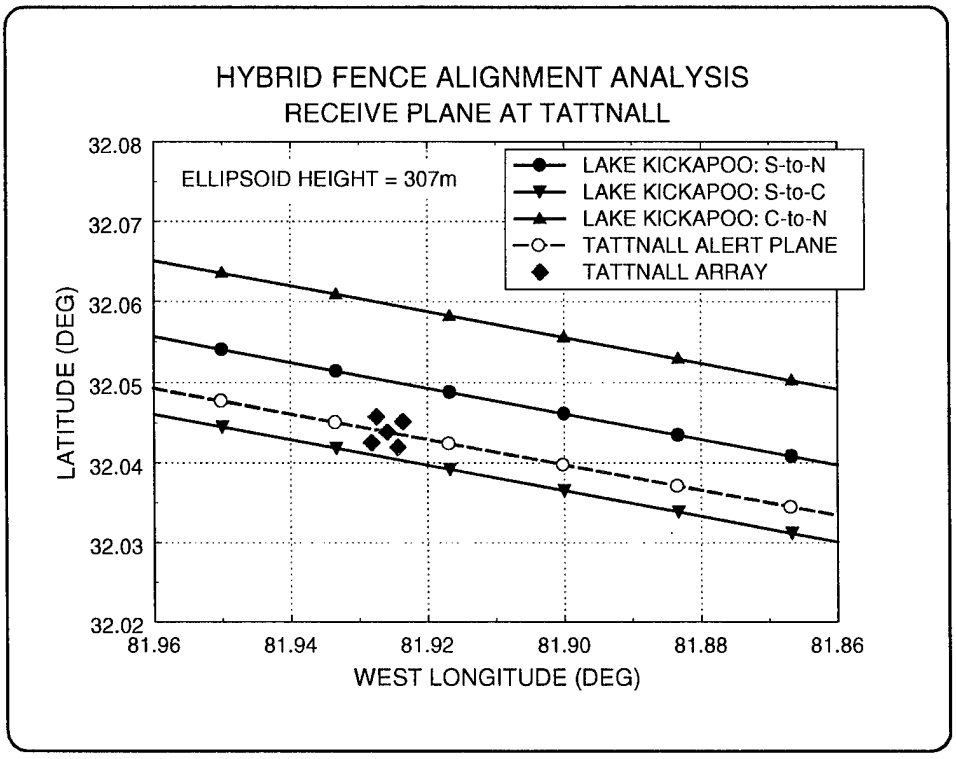

Figure 8—Intersection of the Lake Kickapoo Planes and Tattnall Plane with the Ellipsoid at Tattnall

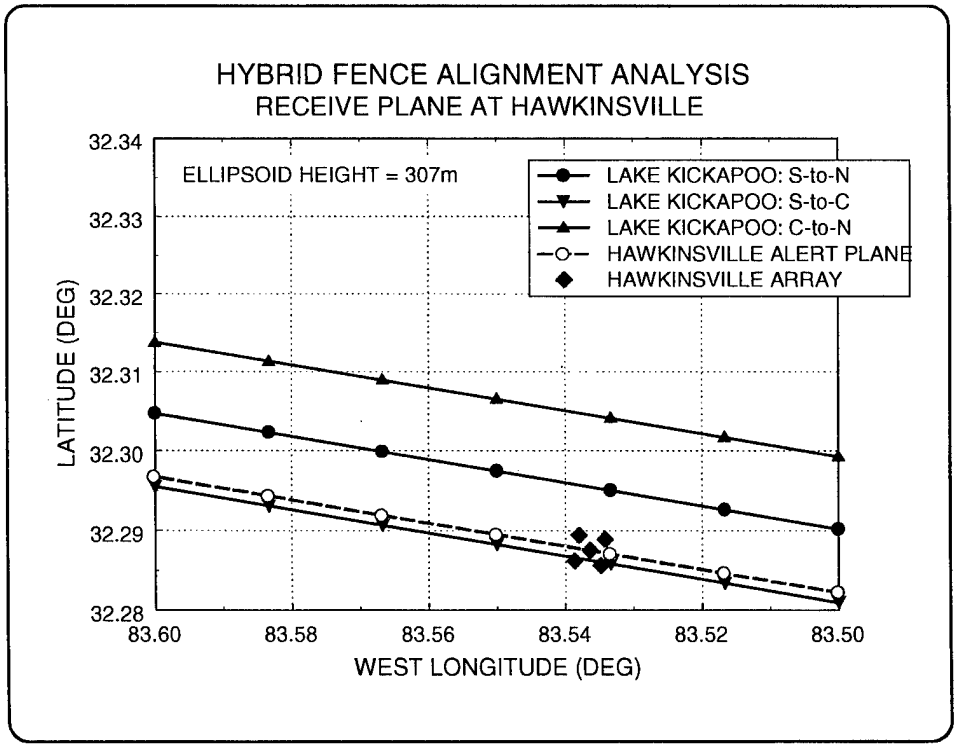

Figure 9—Intersection of the Lake Kickapoo Planes and Hawkinsville Plane with the Ellipsoid at Hawkinsville

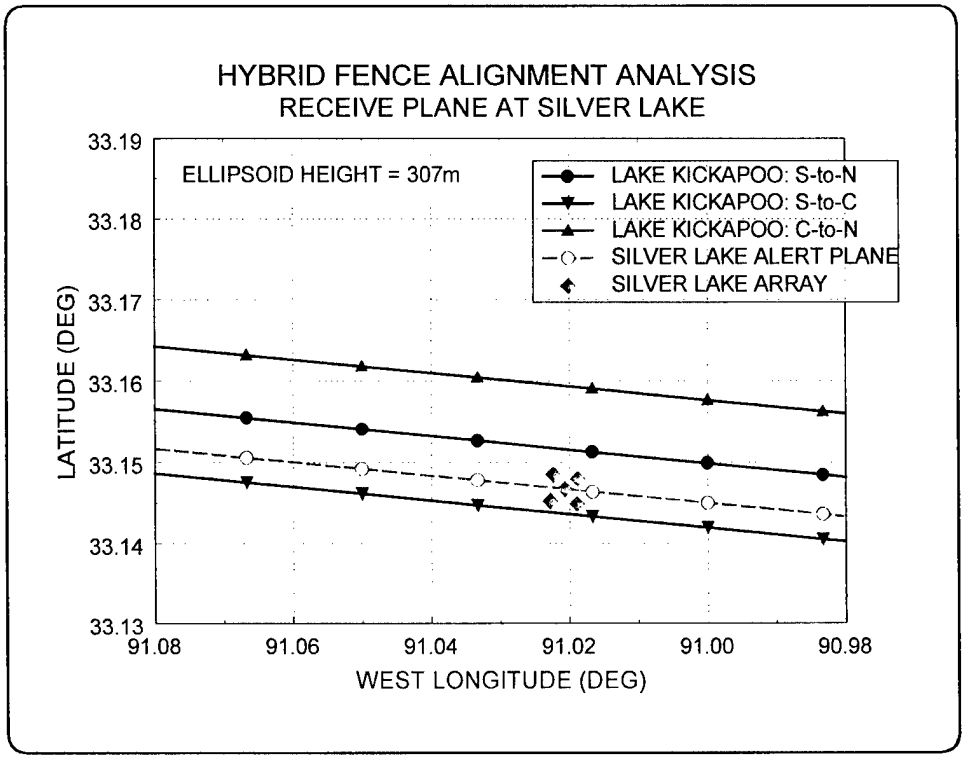

Figure 10—Intersection of the Lake Kickapoo Planes and Silver Lake Plane with the Ellipsoid at Silver Lake

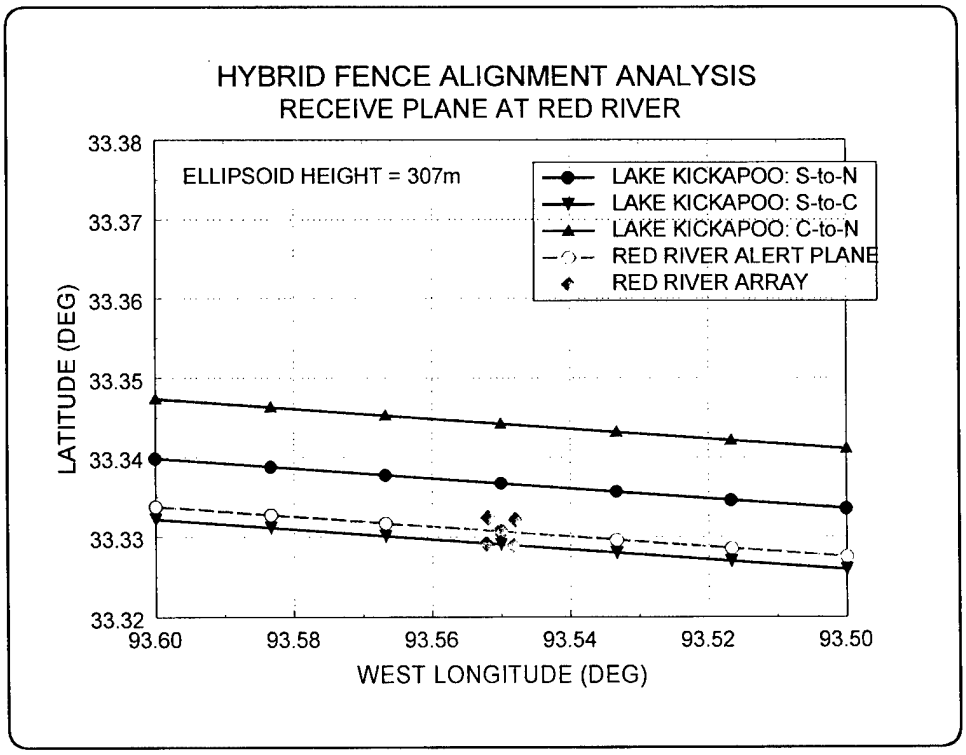

Figure 11—Intersection of the Lake Kickapoo Planes and Red River Plane with the Ellipsoid at Red River

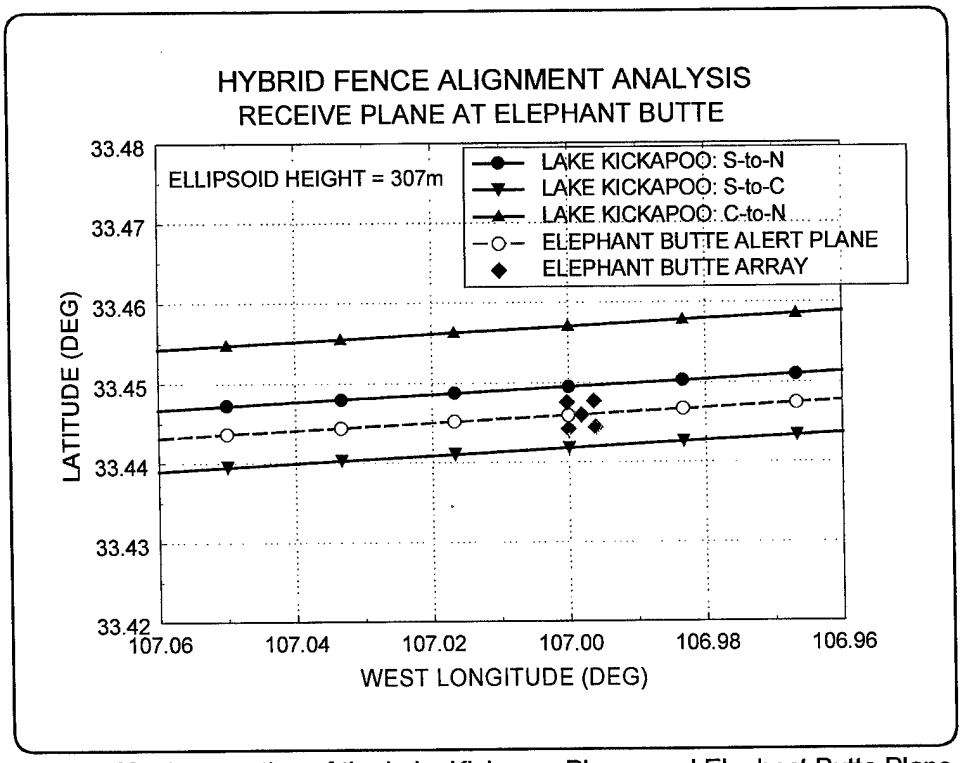

Figure 12—Intersection of the Lake Kickapoo Planes and Elephant Butte Plane with the Ellipsoid at Elephant Butte

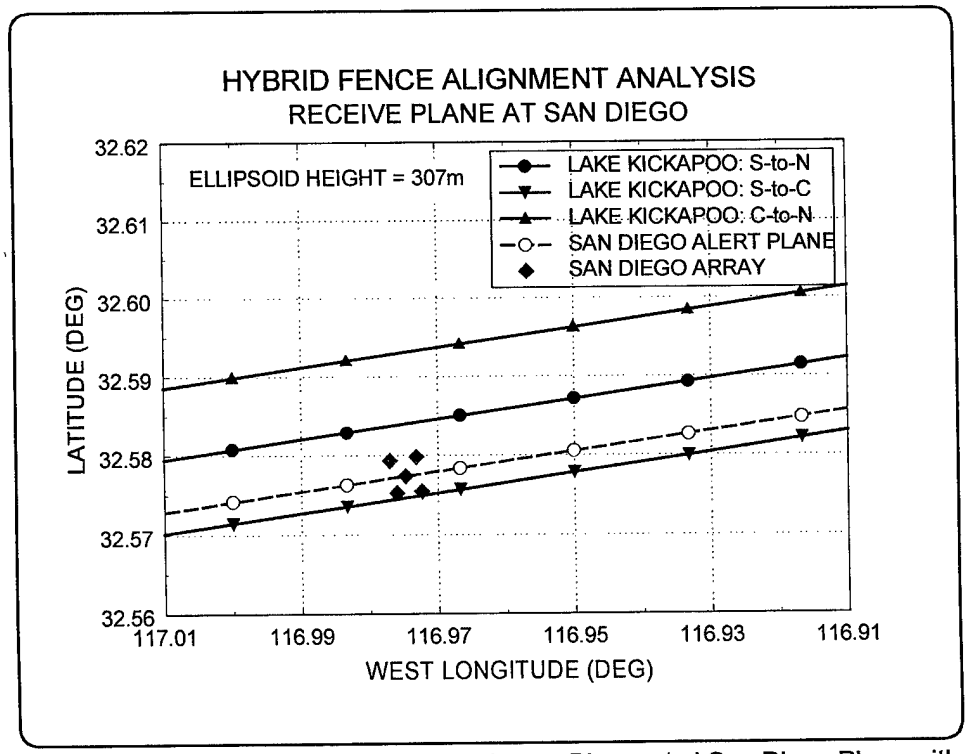

Figure 13—Intersection of the Lake Kickapoo Planes and San Diego Plane with the Ellipsoid at San Diego

can be given a different weight if desired. That is, if it is decided that the transmitter sites should be given more weight than the receiving sites, the weights assigned to each can be adjusted to reflect this emphasis. Also, many of the arrays are defined by their end points; in this case, the midpoint of the line joining the end points can be used as the point to which the average plane must be fit. The formulation described below fits a plane to an array of points. Therefore, the average distance of all point from the plane is minimized (assuming equal weighting). The normal to the average plane is not constrained to be parallel to the lines used to compute the midpoints.

The equation for a plane, defined by Equation (1), can be simplified by dividing through by the D term. The result is shown in Equation (16), where the new coefficients like $\hat{A} = \frac{A}{D}$, etc. We wish to find the coefficients $\hat{A}$, $\hat{B}$, $\hat{C}$ that best solve Equation (16) in a least-squares sense given four or more sets of x, y, z points.

$$\hat{A}x + \hat{B}y + \hat{C}z + 1 = 0 \tag{16}$$

The system of equations to be solved can be written as a matrix equation shown expanded in Equation (17) below and in condensed form in Equation 18. The $\boldsymbol{A}$ in Equation (18) is the *n-by-3* matrix of n points with *3* components each. The $\boldsymbol{X}$ represents the coefficient column vector, and $\boldsymbol{E}$ is the right-hand side column vector of *-1*.

$$\begin{bmatrix} x_1 & y_1 & z_1 \\ x_2 & y_2 & z_2 \\ x_3 & y_3 & z_3 \\ \vdots & \vdots & \vdots \\ x_n & y_n & z_n \end{bmatrix} \cdot \begin{bmatrix} \hat{A} \\ \hat{B} \\ \hat{C} \end{bmatrix} = \begin{bmatrix} -1 \\ -1 \\ -1 \end{bmatrix} \tag{17}$$

$$\boldsymbol{A} \cdot \boldsymbol{X} = \boldsymbol{E} \tag{18}$$

To form the least-squares solution, Equation (18) is premultiplied by $\boldsymbol{A}^T\boldsymbol{W}$, where $\boldsymbol{W}$ is the *n-by-n* weight matrix. This result is shown as Equation (19).

$$\boldsymbol{A}^T\boldsymbol{W}\boldsymbol{A}\boldsymbol{X} = \boldsymbol{A}^T\boldsymbol{W}\boldsymbol{E} \tag{19}$$

Finally, the solution vector is obtained by solving for $\boldsymbol{X}$. The solution equation is given in Equation (20). The inverse product $(\boldsymbol{A}^T\boldsymbol{W}\boldsymbol{A})^{-1}$ is the covariance matrix.

$$X = (A^T W A)^{-1} A^T W E \tag{20}$$

The square root of the diagonal elements of the covariance matrix is the standard deviation of the estimate for the coefficients given by the solution vector X. An example of the solutions obtained by this technique is presented next.

2.6 Error Analysis for a Particular Average Plane

The midpoint of the arrays defined by lines joining surveyed points at all nine sites were used. At the main transmitter, the line used was Lake Kickapoo South-to-North; at the eastern transmitter, Jordan Lake South-to-North; and at the western transmitter, Gila River South-to-North. At the receiver sites, the following lines were used in this example:

- Tattnall 4-to-1
- Hawkinsville 2-to-1
- Silver Lake 4-to-1
- Red River SW-to-NW
- Elephant Butte SW-to-NW
- San Diego 4S-to-1N

All lines were given equal weight in the solution. The coordinates that were used in the A matrix are listed in Table 8. The direction cosines derived from the solution vector and the corresponding standard deviations are listed in Table 9. This solution defines a mean plane that passes a distance of 42342.7 m to the south of the WGS84 origin. The average distance between the nine points and the mean plane is -1.40 m north, with a standard deviation of 258.05 m. The largest distance from the plane is registered at the Red River site, where the alert array midpoint is 446.23 m south of this mean plane. The distances of all midpoints from this mean plane, and the total angle between each array line and the mean plane normal are listed in Table 10.

Table 8—Example Points That Define a Mean Plane

Point	X	Y	Z
Lake Kickapoo S-to-N	-810634.9791	-5258901.6110	3505510.8430
Jordan Lake S-to-N	350280.3390	-5363636.1445	3422238.4975
Gila River S-to-N	-2006012.7940	-4957402.0125	3464669.0785
Tattnall 4-to-1	759886.2934	-5357873.7948	3364594.7148
Hawkinsville 2-to-1	607746.6035	-5362848.5775	3387442.3560
Silver Lake 4-to-1	-95403.9640	-5344740.2845	3467617.9155
Red River SW-to-NW	-330497.5819	-5324197.9756	3484709.8621
Elephant Butte SW-to-NW	-1557933.8200	-5095719.9517	3496112.9541
San Diego 4S-to-1N	-2440165.8760	-4794726.0125	3414651.0640

Table 9—Solution for the Mean Plane

	Direction Cosines	Standard Deviations
l	0.10901032	0.00333804
m	0.54526018	0.01184775
n	0.83114865	0.00806436

The Lake Kickapoo Center point will be adopted as the reference point to define the geodetic vertical direction for all sites. Letting the normal to the average plane extend in the northerly direction, the azimuth angle of the normal is 1.414 deg, and the elevation angle is -0.203 degrees. The total angle column listed in Table 10 can be separated into two components. The first is in the horizontal plane, and the second is in the vertical plane, with respect to the reference point. The angle in the horizontal plane will be called yaw and the angle in the vertical plane, pitch. These two angles, illustrated in Figures 14 and 15, describe the attitude of each line with respect to the normal to the average plane. Together with the offset distance between each midpoint and the average plane, these three parameters describe the relative orientation of the planes defined by the arrays and the average plane. This information can then be used to describe how space is illuminated by the arrays and how efficiently the system transfers energy. Any differences in the roll angles is of no consequence and will not be addressed.

Table 10—Distances and Angles of Defining Points from the Average Plane

Array Line	Distance (m)	Pitch (deg)	Yaw (deg)	Total Angle (deg)
Lake Kickapoo S-to-N	-106.06	0.2028	-0.0046	0.2029
Jordan Lake S-to-N	-338.54	0.2105	-0.0166	0.2111
Gila River S-to-N	-247.69	0.2081	-0.0001	0.2080
Tattnall 4-to-1	-221.24	0.1952	-0.0133	0.1956
Hawkinsville 2-to-1	86.32	0.2143	-0.0040	0.2143
Silver Lake 4-to-1	225.45	0.2091	-0.0083	0.2093
Red River SW-to-NW	446.23	0.2133	-0.0084	0.2135
Elephant Butte SW-to-NW	191.81	0.2074	-0.0002	0.2074
San Diego 4S-to-1N	-48.86	0.2168	-0.0015	0.2169

Errors in the yaw angle, as shown in Figure 14, correspond to a skew between the average plane edge and the particular plane edge. Since the fan beam produced by the arrays will be parallel to the plane edge, a large yaw angle can result in poor energy transfer between a particular array and the average array represented by the average plane. An error in the pitch angle implies that the particular plane and the average plane are parallel but tilted with respect to each other. This is shown in Figure 15. If the tilt is large, the two fan beams may not intersect.

The results listed in Table 10 show that the difference in the yaw angles between the mean plane and each particular plane is small, being 0.017-deg maximum (mean -0.0063 and standard deviation 0.0058). Consequently, the skew between the arrays is small and will be ignored in the analysis of this section. The pitch angle is an order of magnitude larger and is nearly equal to the total angle column. Since the average plane is computed by fitting to the midpoints of lines, it is possible for the normal to be biased with respect to the arrays defined by their surveyed end points. That is the case here; the average plane is biased in pitch with respect to all the particular planes by about 0.21 deg. The

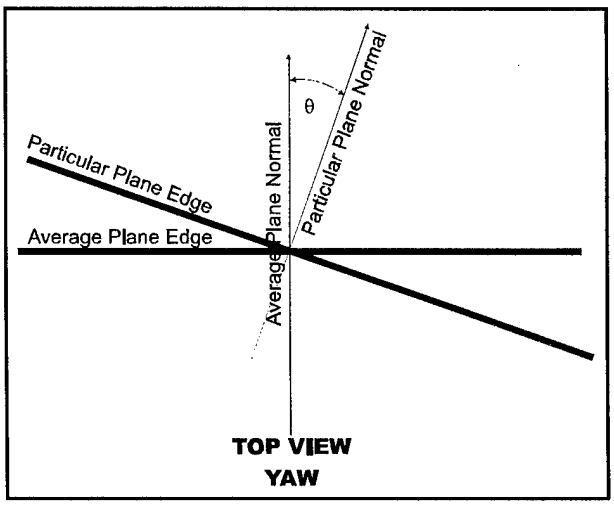

Figure 14—Schematic Diagram of Yaw Angle

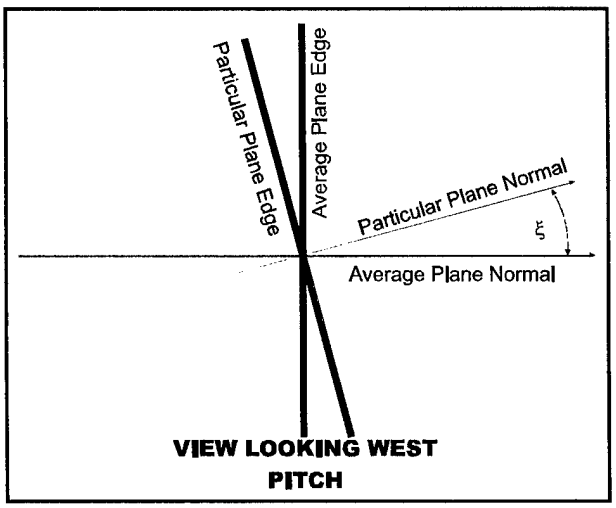

Figure 15—Schematic Diagram of Pitch Angle

relative disagreement among the planes is smaller, being about 0.007 deg. This result indicates that this average plane, containing the average great circle defined by the midpoints of the nine arrays, is not perpendicular to the arrays, but is biased by 0.21 degrees. This number is nearly the same as the elevation angle of the average plane. A logical conclusion is that the arrays were constructed to have an elevation angle of 0 deg (approximately perpendicular to the ellipsoid), while the computation for the normal to the average plane is defined solely by the array midpoints and is not constrained to be perpendicular to anything. As a result, this average plane has an elevation angle of -0.203 deg.

Of the three error sources, the offset distance from the average plane has the largest impact on the magnitude of the misalignment. In order to evaluate the misalignment geometrically, the approximate half-power, far-field beamwidth will be computed. The half-power beamwidth in degrees for long linear arrays can be approximated by the following formula [4]:

$$HPBW \approx \frac{57.3}{L_\lambda} \tag{21}$$

In this simplified expression, the half-power beamwidth depends only on the length of the array in wavelengths. Given that the operational wavelength is about 1.382 m, the corresponding beamwidth can be computed given the physical length of each array. The array lengths [5] and the beamwidth are listed in Table 11.

Table 11—Far-Field, Half-Power Beamwidth of the Longest Arrays

	Length (m)	HPBW
Lake Kickapoo	3249	0.0244
Jordan Lake	315	0.2517
Gila River	500	0.1584
Receiver Alert Low	488	0.1624
Receiver Alert High	2195	0.0361

In order to evaluate the far-field space coverage overlap among the arrays, the beamwidth, the elevation angle, and the distance from the average plane at the Lake Kickapoo center are used to compute a vertical wedge. The information needed to do this is available from Table 10. The area inside the wedge includes the main beam of

the array at the half-power points. The wedges from all arrays should overlap at the far-field altitude for maximum energy transfer between transmitters and receivers. The results from this computation are plotted in Figures 16 through 18. The view is as shown in Figure 15. This view gives a qualitative picture of the effect of the offsets between the arrays in distance and pitch angle. The average plane is also included for reference, but it is not constrained to be aligned with the array normals.

Figure 16 shows the wedges for three transmitter arrays. The vertical lines are curved in the plots because the height axis is plotted on a logarithmic scale. The plane of the paper represents a plane perpendicular to the average plane at the Lake Kickapoo center point and containing the line representing the arrays. As described above, the out-of-plane component of the arrays (yaw angle) is small and will be ignored. The shift to the right or left along the horizontal axis represents the distance offset of the central point of each array from the average plane. The vertical axis is perpendicular to the ellipsoid at the Lake Kickapoo center point. In effect, all the lines representing the arrays have been translated to pass through this point, while remaining parallel. The plot indicates that the overlap of the three transmitters is complete. Because the beamwidth of the Jordan Lake and Gila River transmitters are quite wide, the offset errors are not great enough to cause a misalignment with the narrow Lake Kickapoo beamwidth. Note that the plots depict the far field, while in fact, the wedges are somewhat wider than shown due to near-field effects below a height of 1000 km. Also, this plot assumes that the Lake Kickapoo array is a straight line; the height deviation between the north and south halves of the array discussed in Section 2.3 is not included.

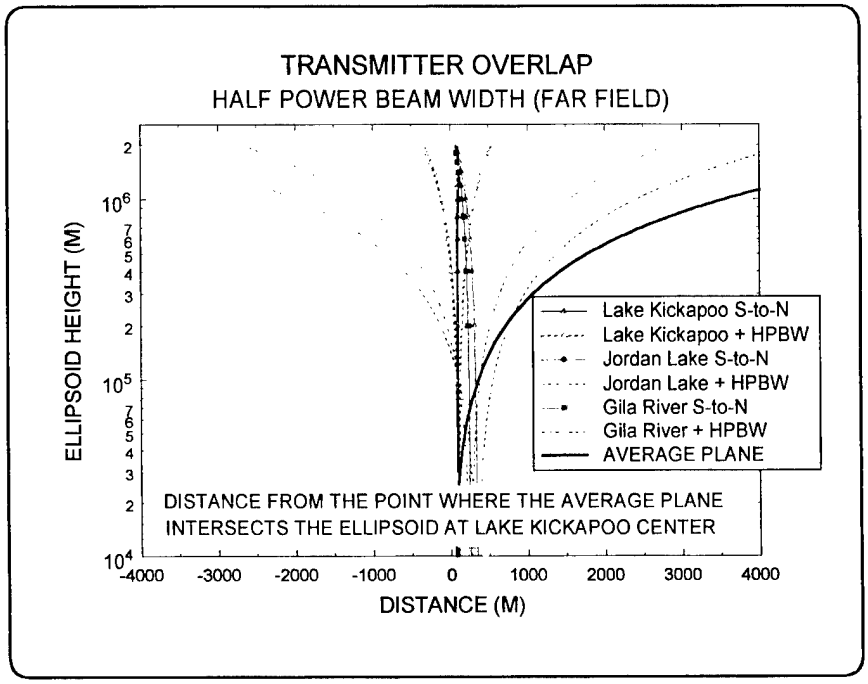

Figure 16—Wedges Computed for the Three Transmitters

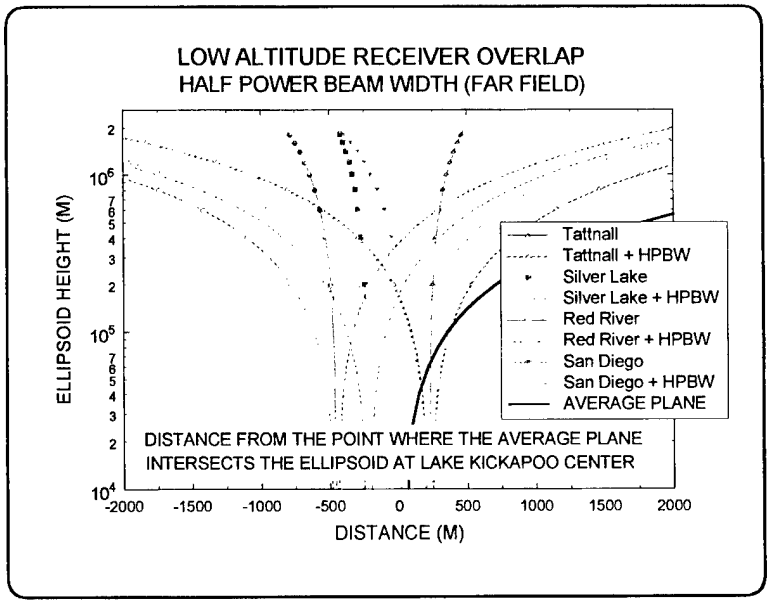

Figure 17—Wedges for the Low-Altitude Alert Arrays

Figure 17 shows the alignment plot for the four low-altitude receiver site

alert arrays, and Figure 18 shows the alignment plot for the two high-altitude alert arrays. Figure 17 indicates that the receiver beamwidth overlap is not as complete as for the transmitters. It indicates that an offset from the average of as little as 500 m from the mean may cause a significant loss of overlap at heights below 1000 km. In Figure 18, the two high-altitude alert arrays, though narrower, overlap each other well and appear to overlap a portion of the other four receiver beamwidths as well. However, the overlap between Lake Kickapoo and these two alert arrays appears to be deficient. Only about half of the beamwidths overlap at heights above 1000 km. A more quantitative discussion of the energy exchange between the transmitters and receivers will be presented in Section 3.

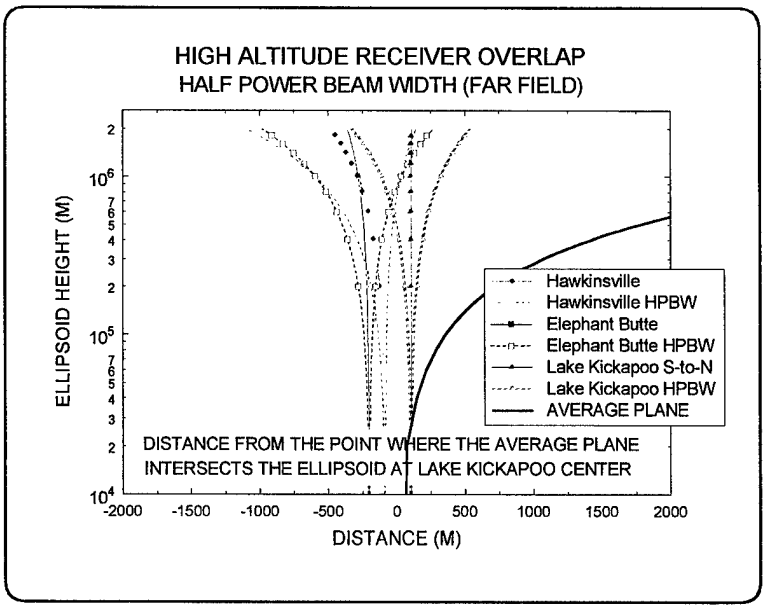

Figure 18—Wedges for the High-Altitude Alert Arrays

2.7 East and West Subarrays

The independent alignment of the east and west sections of the Space Surveillance System is of interest for future development and operation. The eastern arrays include Tattnall, Hawkinsville, Jordan Lake, Silver Lake, and Red River. The western arrays include Elephant Butte, Gila River, and San Diego. Each section includes a transmitter site, which is used as the reference point. The alignment of the two sections can be evaluated by fitting a plane to the midpoints of each array and looking at the half-power beamwidth overlap at the transmitter site. The midpoints used for each array are those listed in Table 8. The results from the fits to the east and west sections are shown in Tables 12 and 13, respectively.

Table 12—Distances and Angles of Defining Points from the Average East-Section Plane

Array Line	Distance (m)	Pitch (deg)	Yaw (deg)	Total Angle (deg)
Jordan Lake S-to-N	11.93	1.7968	-0.0589	1.7978
Tattnall 4-to-1	-276.09	1.7823	-0.0529	1.7832
Hawkinsville 2-to-1	269.61	1.8028	-0.0472	1.8034
Silver Lake 4-to-1	168.65	1.7969	-0.0506	1.7976
Red River SW-to-NW	-175.05	1.8011	-0.0514	1.8018
Average	-0.19	1.7960	-0.0522	1.7968
Standard Deviation	228.11	0.0081	0.0043	0.0080

Table 13—Distances and Angles of Defining Points from the Average West-Section Plane

Array Line	Distance (m)	Pitch (deg)	Yaw (deg)	Total Angle (deg)
Gila River S-to-N	0.0046	1.2961	0.0240	1.2963
Elephant Butte SW-to-NW	0.0048	1.2955	0.0238	1.2957
San Diego 4S-to-1N	0.0044	1.3050	0.0243	1.3052
Average	0.0046	1.2989	0.0240	1.2991
Standard Deviation	0.0002	0.0053	0.0003	0.0053

The average planes are fits to the midpoints of the arrays—not to the direction cosines of the line joining the end points of the arrays. Consequently, the direction cosines of the average plane may be biased with respect to the direction cosines of each individual array. This indicates that the arrays are not necessarily perpendicular to the average plane defined by the midpoints. The arrays themselves are well aligned. The mean pitch and yaw angles have standard deviations smaller than 0.01 deg. The distance offsets for the western section are on the order of millimeters because there are only three points to consider.

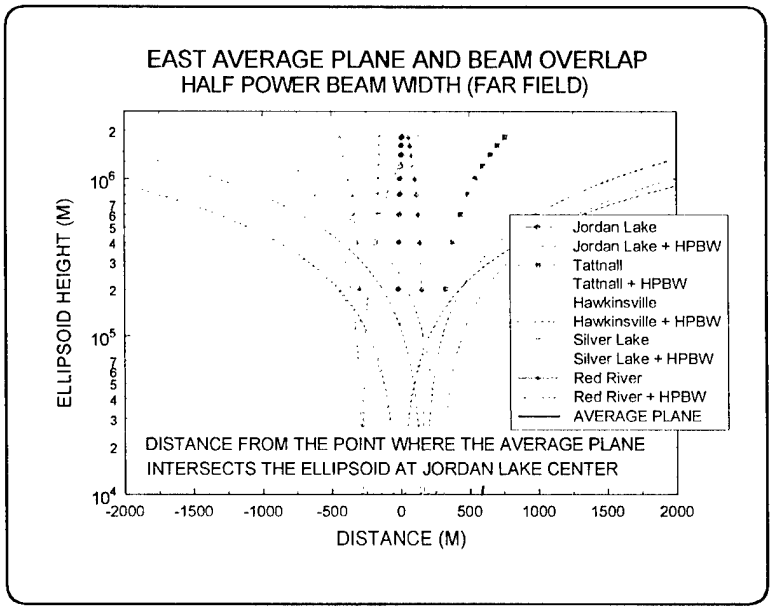

Figure 19—Wedges for the East Section

The misalignment among the eastern sites from the eastern mean plane is illustrated in Figure 19. The wide beamwidth from all sites, except Hawkinsville, allows for reasonable overlap despite the significant offsets. The alignment improves at higher altitudes as the wide beamwidths begin to include the narrow volume occupied by Hawkinsville.

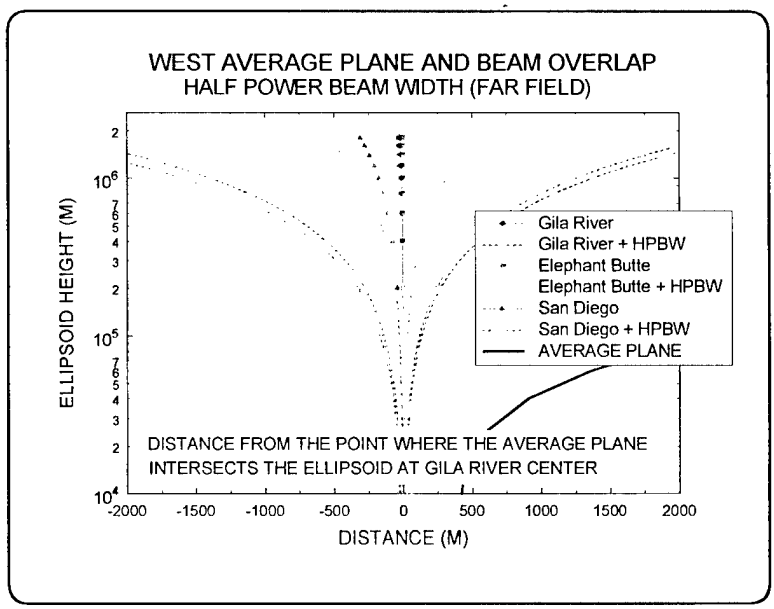

Figure 20—Wedges for the West Section

In the west, the presence of only three sites makes alignment easy (see Figure 20). The three array midpoints define their own plane; consequently, there is no offset. The angle

alignment is good, with the narrow beam Elephant Butte site situated in the center of the other two wide beams.

2.8 A Fit to All Center Points

Another way to define a mean plane would be to do a fit to all the surveyed center points of the arrays. If these points are centrally located on the site property, these results may be of interest to the designer of new arrays who wishes to stay within the existing property lines of the nine sites. The offsets of the central points from this fitted plane are listed in Table 14. The largest positive offset is at Red River (440 m south of the plane), and the largest negative offset is at Jordan Lake (340 m north of the plane). Plots of the location of the mean plane with respect to existing survey markers at each of the sites are presented in Figures 21 through 29. The symbols represent the surveyed points, while the horizontal line is the location of the mean plane. In the case on Jordan Lake, the plane passes south of the southern point of the array, and in the case of Red River, the plane passes north of the northern point. At all other sites, the plane passes close to the edge, or somewhere through the existing array.

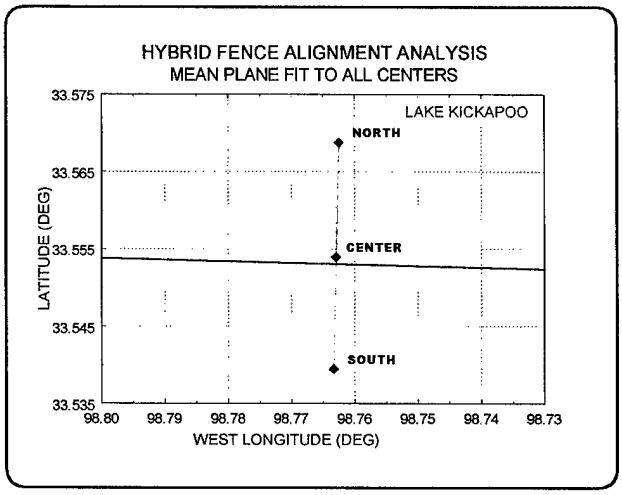

Figure 21—Lake Kickapoo Offset

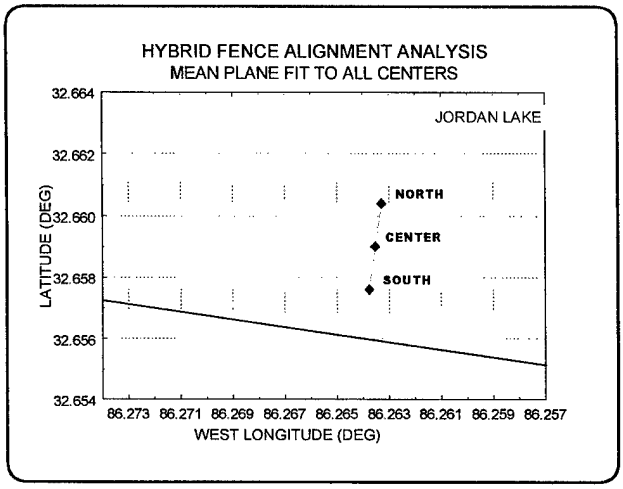

Figure 22—Jordan Lake Offset

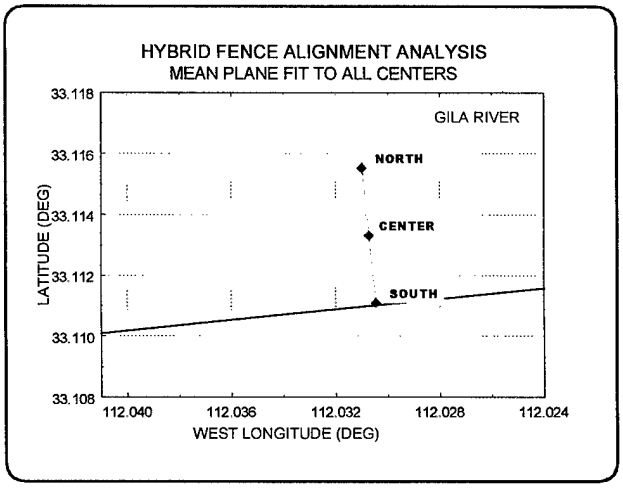

Figure 23—Gila River Offset

Table 14—Offset Between Fit Plane and All Center Points

Point	Offset (meters)
Lake Kickapoo Center	-97.14
Jordan Lake Center	-339.61
Gila River Center	-249.04
Tattnall TAT CNTR 1992	-217.46
Hawkinsville CNTR 1992	88.30
Silver Lake CNTR 1992	220.60
Red River CNTR	440.09
Elephant Butte CNTR	186.75
San Diego PT13	-44.90
Average	-1.38

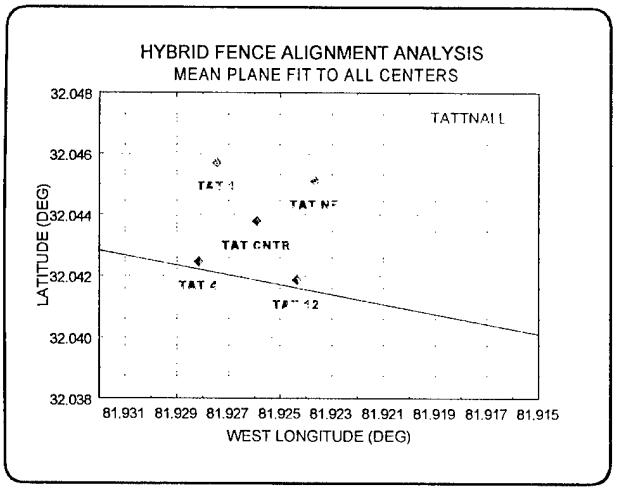

Figure 24—Tattnall Offset

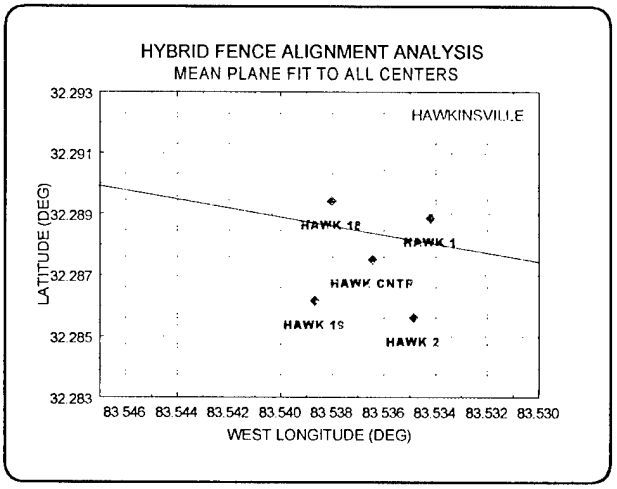

Figure 25—Hawkinsville Offset

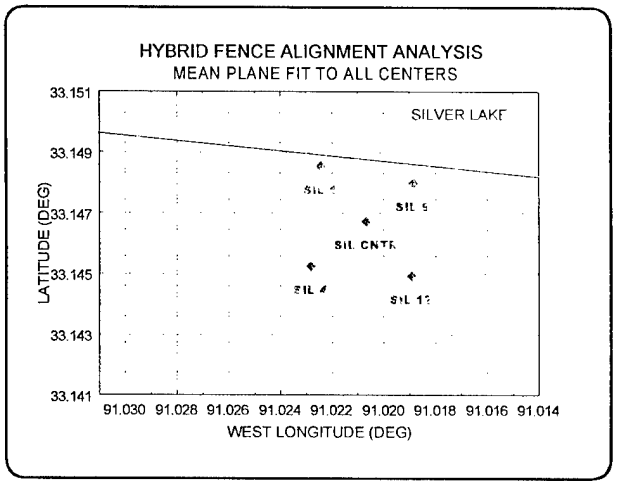

Figure 26—Silver Lake Offset

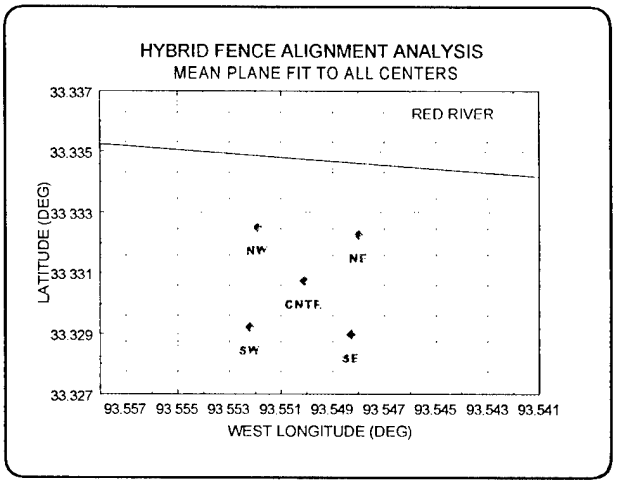

Figure 27—Red River Offset

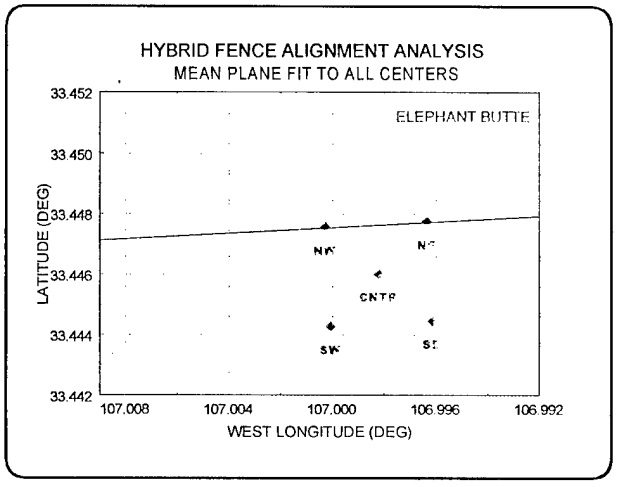

Figure 28—Elephant Butte Offset

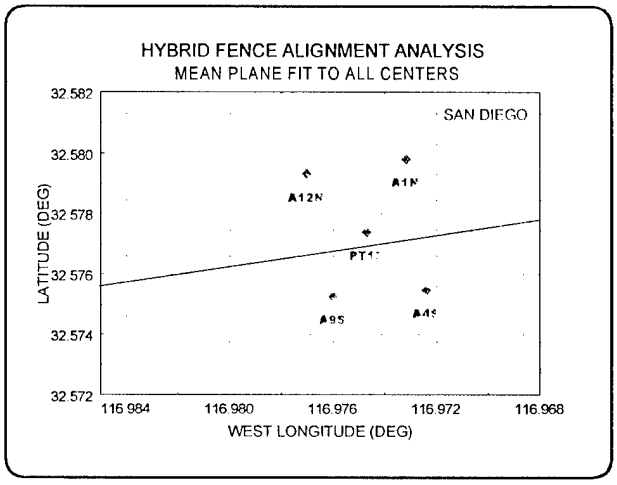

Figure 29—San Diego Offset

3.0 SYSTEM ALIGNMENT MODEL

The geometrical analysis described in the previous sections can be used to estimate the average losses between any of the transmitter and receiver pairs. In order to do this, the geometrical misalignments between arrays and the theoretical far-field array factor need to be computed. The misalignments consist of offsets from the planes defined by the transmitter arrays, and the nonparallelism between arrays described by the pitch and yaw angles discussed before. The array factors are the theoretical illumination of space for a broadside array of a given size. Treating all arrays as if they were transmitters allows for the overlap of the array factors between pairs of arrays to be computed over the entire longitude range of interest.

3.1 Array Factors

The array factors for broadside linear arrays are generated from knowledge of the number of elements constituting the array, the separation between elements in wavelengths, and the electrical properties of each element. For the purposes of this analysis, a broadside linear array is one in which all elements radiate in phase so that the maximum far-field radiation lies on a circle perpendicular to the line of the array. The number of elements will be taken as even with the phase center of the array at its midpoint, and a uniform amplitude distribution. In the far field, the physical separation between the elements (assumed isotropic) introduces a phase shift that causes the wavefronts from each element to interfere in such a manner as to produce a unique radiation pattern called the array factor.

Since all elements are in phase and have equal amplitude, the maximum points on the array factor will lie on a circle whose center is the midpoint of the array and which is perpendicular to the line joining all elements. In practice, the array factor is modified by the element factor so that the perfect symmetry due to the array is destroyed. Since the alignment is set by the array and not the elements, the effects of the elements are not considered in the analysis in this section.

In order to map the array factor onto a grid of points in geodetic coordinates, a transformation between the array and WGS84 is required. If the midpoint of the array is taken as the origin of the array, a coordinate system can be defined where one axis is along the line of the array, the second is perpendicular to the array in the vertical direction, and the third is the cross product of the first two. This coordinate system is coincident with the array geometry and can be related to WGS84. One way to do this is as follows.

3.2 Coordinate Transformation

The end points of the array are known in WGS84 coordinates from the NIMA survey. With the end points given, the midpoint can be found. This midpoint will be the array origin for the purposes of this development. The midpoint coordinates can be transformed into geodetic longitude λ_m, latitude ϕ_m, and height h_m above the ellipsoid. The local vertical unit vector $\mathbf{u}$ is then found from Equation (22). This vector is perpendicular to the ellipsoid but not necessarily perpendicular to the array.

$$\begin{aligned} \hat{u}_{xm} &= \cos\phi_m \cos\lambda_m \\ \hat{u}_{ym} &= \cos\phi_m \sin\lambda_m \\ \hat{u}_{zm} &= \sin\phi_m \end{aligned} \tag{22}$$

The direction cosines of the array are its unit vector. These can be found by differencing the coordinates of the north point from the south point and dividing by the length, as in Equation (23).

$$\begin{aligned} \hat{a}_x &= \frac{x_n - x_s}{\sqrt{(x_n - x_s)^2 + (y_n - y_s)^2 + (x_n - x_s)^2}} \\ \hat{a}_y &= \frac{y_n - y_s}{\sqrt{(x_n - x_s)^2 + (y_n - y_s)^2 + (x_n - x_s)^2}} \\ \hat{a}_z &= \frac{z_n - z_s}{\sqrt{(x_n - x_s)^2 + (y_n - y_s)^2 + (x_n - x_s)^2}} \end{aligned} \tag{23}$$

The cross product $\hat{\mathbf{a}}\times\hat{\mathbf{u}}$ will be in the easterly direction, perpendicular to the array and perpendicular to the local vertical at the midpoint. A reference plane can be defined from the following three points: the midpoint of the array, the midpoint plus the unit vector in the $\hat{\mathbf{a}}$ direction, and the midpoint plus the unit vector in the $\hat{\mathbf{a}}\times\hat{\mathbf{u}}$ direction. A normal to this plane will be defined as normal to the array. With this construction, the grid of geodetic coordinates can be transformed into azimuth and elevation angles with respect to the array factor. The azimuth angle is measured in the plane containing both the $\hat{\mathbf{a}}$ and $\hat{\mathbf{a}}\times\hat{\mathbf{u}}$ vectors. The elevation angle is the complement of the zenith angle measured from the normal vector. These vectors are illustrated in Figure 30. The azimuth and elevation angles of any given grid point G(x, y, z) can be found by the dot product of $\hat{\mathbf{G}}$ with the array coordinates. These relationships are listed as Equation (24).

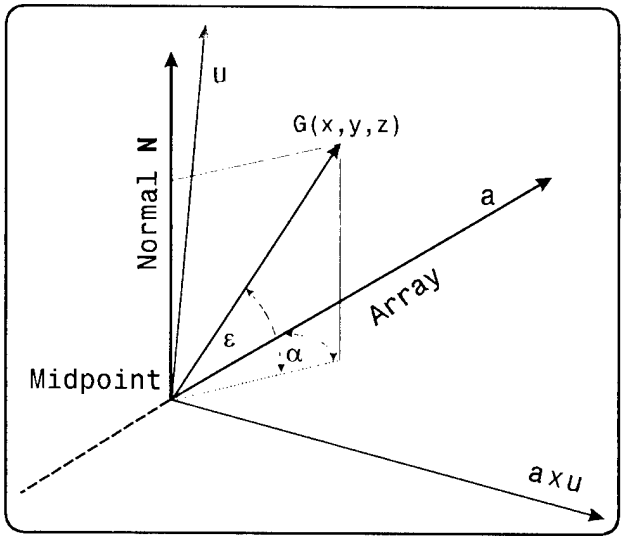

Figure 30—Array Coordinate System

$$\begin{aligned} \alpha &= \arctan\left(\frac{\hat{\boldsymbol{G}}\cdot\hat{\mathbf{a}}\times\hat{\mathbf{u}}}{\hat{\boldsymbol{G}}\cdot\hat{\mathbf{a}}}\right) \\ \epsilon &= \frac{\pi}{2} - \arccos\left(\hat{\boldsymbol{G}}\cdot\hat{\boldsymbol{N}}\right) \end{aligned} \tag{24}$$

In this way, the array factor value for any grid point can be determined and plotted. Given the coordinates of a grid point, the array factor at this point from any of the Space Surveillance arrays can be computed and compared with the array factor from any other of the arrays. Multiplying the values from pairs of arrays will give an estimate of the overlap between them. The better the alignment between the arrays, the better the overlap will be.

3.3 Transmitter Array Factors

The expression for the array factors is given in Equation 25. This applies to receiver sites as well as transmitter sites. In the far field, it is a function of the number of elements (n), their spacing in wavelengths (d), and the elevation and azimuth angles (ϵ, α). In the special case where $\epsilon \rightarrow 90$ deg, at any azimuth angle, the argument of the sine functions approaches zero and can be replaced by the arguments themselves, giving the result $F = F_0$.

$$F = \frac{F_0}{n} \frac{\sin(n\pi d \cos\epsilon \cos\alpha)}{\sin(\pi d \cos\epsilon \cos\alpha)} \tag{25}$$

The Lake Kickapoo transmitter far-field array factor as a function of geodetic west longitude and north latitude is shown in Figure 31. The curve of the maxima, in this and the following figures, traces the projection of the great circle on the ellipsoid. The darker areas represent the underside of the plotted surface. The vertical scale is in decibels with an arbitrary zero reference. The first sidelobe is 13.5 dB below the maxima, as expected. Similar plots for the other two transmitters are shown in Figures 32 and 33. Because these secondary arrays are considerably shorter, the array factor maximum is much broader and not as sensitive to a misalignment with respect to the other arrays.

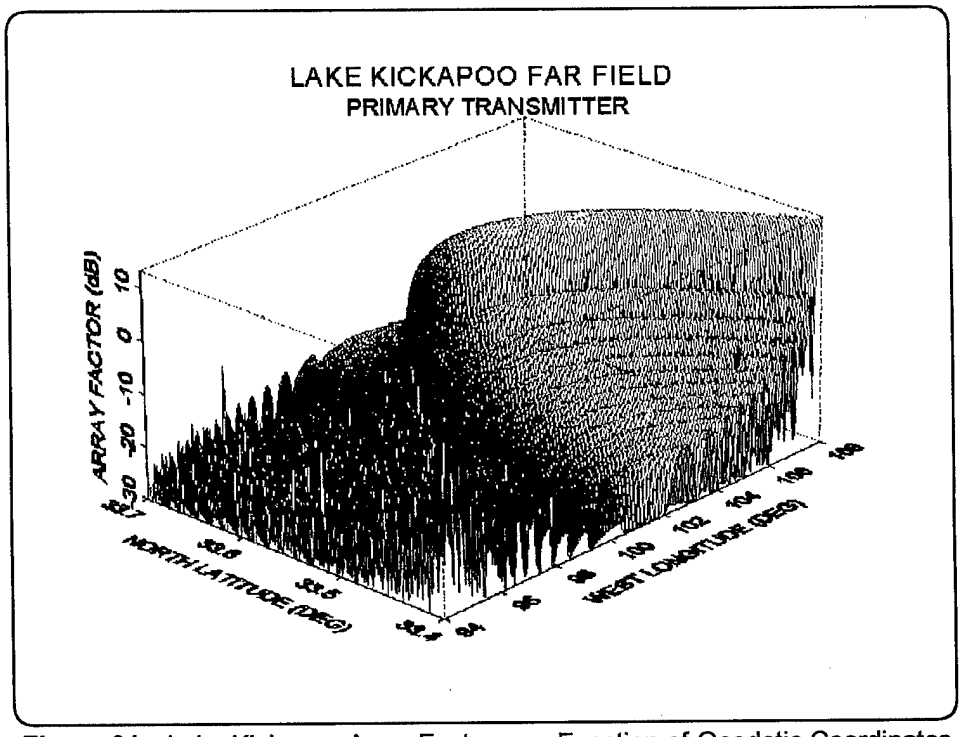

Figure 31—Lake Kickapoo Array Factor as a Function of Geodetic Coordinates

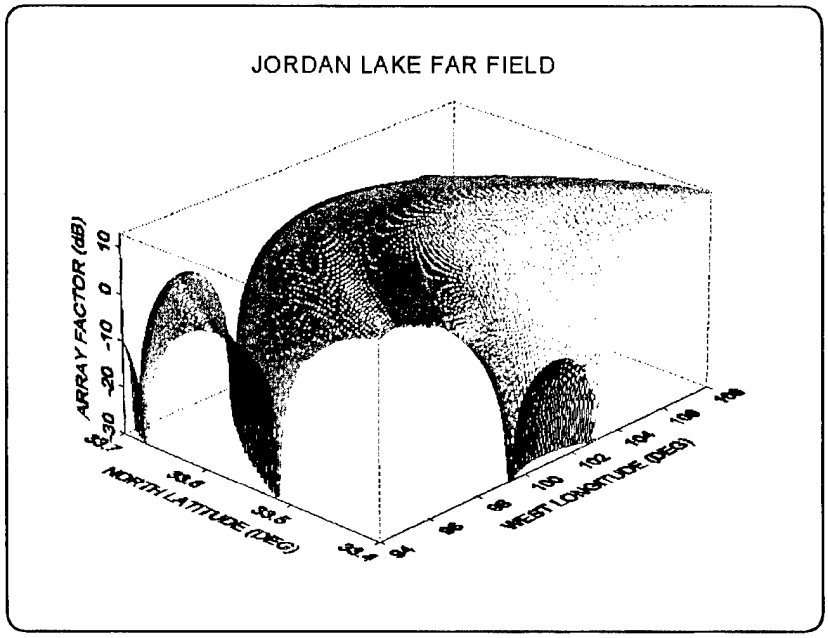

Figure 32—Jordan Lake Array Factor as a Function of Geodetic Coordinates

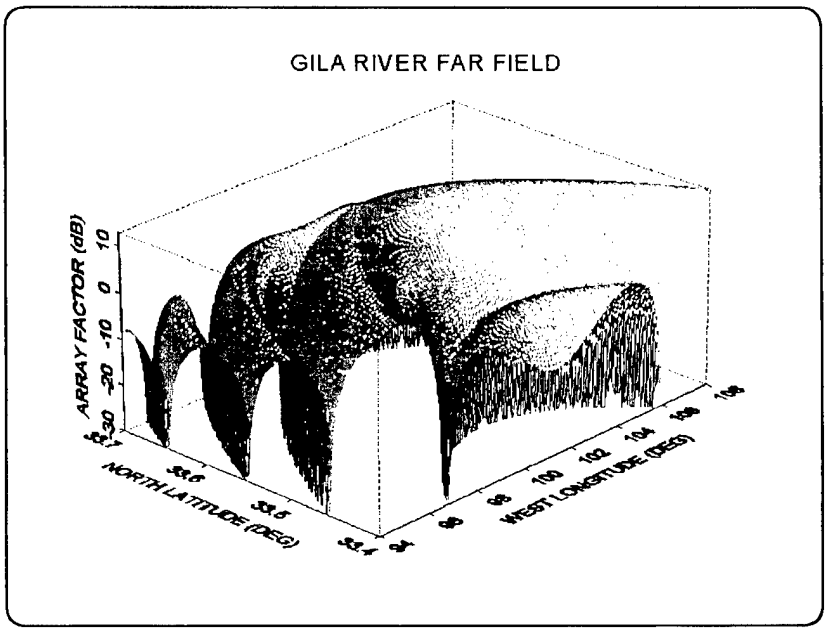

Figure 33—Gila River Array Factor as a Function of Geodetic Coordinates

3.4 Receiver Array Factors

There are two types of receiver sites: high altitude and low altitude. Each type consists of many linear arrays of different lengths arranged so that the phase centers of the arrays are arranged in a specific way. The multiple arrays are used as an interferometer to perform specialized analyses on the signals scattered from orbiting targets. The arrays at the high-altitude sites are longer and have greater sensitivity to high-altitude targets than the low-altitude sites. For the purposes of the alignment problem addressed by this report, only the longest arrays at each site will be of interest. This is primarily because the NIMA survey presented positions of only a few points on the arrays at the receiver sites. An analysis of the alignment of all arrays would require a more complete survey. A secondary reason is that the short arrays have a broad array factor and would not be sensitive to the small alignment errors typical of the Space Surveillance Fence.

The array factors for the four low-altitude sites are represented by the Red River site shown in Figure 34. The two high-altitude sites are represented by Elephant Butte, as shown in Figure 35.

3.5 Products and Ratios of Array Factors

To address the effects of the misalignment of the arrays on performance, each transmitter site will be paired with a receiver site. The actual positions of each array will be used to produce an array factor value on a grid of geodetic points in the far field. The array factor values for each pair of sites will be multiplied together (by adding dB values) at common grid points. This result represents the total energy transfer between the two arrays. This same process will be repeated for each pair, with the receiver sites shifted to be in perfect alignment with the plane defined by the particular transmitter array. The first set of values will be referred to as the actual product and the second as the ideal product. The product values in each case will be truncated to keep only the largest values, those greater than -26 dB below the maximum. All truncated grid points are set to 0 dB. This truncation removes all contributions from the array sidelobes. Finally, the actual products are divided by the ideal

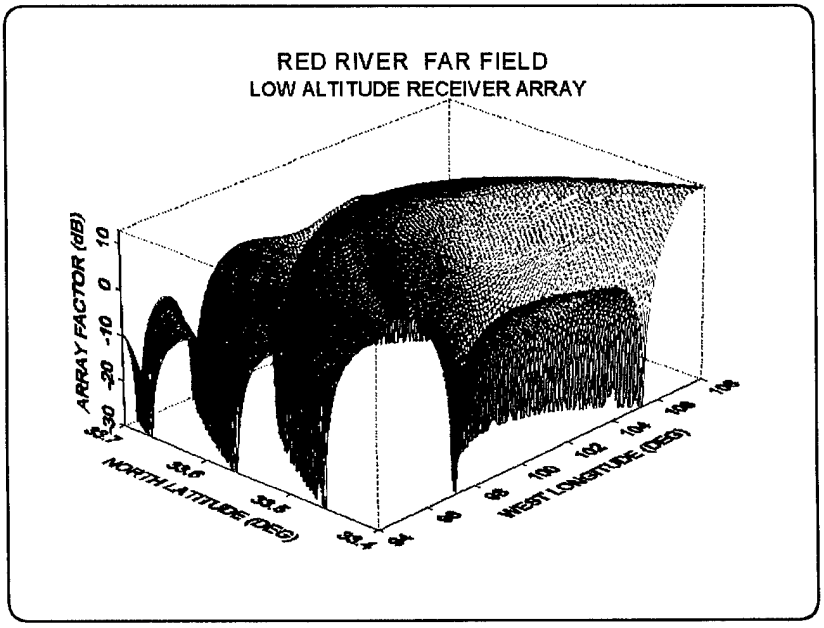

Figure 34—A Low-Altitude Array Factor as a Function of Geodetic Coordinates (Red River)

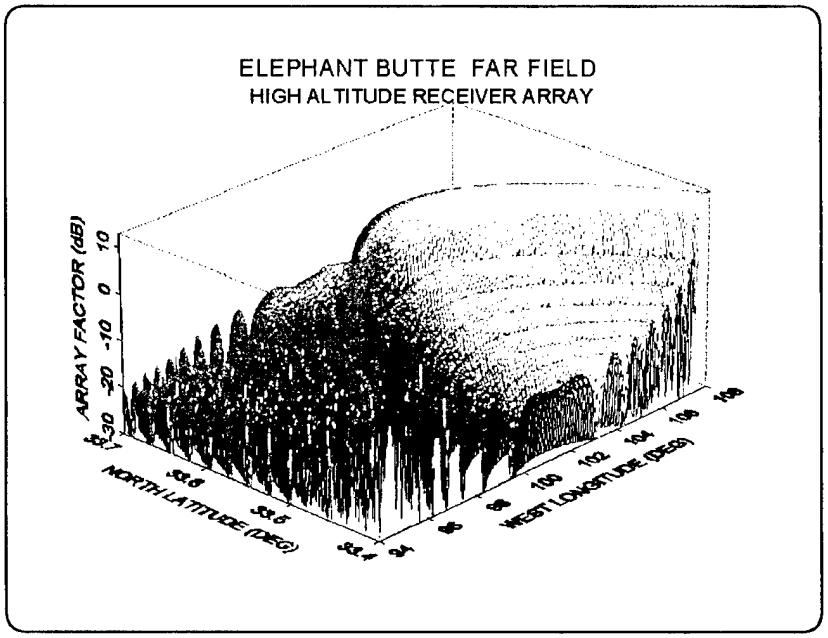

Figure 35—A High-Altitude Array Factor as a Function of Geodetic Coordinates (Elephant Butte)

products (by differencing the dB values) to form a plot of the deviations of the actual pair from the ideal. The mean of this difference over the entire nonzero grid represents the loss incurred by the misalignment of that pair of arrays.

Section 3.6 shows the actual and ideal product plots for one transmitter and receiver pair. Section 3.7 shows the difference plots for all combinations. The geodetic grid ranges from 80 to 118 deg west longitude and 31.5 to 34 deg north latitude.

3.6 Misalignments and Product Plots

For each transmitter, a plane can be defined. The offsets and the errors in direction (pitch and yaw angles) for each receiver are computed relative to the specific transmitter plane. These errors are listed in Tables 15 through 17. The offset errors appear to be the most important, especially in the cases where two high-gain (narrow array factor) arrays are paired. Table 15 shows that the Hawkinsville array has the largest offset relative to Lake Kickapoo. Both are high-gain arrays, and the mean loss computed by the method outlined in Section 3.5 is the largest of all transmitter-receiver pairs. As before, the sign of the offset indicates on which side of the plane the midpoint of each array lies. A positive offset indicates that the point is south of the plane. These results are consistent with the plots shown as Figures 8 through 13. The senses for the angles are described in Figures 14 and 15.

Two representative plots of the sum of a pair of array factors are shown in Figures 36 and 37. Note that the sidelobes are removed, and that the maximum is about +26dB.

Table 15—Misalignments of Receiver Arrays with Lake Kickapoo Transmitter

ACTUAL RECEIVER ARRAY	OFFSET (m)	PITCH (deg)	YAW (deg)
TATTNALL 4-to-1	703.32	-0.0076	-0.0087
HAWKINSVILLE 2-to-1	871.31	0.0114	0.0006
SILVER LAKE 4-to-1	534.46	0.0063	-0.0037
RED RIVER SW-to-NW	657.18	0.0105	-0.0038
ELEPHANT BUTTE SW-to-NW	395.10	0.0046	0.0044
SAN DIEGO 4S-to-1N	721.53	0.0140	0.0031

Table 16—Misalignments of Receiver Arrays with Jordan Lake Transmitter

ACTUAL RECEIVER ARRAY	OFFSET (m)	PITCH (deg)	YAW (deg)
TATTNALL 4-to-1	559.89	-0.0145	0.0060
HAWKINSVILLE 2-to-1	691.69	0.0060	0.0117
SILVER LAKE 4-to-1	192.69	0.0000	0.0084
RED RIVER SW-to-NW	263.06	0.0043	0.0076
ELEPHANT BUTTE SW-to-NW	-257.08	-0.0000	0.0167
SAN DIEGO 4S-to-1N	-98.74	0.0090	0.0137

Table 17—Misalignments of Receiver Arrays with Gila River Transmitter

ACTUAL RECEIVER ARRAY	OFFSET (m)	PITCH (deg)	YAW (deg)
TATTNALL 4-to-1	309.29	-0.0101	-0.0154
HAWKINSVILLE 2-to-1	485.72	0.0069	-0.0026
SILVER LAKE 4-to-1	192.73	0.0026	-0.0079
RED RIVER SW-to-NW	331.87	0.0068	-0.0071
ELEPHANT BUTTE SW-to-NW	170.00	-0.0006	-0.0002
SAN DIEGO 4S-to-1N	584.91	0.0089	0.0003

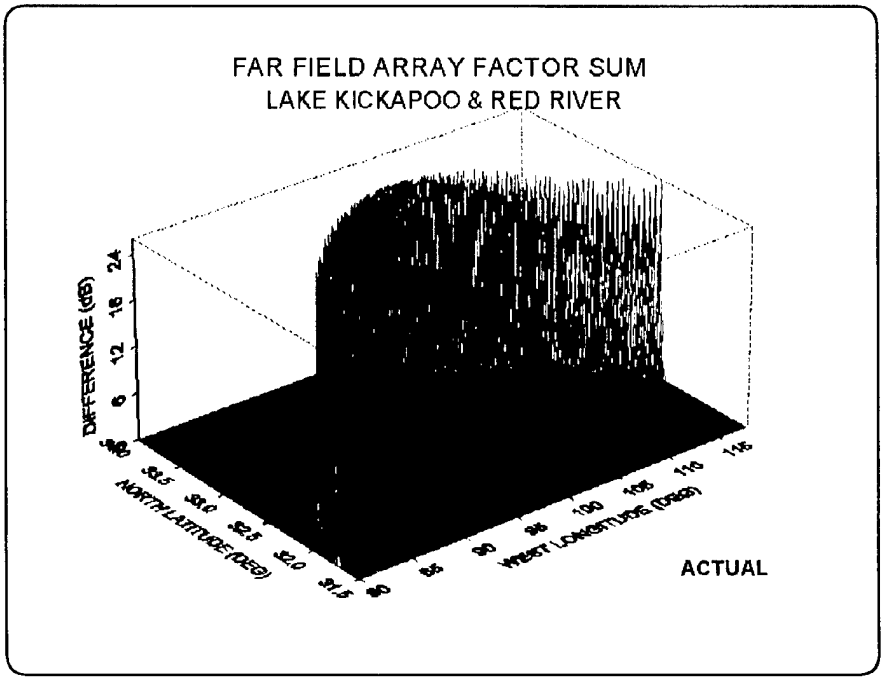

Figure 36—The Sum (dB) of the Lake Kickapoo Transmitter and the Red River Receiver (Actual)

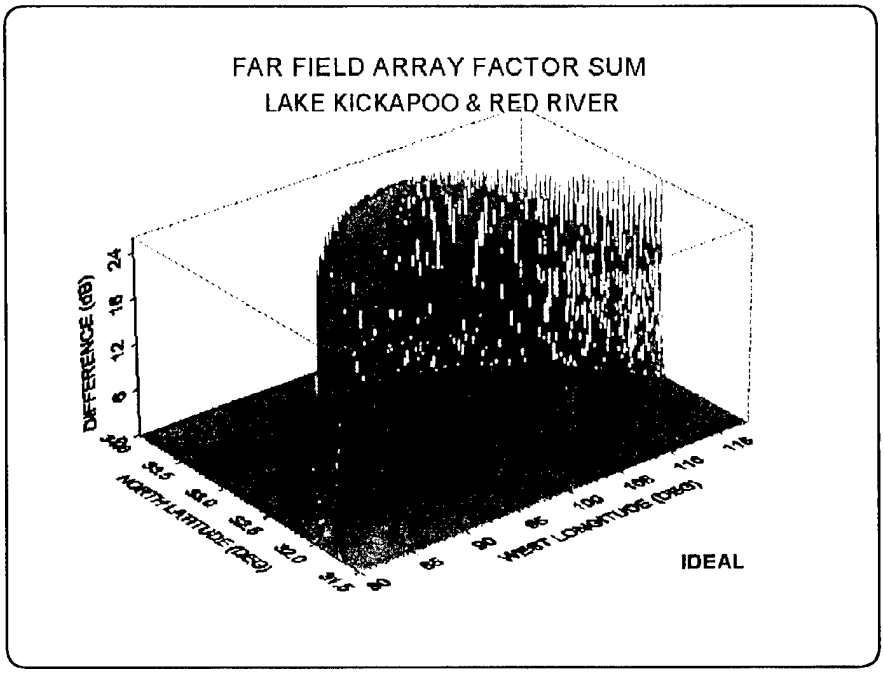

Figure 37—The Sum (dB) of the Lake Kickapoo Transmitter and the Red River Receiver (Ideal)

3.7 Far-Field Ratio Plots

The differences (dB) between the actual and ideal array factors summarize the effect of the misalignment of the transmitter and receiver arrays relative to each other. These statistics are valid only for the grid points considered, that is, all those greater than 0 dB in the sum plots. The minimum, maximum, and mean values listed in Table 18 indicate that only the Lake Kickapoo-Hawkinsville pair has a mean loss greater than 1 dB. The large maxima and minima at some other pairs average out resulting in a small mean value. The difference plots for all 18 pairs are presented as Figures 38 through 55. These show the nature and magnitude of the error in each pair as a function of longitude and latitude.

Table 18—Statistics of the Differences Between Actual and Ideal Pairs (dB)

LAKE KICKAPOO	TATTNALL	HAWKINS-VILLE	SILVER LAKE	RED RIVER	ELEPHANT BUTTE	SAN DIEGO
Min	-0.85	-11.83	-0.95	-1.30	-4.85	-1.41
Max	0.78	5.06	0.83	1.24	3.03	1.53
Mean	-0.01	-4.93	-0.03	-0.00	-0.84	-0.05
JORDAN LAKE						
Min	-6.51	-16.57	-2.05	-3.07	-15.37	-5.25
Max	6.01	16.41	2.09	3.02	15.74	4.86
Mean	-0.07	-0.00	-0.00	-0.01	-0.00	-0.03
GILA RIVER						
Min	-3.88	-15.73	-1.07	-2.02	-0.24	-2.48
Max	3.23	15.37	1.01	1.77	0.27	2.13
Mean	-0.13	-0.03	-0.01	-0.05	-0.00	-0.11

High spacial resolution analysis of the Lake Kickapoo-Hawkinsville pair illustrates how the large offset, combined with the narrow array factors, can cause a signal loss. The center of the Hawkinsville array is 871-m south (at the longitude of Hawkinsville) of the Lake Kickapoo-defined plane. In the far field, this causes the array factors to miss precise alignment. The array factors for both arrays are illustrated in Figure 56. The first southern sidelobe of the Lake Kickapoo array is inside the main lobe of the Hawkinsville array factor. Also, the main lobe of the Hawkinsville array cuts off the northern edge of the Lake Kickapoo array factor. These two effects account for the mean error of almost 5 dB listed in Table 18. If the alignment were perfect, the two array factors would overlap, as illustrated in Figure 57. Figures 58 and 59 show the product of the actual and ideal array factors for the longitudes between 89 and 90 deg. Figure 60 shows the ratio of the actual to the ideal products. This scale of plots is expanded, compared with Figures 36 and 37, in order to include some sidelobes and better illustrate the cause of the misalignment.

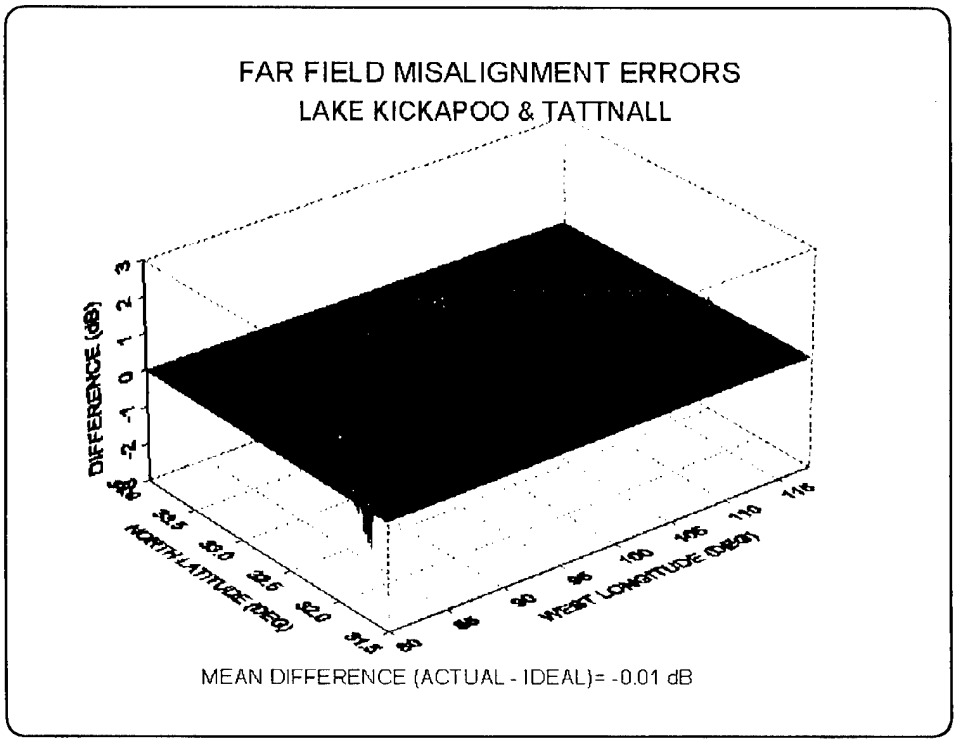

Figure 38—Difference (dB) Between the Actual and Ideal Sums for the Lake Kickapoo and Tattnall Pair

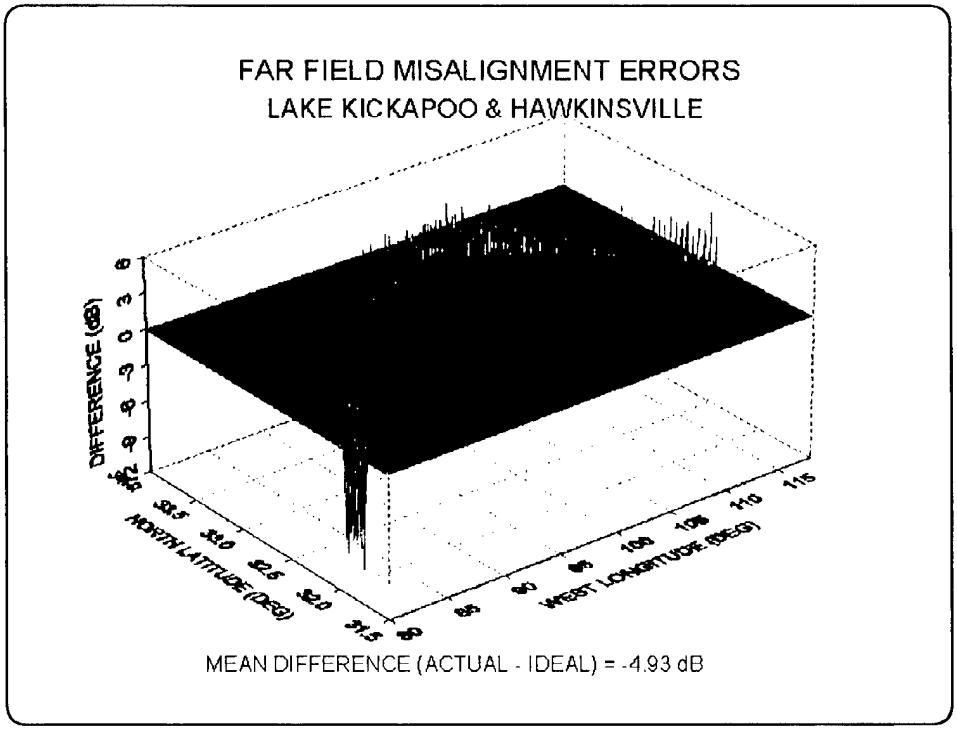

Figure 39—Difference (dB) Between the Actual and Ideal Sums for the Lake Kickapoo and Hawkinsville Pair

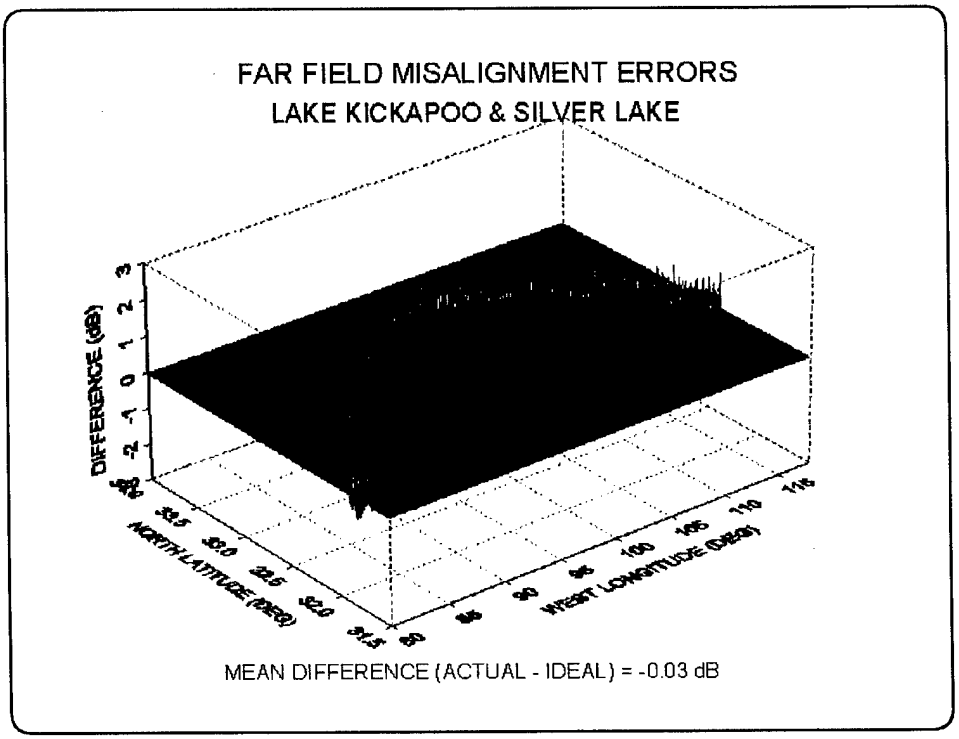

Figure 40—Difference (dB) Between the Actual and Ideal Sums for the Lake Kickapoo and Silver Lake Pair

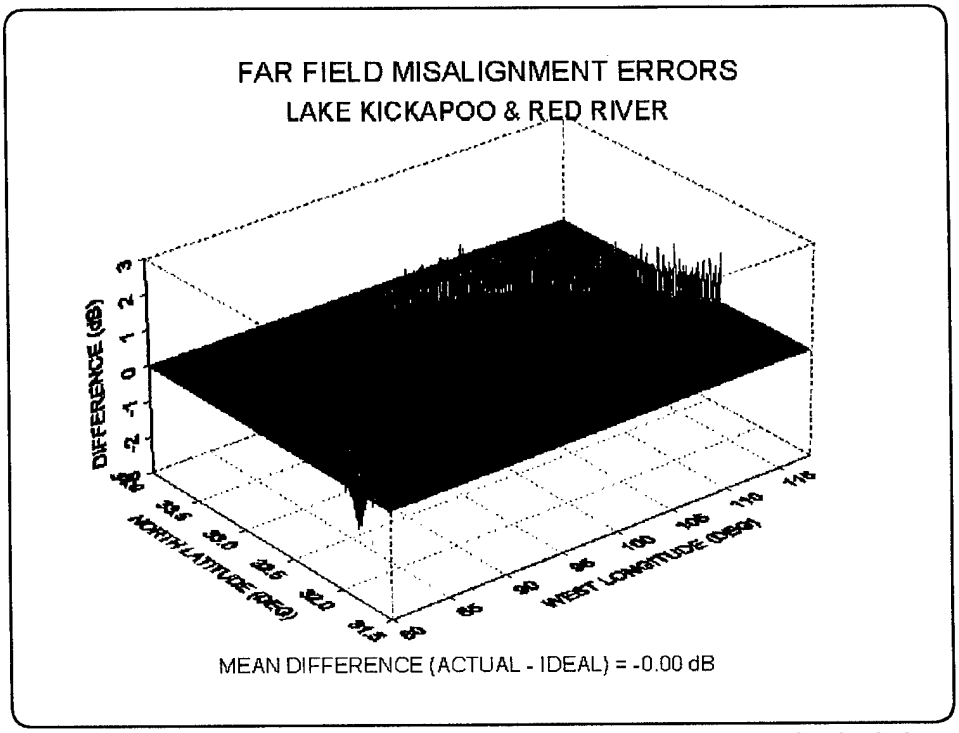

Figure 41—Difference (dB) Between the Actual and Ideal Sums for the Lake Kickapoo and Red River Pair

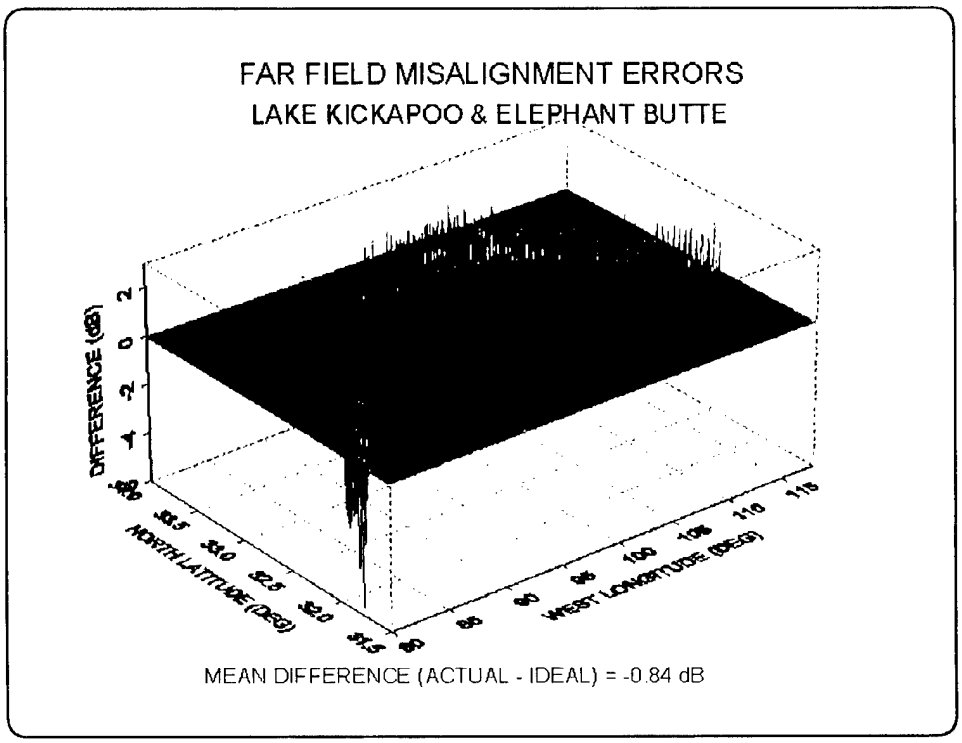

Figure 42—Difference (dB) Between the Actual and Ideal Sums for the Lake Kickapoo and Elephant Butte Pair

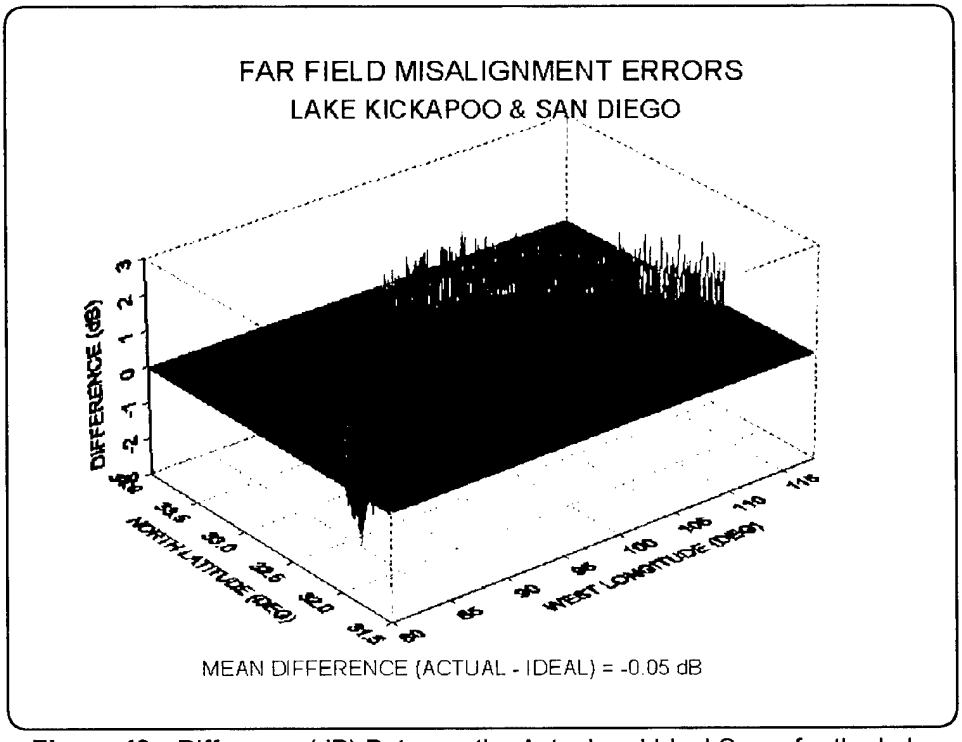

Figure 43—Difference (dB) Between the Actual and Ideal Sums for the Lake Kickapoo and San Diego Pair

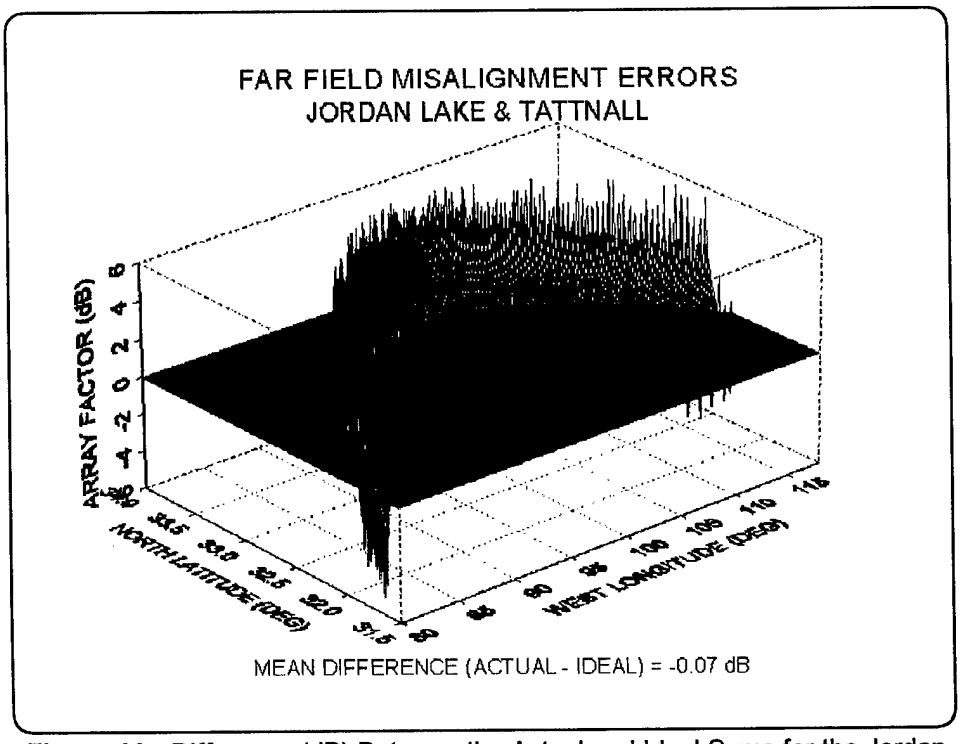

Figure 44—Difference (dB) Between the Actual and Ideal Sums for the Jordan Lake and Tattnall Pair

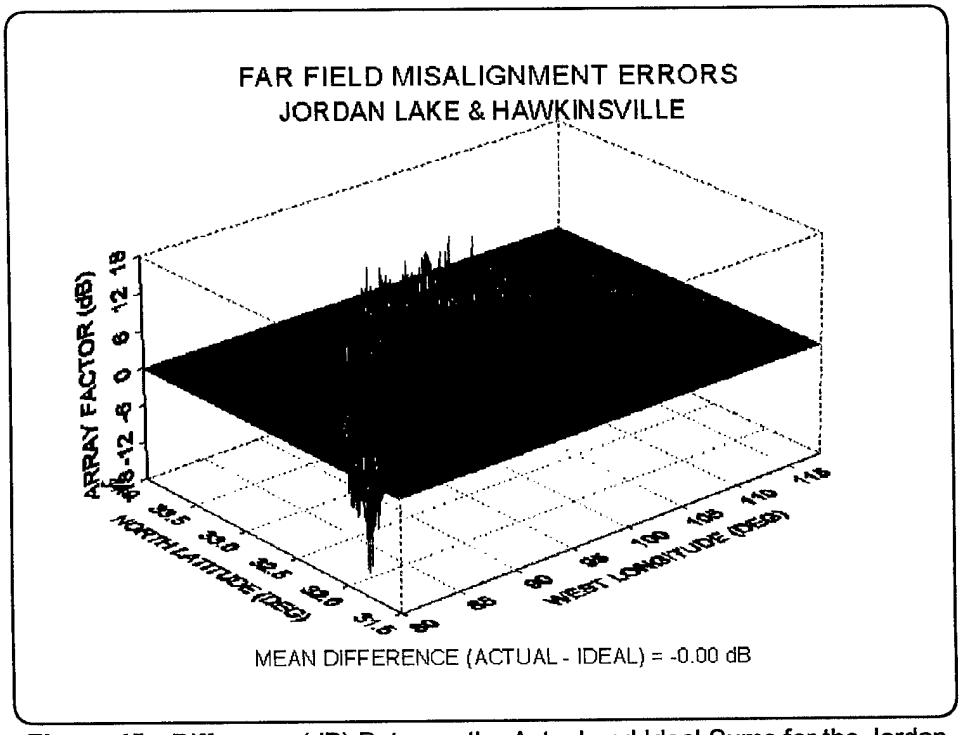

Figure 45—Difference (dB) Between the Actual and Ideal Sums for the Jordan Lake and Hawkinsville Pair

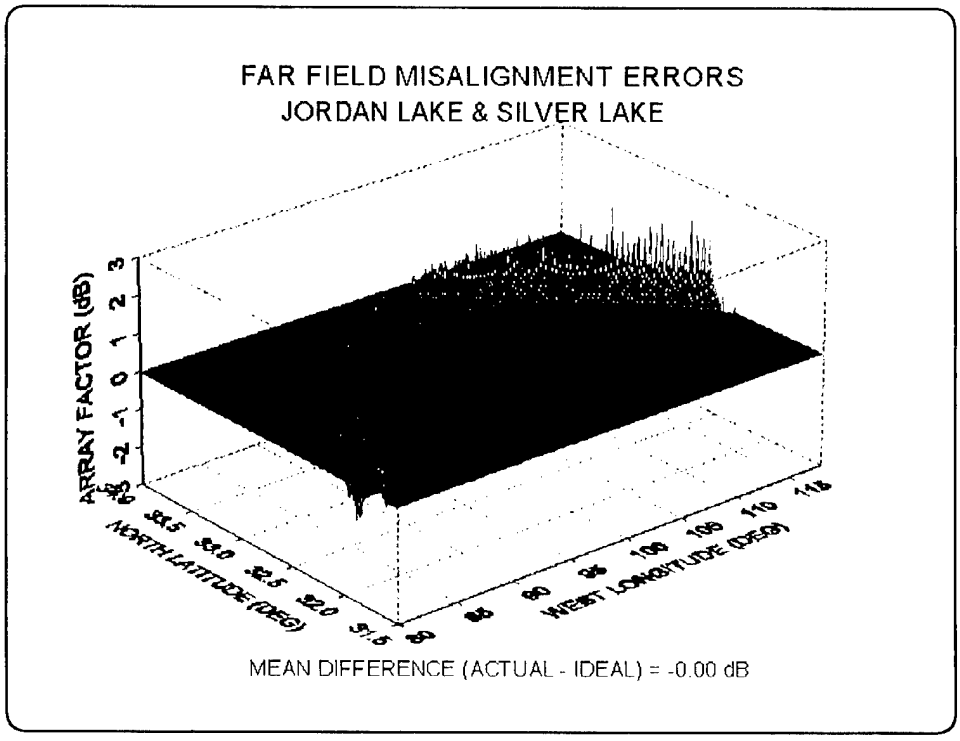

Figure 46—Difference (dB) Between the Actual and Ideal Sums for the Jordan Lake and Silver Lake Pair

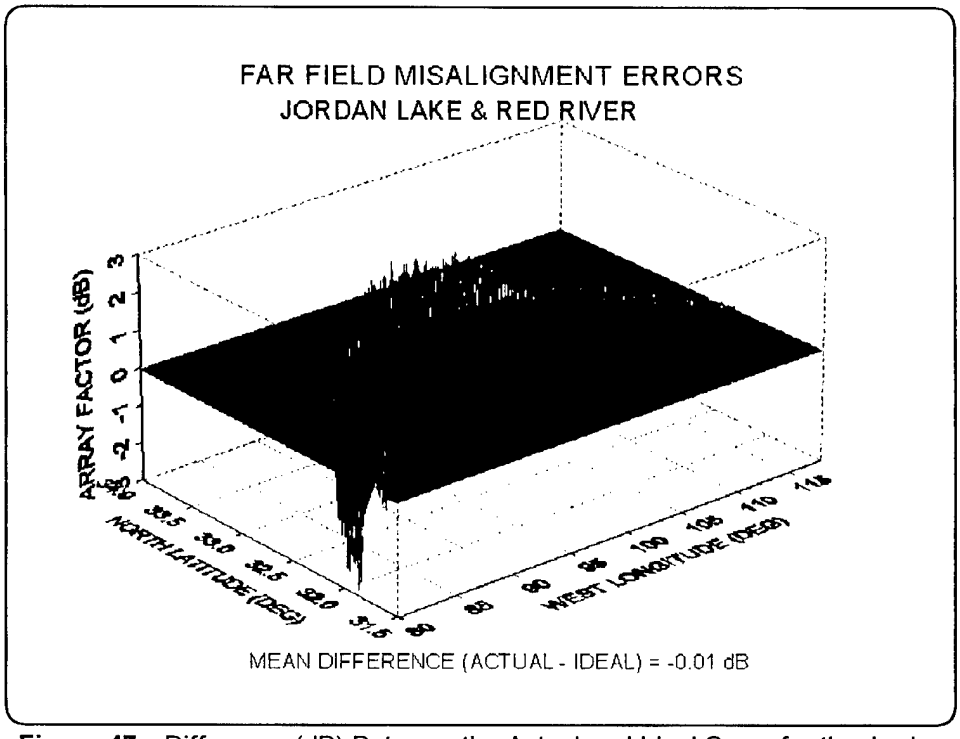

Figure 47—Difference (dB) Between the Actual and Ideal Sums for the Jordan Lake and Red River Pair

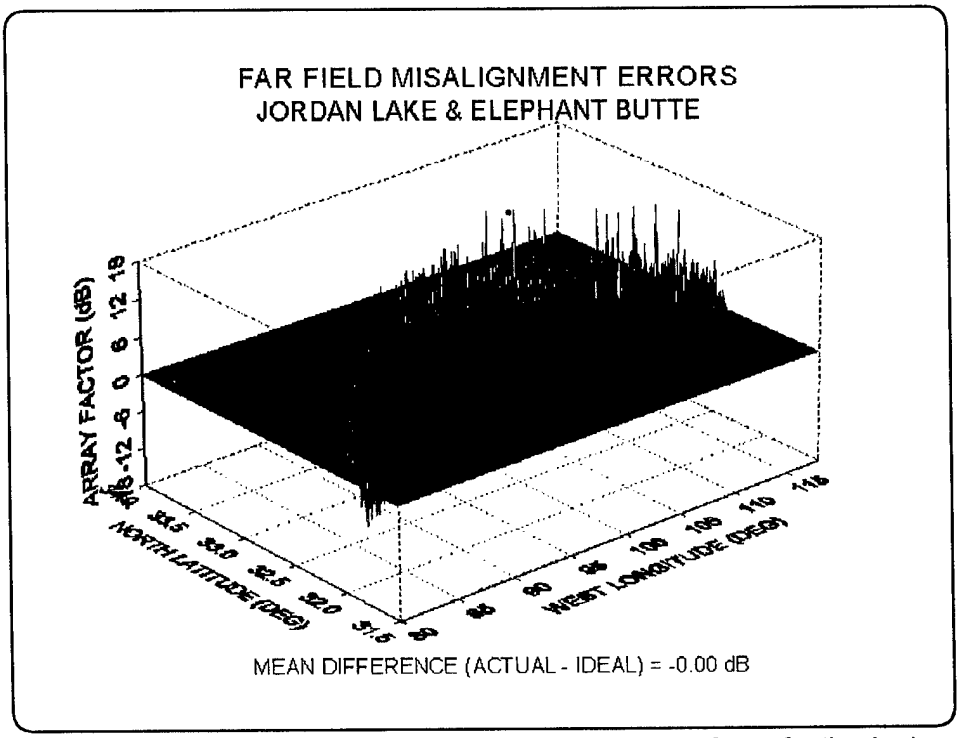

Figure 48—Difference (dB) Between the Actual and Ideal Sums for the Jordan Lake and Elephant Butte Pair

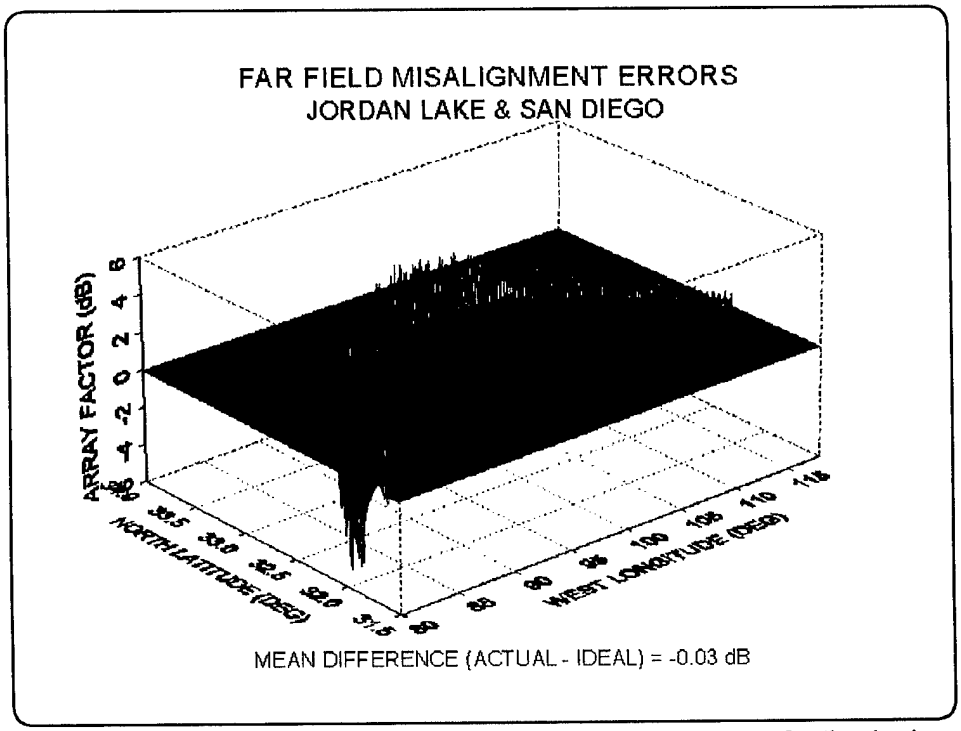

Figure 49—Difference (dB) Between the Actual and Ideal Sums for the Jordan Lake and San Diego Pair

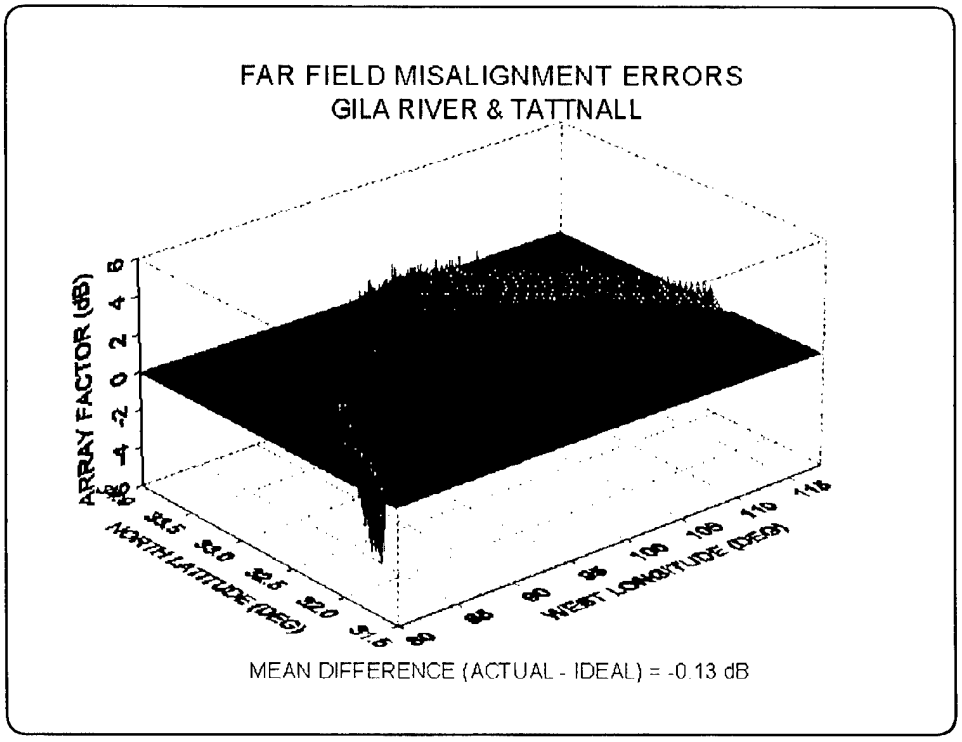

Figure 50—Difference (dB) Between the Actual and Ideal Sums for the Gila River and Tattnall Pair

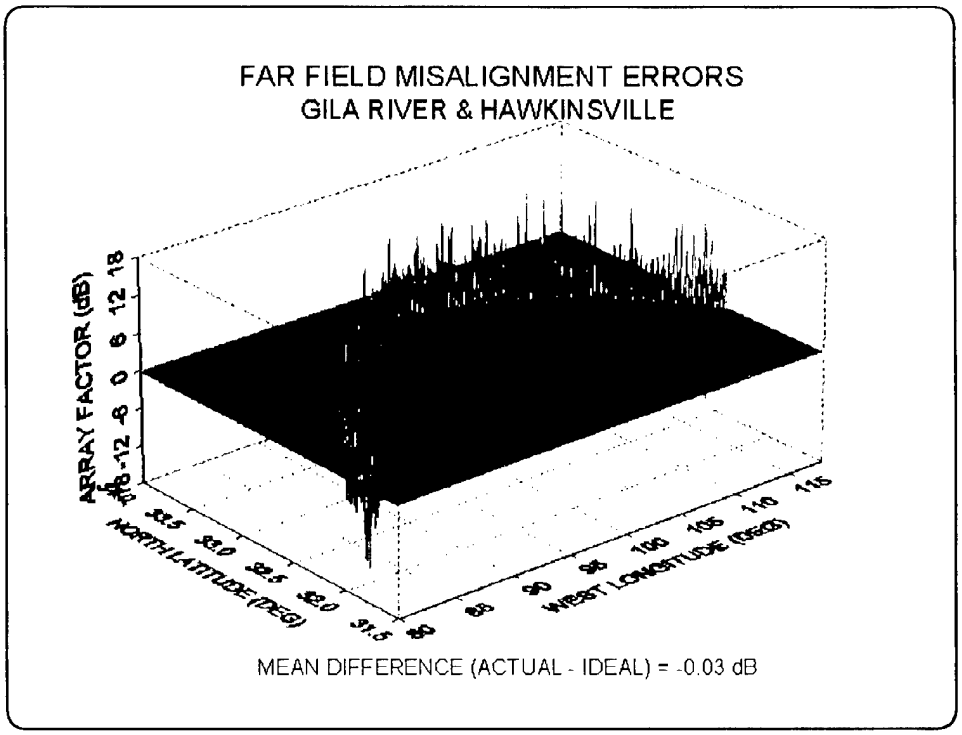

Figure 51—Difference (dB) Between the Actual and Ideal Sums for the Gila River and Hawkinsville Pair

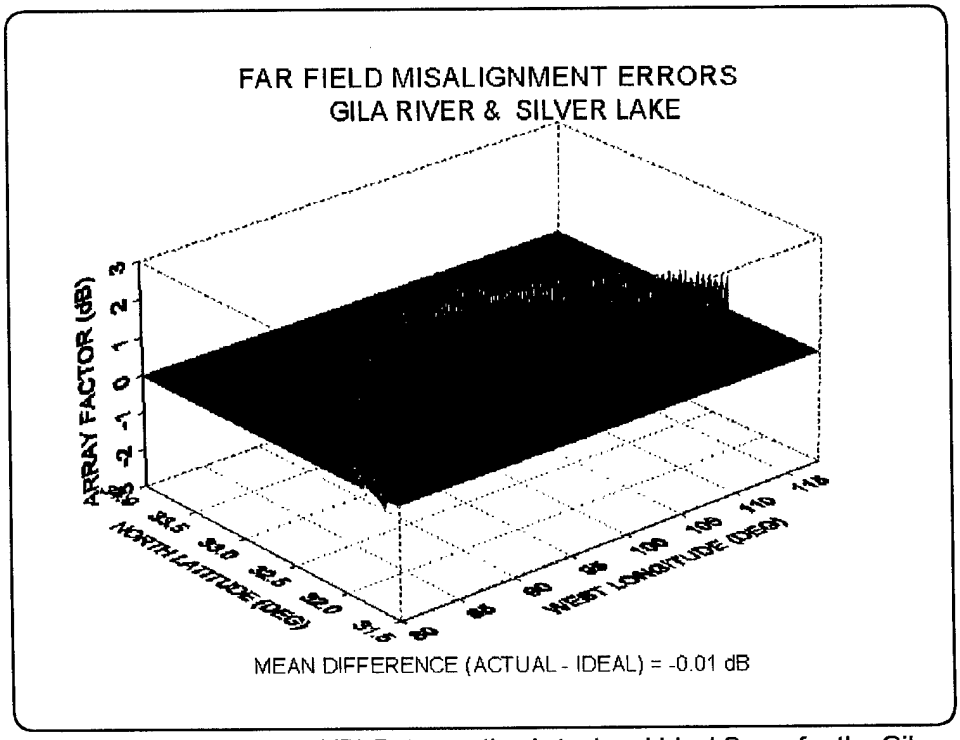

Figure 52—Difference (dB) Between the Actual and Ideal Sums for the Gila River and Silver Lake Pair

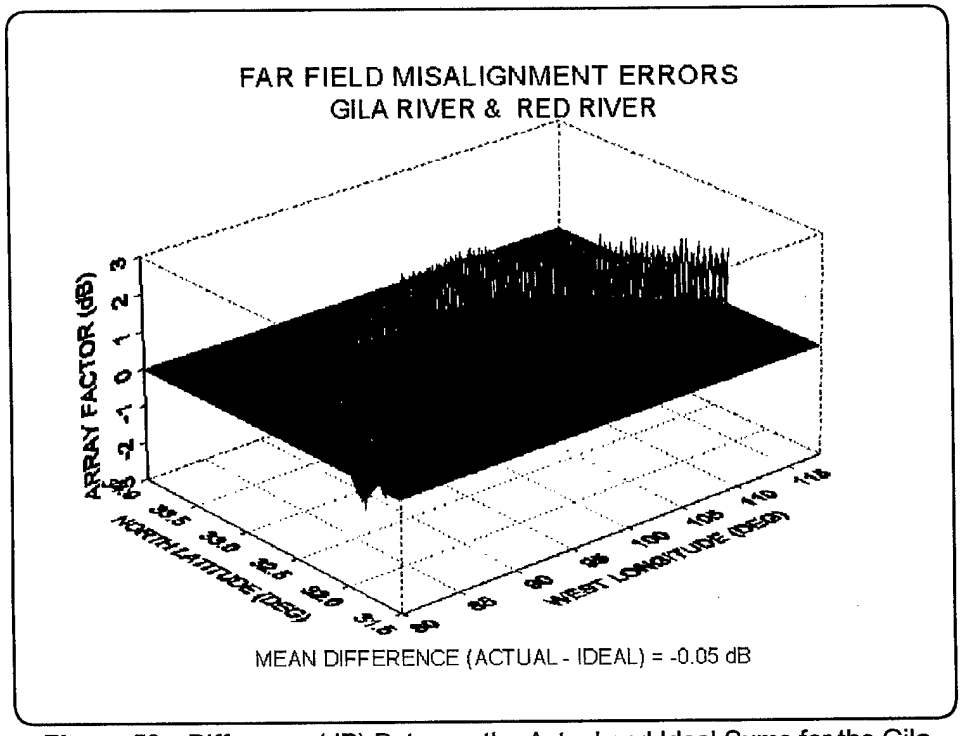

Figure 53—Difference (dB) Between the Actual and Ideal Sums for the Gila River and Red River Pair

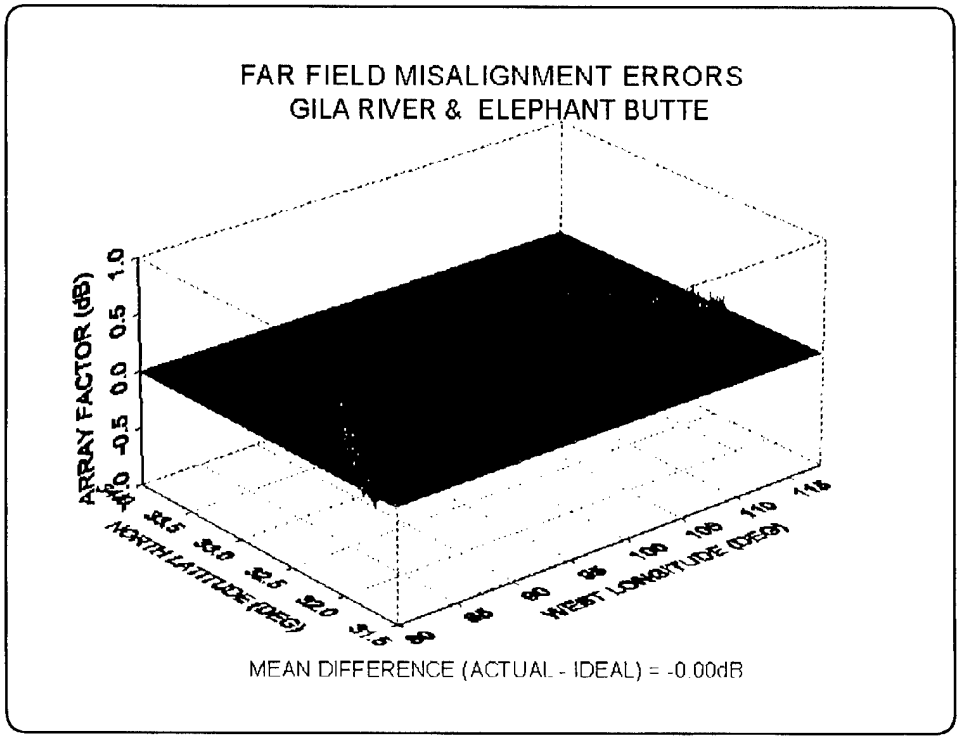

Figure 54—Difference (dB) Between the Actual and Ideal Sums for the Gila River and Elephant Butte Pair

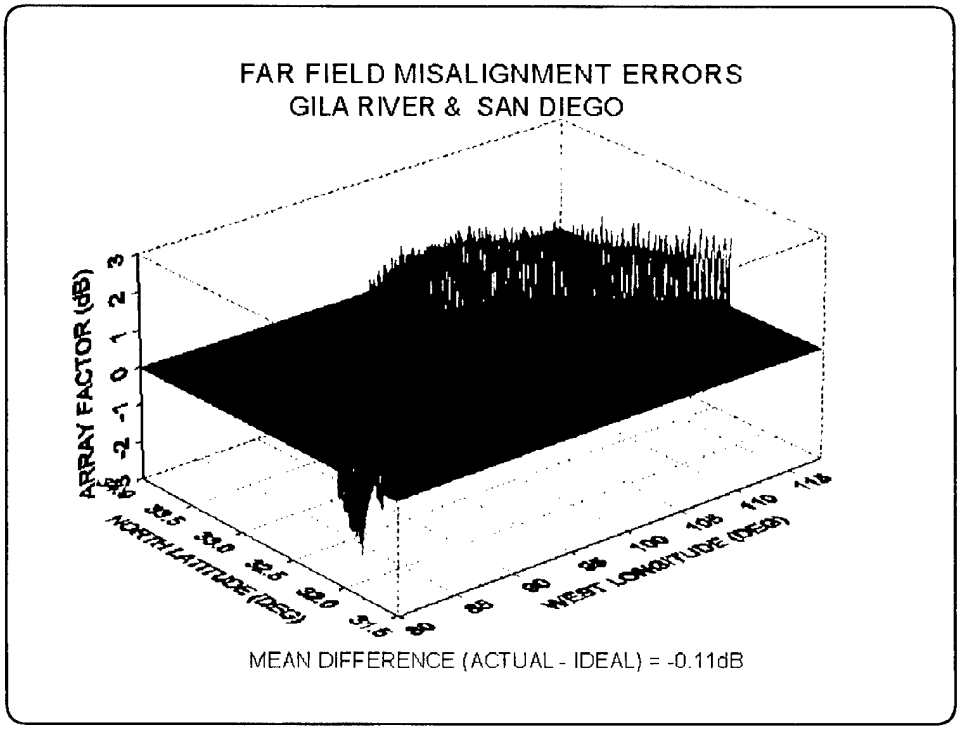

Figure 55—Difference (dB) Between the Actual and Ideal Sums for the Gila River and San Diego Pair

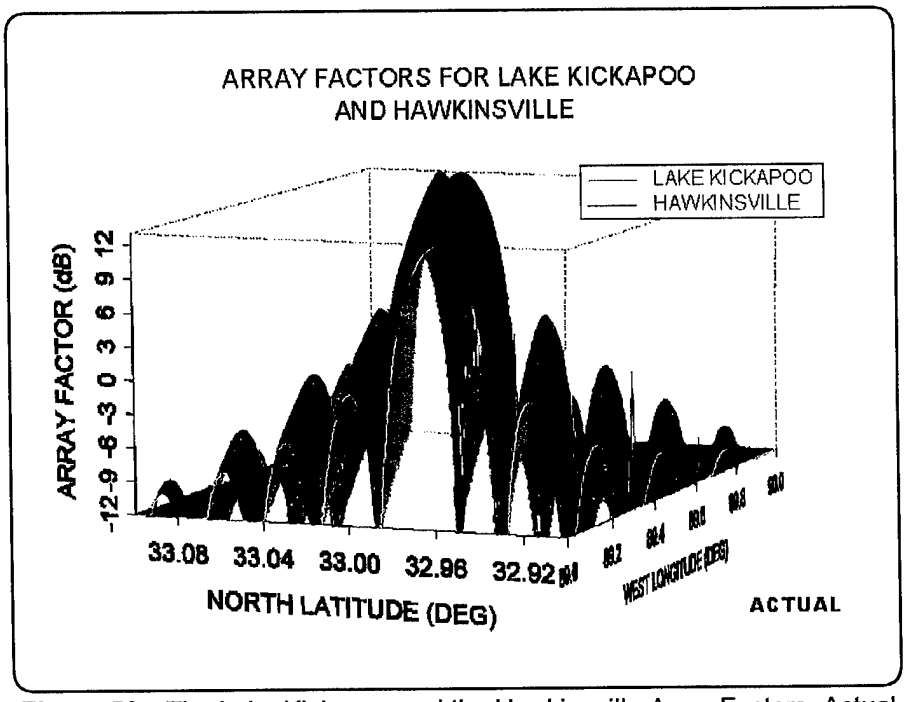

Figure 56—The Lake Kickapoo and the Hawkinsville Array Factors, Actual Alignment

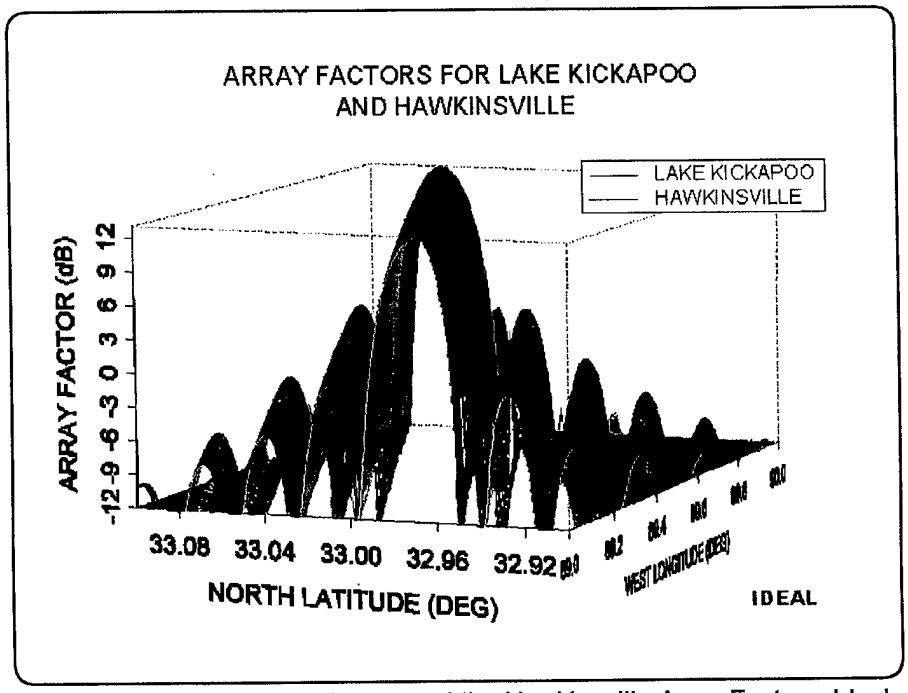

Figure 57—The Lake Kickapoo and the Hawkinsville Array Factors, Ideal Alignment

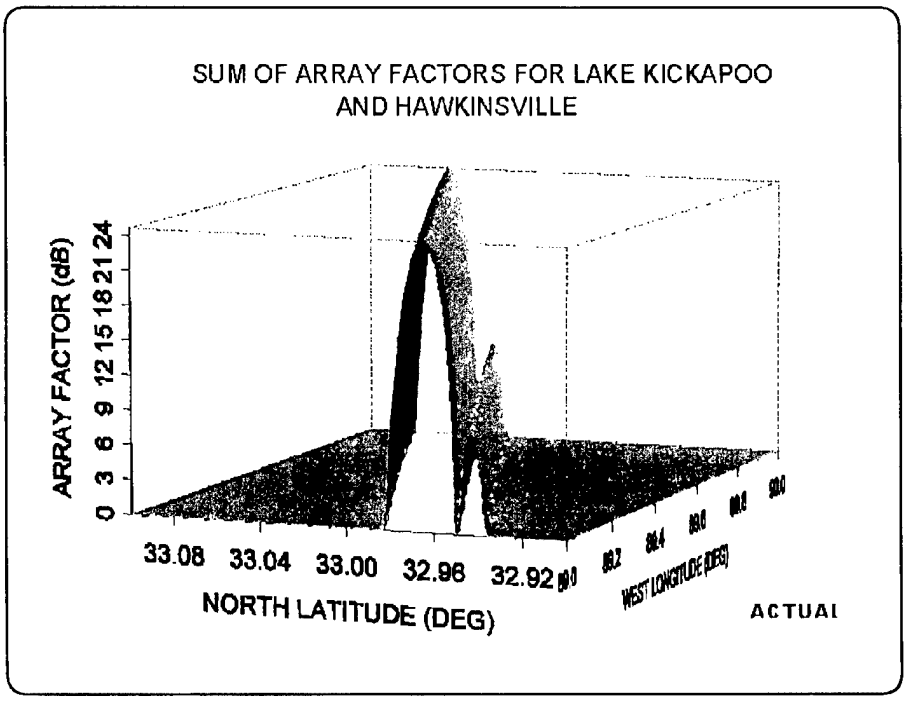

Figure 58—The Product of the Lake Kickapoo and the Hawkinsville Array Factors, Actual Alignment

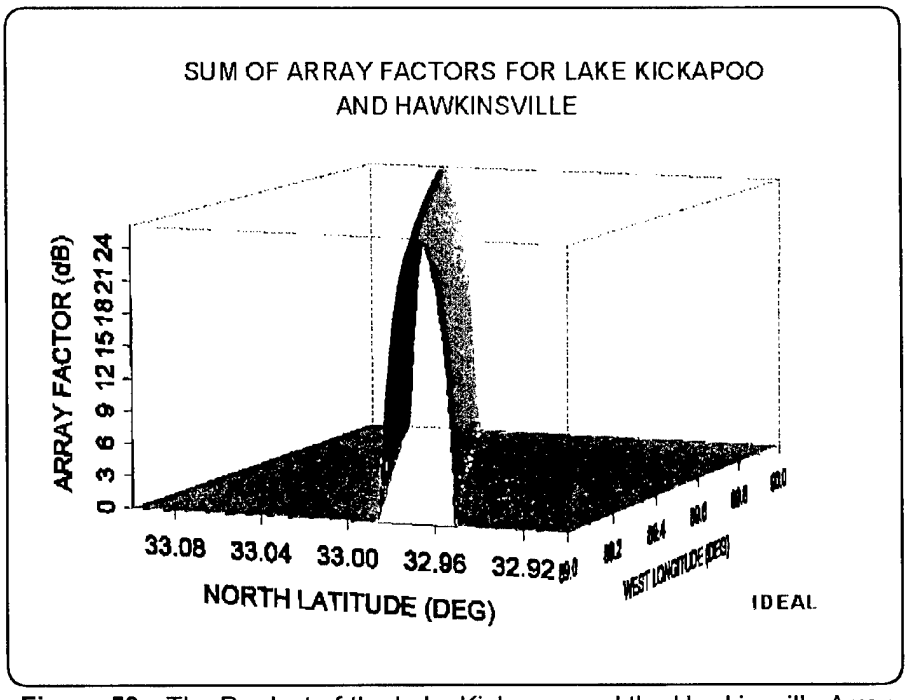

Figure 59—The Product of the Lake Kickapoo and the Hawkinsville Array Factors, Ideal Alignment

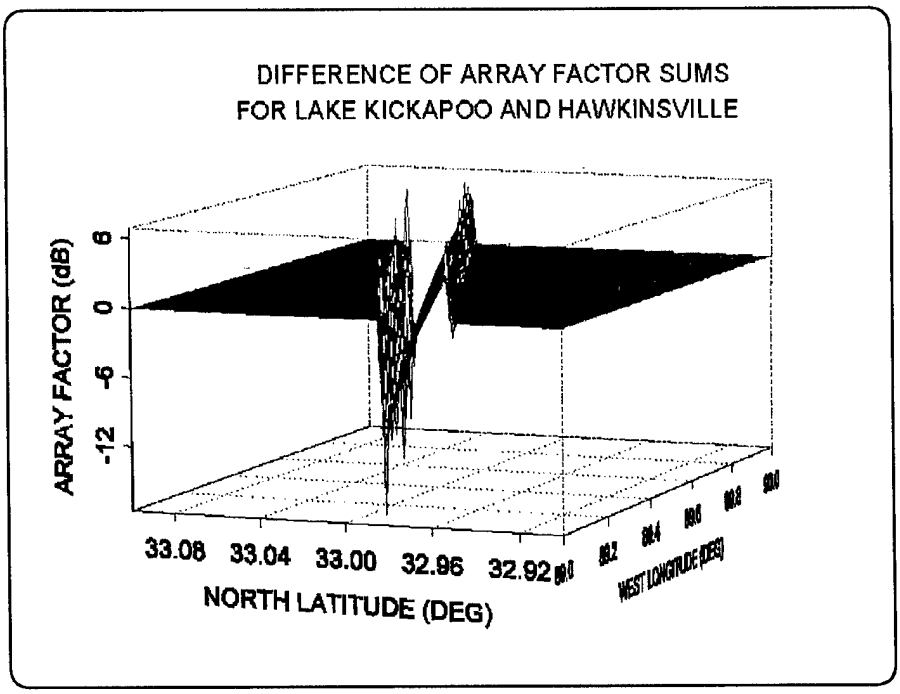

Figure 60—The Ratio of the Lake Kickapoo and the Hawkinsville Actual and Ideal Array Factor Products

4.0 PRODUCT OF THE RECEIVER-TRANSMITTER INTENSITIES AS A MEASURE OF THE ALIGNMENT

In order to examine more completely the effect of a misalignment between and among the arrays at each of the stations that constitute the Naval Space Surveillance radar fence, a detailed computer model of the electromagnetic fields of the arrays was employed. This model yields realistic radiation patterns for the transmitter and receiver elements and arrays, and is applicable to both near- and far-field operation. This model was developed by Dr. Steven Berg, Interferometrics Inc., for the Naval Research Laboratory in 1988[6] to investigate the transmitter performance. The Lorentz Reciprocity Theorem for electromagnetic fields implies that the patterns of the receiver arrays can be obtained by measuring their fields while they act in a transmitting mode[7]. This enables the use of fictitious "receiver fields" to be constructed in conjunction with the actual transmitter fields for a study of the interaction between the two.

For a given radar system, any "true" efficiency measure is properly dependent on the shape, size, and composition of the object illuminated, and viewed by the system via the frequency and angular-dependent scattering cross section. However, this analysis is confined to situations where the objects at hand possess uniform scattering cross sections. A justification for this kind of an approach follows.

If the points in space associated with the origin of the earth—the Tattnall receiver station, the San Diego receiver station, and the point of observation—be denoted as O, T, S, and P, respectively (as shown in Figure 61), then the earth-centered angle $\angle TOS$ can be found by using the identity in Equation (26).

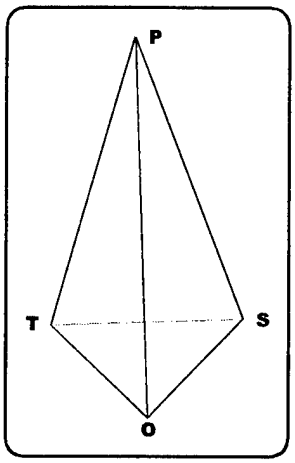

Figure 61—Earth-Centered Extremities of the Fence Sites

$$\angle TOS = \arccos\left(\frac{\vec{T}}{|\vec{T}|} \cdot \frac{\vec{S}}{|\vec{S}|} \right) \tag{26}$$

When Equation (26) is evaluated, the angle is approximately 29.5°. Thus it is clear that the values of the angles ∠TOP and ∠POS for all the points directly above the extremities of the fence are limited to the interval between zero and 29.5°. This, in turn, imposes a constraint on the size of the ∠TPS, which can be seen in Equation (27). This equation computes the angle ∠TPS as the sum of the two smaller angles, ∠TPO and ∠SPO, where the lengths OT, OS, and OP are known.

$$\angle TPS = \arctan\left(\frac{|OT| \sin(\angle TOP)}{|OP| - |OT| \cos(\angle TOP)} \right) + \arctan\left(\frac{|OS| \sin(\angle POS)}{|OP| - |OS| \cos(\angle POS)} \right) \tag{27}$$

Now, letting OT≈OS and making the somewhat rough, small-angle approximation by treating the above sines of angles as the angles' radian measure and the cosines of the above angles as unity, simplifies the expression to that shown as Equation (28). This shows that for the observation points P several radii from the surface of the earth, the ratio of the angles TPS to TOS is approximately inversely proportional to the ratio of the lengths of the segments TP and OT.

$$\angle TPS = \arctan\left(\frac{\angle TOP}{\frac{|OP|}{|OT|} - 1} \right) + \arctan\left(\frac{\angle POS}{\frac{|OP|}{|OT|} - 1} \right) \tag{28}$$

We can see then that the range of ∠TPS is limited to a fraction of the aforementioned 29.5° ∠TOS. For most conventionally shaped objects, the cross section does not vary wildly within such a range of angles. Thus it is expected that the incoherent coupling of the array patterns of a pair of receiver and transmitter sites Λ^2 through a particular object with differential cross section $\Omega(\hat{r}_1, \hat{r}_2)$ is given by the expression in Equation (29).

$$\Lambda^2(x,y,z) \equiv I_1(x,y,z)\, \Omega^2(\hat{r}_1, \hat{r}_2)\, I_2(x,y,z) \tag{29}$$

The argument {x, y, z} represents the coordinates of the point at which the coupling is considered, I_1, I_2 are the respective intensities of the receiver and transmitter fields, and $(\hat{r}_1, \hat{r}_2)$ are the unit vectors in the direction from the phase centers of the chosen receiver and transmitter sites to the "observation" point.

Since the coupling in question is of interest only up to an overall constant, and bearing in mind the aforementioned mild variation of the scattering cross section, the characteristics of the scatter at P will be assumed to be uniform. Equation (29) is then simplified to be the product of the receiver and transmitter site intensities, as shown in Equation (30), rather than that of the coupling Λ^2 itself.

$$\tilde{\Lambda}^2_{1,2}(x,y,z) \equiv I_1(x,y,z)\, I_2(x,y,z) \tag{30}$$

Furthermore, due to the fact that all the antenna dipoles for the transmitter sites on one hand and for the receiver sites on the other are similar, it makes sense for this study to consider combined couplings of the fields of the different receivers with the different transmitters. This is expressed in Equation (31) as the sum over all combinations of transmitter and receiver sites. The subscripts (i, j) represent the transmitter and receiver site indices, respectively.

$$\bar{\Lambda}^2(x,y,z) \equiv \sum_{\forall i,j} \tilde{\Lambda}^2_{i,j}(x,y,z) \tag{31}$$

One can substitute into Equation (31) the expression, Equation (30), to obtain the expanded form shown in Equation (32). Both Equations (30) and (32) will be used for the alignment study.

$$\bar{\Lambda}^2(x,y,z) \equiv \sum_{\forall i} I_i(x,y,z) \sum_{\forall j} I_j(x,y,z) \tag{32}$$

4.1 Realistic Fence Transmitter and Receiver Field Equations

The formalism appearing below is a condensed version of the one contained in the 1988 report by Berg cited earlier. Neglecting the mutual impedance of the antenna monopoles for both the receiver and transmitter antennas, and assuming that the antenna dipoles lie in the x-z plane, the following "free" space far-electrical-field expression can be derived for spherical coordinates for both the receiver and transmitter antenna elements.

$$\boldsymbol{E}(r,\theta,\phi) = \epsilon(r,\theta,\phi) \equiv$$

$$E_0 \frac{e^{-ikr}}{r} \frac{e^{-i\frac{\pi}{2}(\sin\delta\cos\theta + \cos\delta\sin\theta\cos\phi)} + i(\sin\delta\cos\theta + \cos\delta\sin\theta\cos\phi)}{1 - (\sin\delta\cos\theta + \cos\delta\sin\theta\cos\phi)^2} \times$$

$$[(\sin\delta\cos\theta + \cos\delta\sin\theta\cos\phi)\,\hat{\boldsymbol{\Theta}} + \cos\delta\sin\phi\,\hat{\boldsymbol{\Phi}}] + \tag{33}$$

$$E_0 \frac{e^{-ikr}}{r} \frac{e^{-i\frac{\pi}{2}(\sin\delta\cos\theta - \cos\delta\sin\theta\cos\phi)} + i(\sin\delta\cos\theta - \cos\delta\sin\theta\cos\phi)}{1 - (\sin\delta\cos\theta - \cos\delta\sin\theta\cos\phi)^2} \times$$

$$[-(\sin\delta\cos\theta - \cos\delta\sin\theta\cos\phi)\,\hat{\boldsymbol{\Theta}} + \cos\delta\sin\phi\,\hat{\boldsymbol{\Phi}}]$$

In Equation (33) above, the δ is the "droop" angle (55° for the transmitters and 0° for the receivers), and the unit vectors $\hat{\Theta}$ and $\hat{\Phi}$ are in the spherical coordinate directions Θ and Φ, respectively.

The field pattern of the receiver element placed over the finite ground screen was calculated using the perfect image approximation that is based on the unrealistic assumption that the underlying screen is infinite in its extent, that it is a perfect conductor, and that it has no reactance. Given the geometry of the receiver array—namely, that the element's monopoles are parallel to the axis of the receiver array as a whole—such approximation is more reasonable than it would be for the transmitter arrays whose element monopoles are orthogonal to the axis, albeit they are drooped. Placing the 180° out-of-phase image source at an equal distance below the conducting screen results in the field pattern expressed in Equation (34), where $\epsilon(r, \theta, \phi)$ was defined in Equation (33), and $\epsilon^*(r, \theta, \phi)$ is its complex conjugate.

$$\boldsymbol{E}(r, \theta, \phi) = \epsilon(r, \theta, \phi) - e^{-i\frac{3\pi}{2}\cos\theta}\epsilon^*(r, \theta, \phi) \tag{34}$$

Taking accurate account of the finite extent of the ground screen calls for a more elaborate treatment of the problem at hand. The imposition of the scattering boundary conditions along the surface of the ground screen leads in a natural way to an implicit expression for the scattered field, which in combination with the antenna element's own field, provides the total field in the observation region. A common method to satisfy the boundary conditions for these types of problems is through the introduction of the induced current, which generates an electromagnetic field that properly balances the incoming scattering field. For a single wire, this approach leads to a one-dimensional integral equation.

The aforementioned integral equation is equivalent to an infinite number of boundary conditions—one for each point on the conducting interface. The numerical handling of such problems normally requires some sort of a discretization. One such method has to do with the replacement of the current distribution with its approximate representation in the basis of a finite number of suitably chosen piecewise sinusoids. If the sinusoids are weighted in a manner that reduces the average errors due to the discretization over each of the discrete segments, and the weighting function themselves are chosen to be proportional to the same piecewise sinusoids, the determination of the weighting constants of proportionality is referred to as the Galerkin Method.

This approach was used to obtain the free-space expression for the field of a single element of the transmitters over the conducting ground screen. This expression is reproduced as Equation (35), where r_1 and r_2 are the distances from the first and second end points of the dipole to the observation point.

Equations (34) and (35) are the primary equations used for the computation of the electrical fields due to the receiver and transmitter antenna elements over the ground screen. The actual fields of the transmitters and receivers of the space surveillance system are then obtained by the superposition of these elemental fields.

$$
\begin{aligned}
\mathbf{E}(r,\theta,\phi) = {} & E_0\left[\frac{\pi}{2kr}\left(\frac{e^{-ikr_2}}{r_2} - \frac{e^{-ikr_1}}{r_1}\right)\right]\hat{\boldsymbol{r}} - \\
& E_0\left[\frac{e^{-ikr}}{r}\,2i\,(\sin^2\delta - \cos^2\delta\cos^2\phi)\right] + \\
& E_0\left[\frac{e^{-ikr_1}}{r_1} - \frac{e^{-ikr_2}}{r_2}\right]\left[\sin\delta\cos\theta + \frac{\pi}{2kr}\sin\theta\cos\theta(\sin^2\delta - \cos^2\delta\cos^2\phi)\right] - \\
& E_0\left[\frac{e^{-ikr_1}}{r_1} - \frac{e^{-ikr_2}}{r_2}\right]\left[\cos\delta\cos\theta\cos\phi + \frac{\pi}{2kr}\sin\delta\cos\delta\cos\phi(\sin^2\theta - \cos^2\theta)\right] \times \\
& \left[1 - (\sin\delta\cos\theta - \cos\delta\sin\theta\cos\phi)^2\right]^{-1}\hat{\boldsymbol{\theta}} - \\
& E_0\left\{\frac{e^{ikr}}{r}\,2i\cos\delta\sin\theta\cos\phi - \left[\frac{e^{-ikr_1}}{r_1} + \frac{e^{-ikr_2}}{r_2}\right]\left[1 + \frac{\pi}{2kr}\sin\delta\cos\theta\right]\right\}\cos\delta\sin\phi \times \\
& \left[1 - (\sin\delta\cos\theta - \cos\delta\sin\theta\cos\phi)^2\right]^{-1}\hat{\boldsymbol{\Phi}}
\end{aligned}
\tag{35}
$$

4.2 Fence-Field Computations

The field for each of the arrays is computed with respect to the spherical coordinate system associated with the phase center of the array. The local reference frame has the z-axis aligned with the arrays and points in the southerly direction. This is at odds with the WGS84 global geodetic system and requires a that transformation has to be constructed to apply the model.

The transformation has to take a given point specified in the WGS84 geodetic system and convert it to the equivalent coordinates in the local (associated with a given array) spherical coordinate system. The transformation requires a translation and rotation of the coordinate axes.

4.3 Results from the Model

A number of runs of the new code were performed over two-dimensional geodetic regions parallel to the surface of the earth for several different heights. Not only were the individual fields of the different arrays of interest, but as mentioned earlier, the products of such patterns as well. The latter represent the overlap between the fields of the different transmitters and receivers. Figures 62 through 74 show a number of examples of such computations for the heights of 5000 km and 20,000 km over the surface of the earth. All computations were performed on a geodetic grid of constant height over the surface of the earth. Figures 62 and 63 represent plots of power due to Tattnall and Elephant Butte receiver stations, correspondingly. The geodetic computational domain in both cases is between 98° and 108° West longitude, between 33° and 34° North latitude, and at an ellipsoid height of 5000 km. It is easy to see that the field due to the Tattnall site is significantly more spread in the North-South direction than that due to the Elephant Butte site. This has to do with the fact that while both sites have antennas made of the same type elements, the overall lengths of the antenna arrays

employed in the latter case are greater. This leads to the well-known result that longer arrays produce tighter fields. The main lobes in both cases are the most prominent features on the plots. Because most of the distance separation between the observation points and the arrays comes from the vertical separation of 5000 km here, no prominent variation in the shapes and sizes of the lobes with longitude is observed here.

Figures 64 and 65 contain plots of the fields due to the Jordan Lake and Kickapoo complex transmitter arrays. The computational domain is the same as above. Again, the much longer Kickapoo complex array produced a significantly narrower main beam than the Jordan Lake array. Incidentally, the craggy appearance of the crest on the plot of the Kickapoo field intensity is just an artifact of the insufficiently dense computational grid. Given the state of computer technology at this writing, a tradeoff had to be made between grid density and the time needed to complete the computations. For example, the Kickapoo calculations take a couple of days computer time to finish. Given the facts that the undersampling effect is neither very significant here nor is it very important for our study, we elected not to pursue a higher computational resolution.

Although in our work the RMS currents driving the receiver and transmitter elements were arbitrary, they were the same for all the receiver elements on one hand, and for the transmitter elements on the other. Therefore, the relative magnitudes of fields attributable to the different receiver or transmitter arrays are strongly dependent on the relative numbers of the antenna elements they possess. This is in accord with what we see on Figures 64 and 65, where the Kickapoo field amplitude is significantly higher than that of the Jordan Lake transmitter. Figure 66 contains a plot of the combined product intensities in accordance with Equation (32) above. The results had been scaled by a small factor to reduce the size of the numbers appearing on the plot. The computational domain is the same as the one listed at the beginning of this section. We can see that the shape of this plot is almost indistinguishable from that of the intensity of the Kickapoo complex alone. There are two obvious reasons for that: a) the intensity products with the participation of the Kickapoo transmitter array dominate those with the participation of the Gila River and Jordan Lake transmitters; b) the field intensity spatial distributions are so much wider for the low-altitude receiver stations than that of the Kickapoo array that the former can be simply viewed as windowing functions upon the latter, allowing all its features to come through.

The second set of examples deals with the field computations for a geodetic domain, all of whose points lie at the height of 20,000 km. The sequence of Figures 67 through 70 are exactly the same as that for the above Figures 62 through 65. The comments are basically the same too. We can notice, however, that the intensities have dropped considerably compared to those corresponding to the near-field, 5000-km cases. Figures 70 through 72 provide a further example of the dominance of the Kickapoo site compared to the other two transmitter sites.

Figure 73 illustrates the alignment of the fields of the Kickapoo transmitter and of Jordan Lake transmitter. The intensities of both fields had been premultiplied by factors that make their corresponding crests comparable in size. We can see that the fields are, in fact, aligned quite nicely, with the narrower Kickapoo main beam being wholly hidden within the Jordan Lake beam. Similarly, Figure 74 shows that the "field" of the San Diego receiver site is well aligned with that of the Kickapoo field.

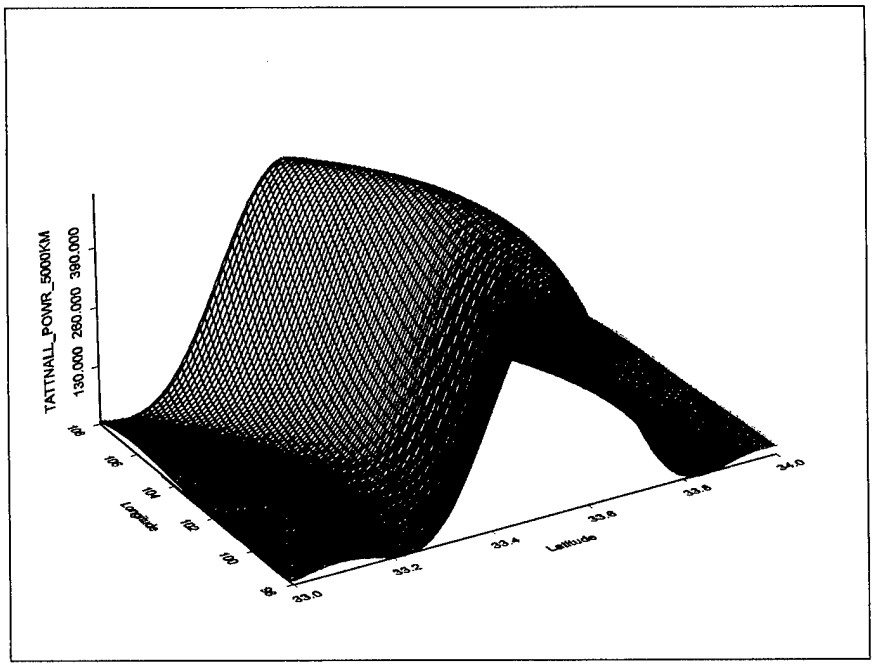

Figure 62—"Field" Intensity of the Tattnall Receiver Station at the Height of 5000 km

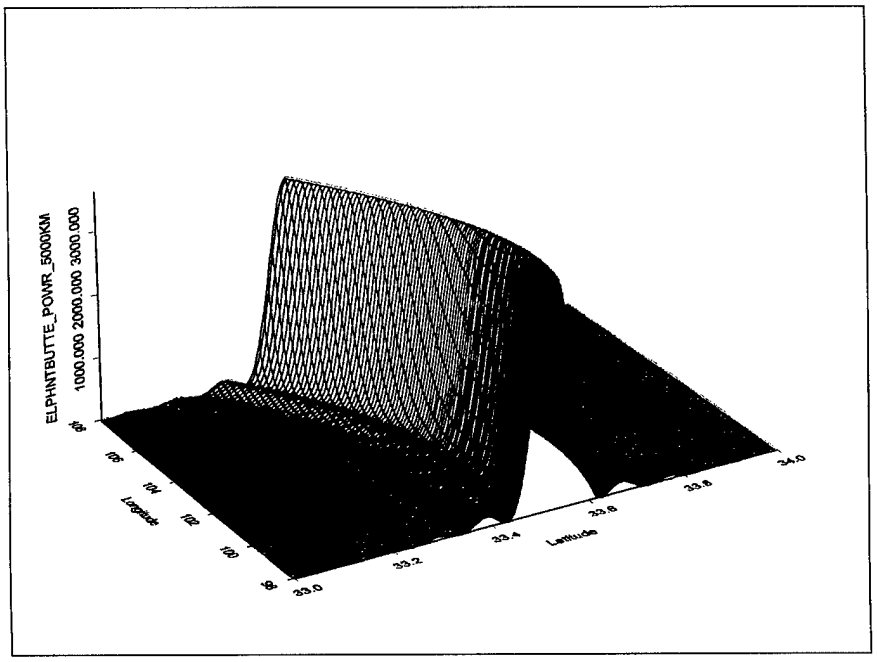

Figure 63—"Field" Intensity of the Elephant Butte Receiver Station at the Height of 5000 km

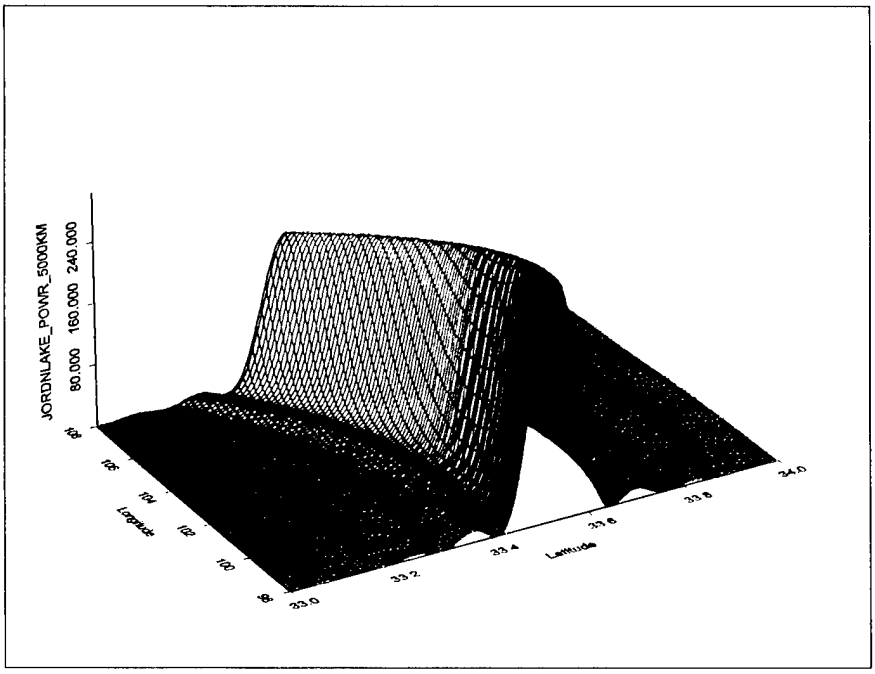

Figure 64—"Field" Intensity of the Jordan Lake Transmitter Station at the Height of 5000 km

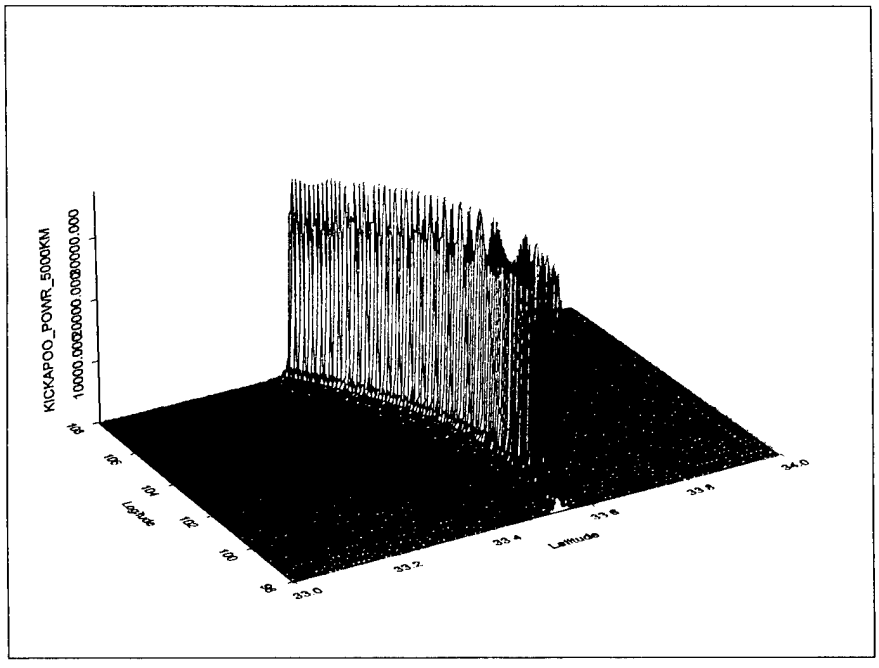

Figure 65—"Field" Intensity of the Kickapoo Complex at the Height of 5000 km

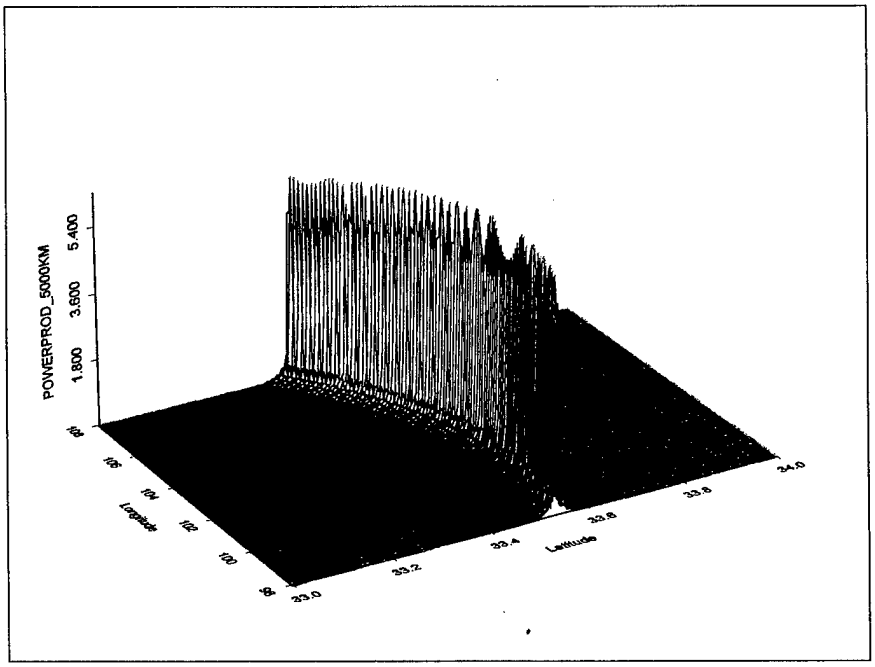

Figure 66—Combined Product Intensities in Accordance with Equation (32) at the Height of 5000 km

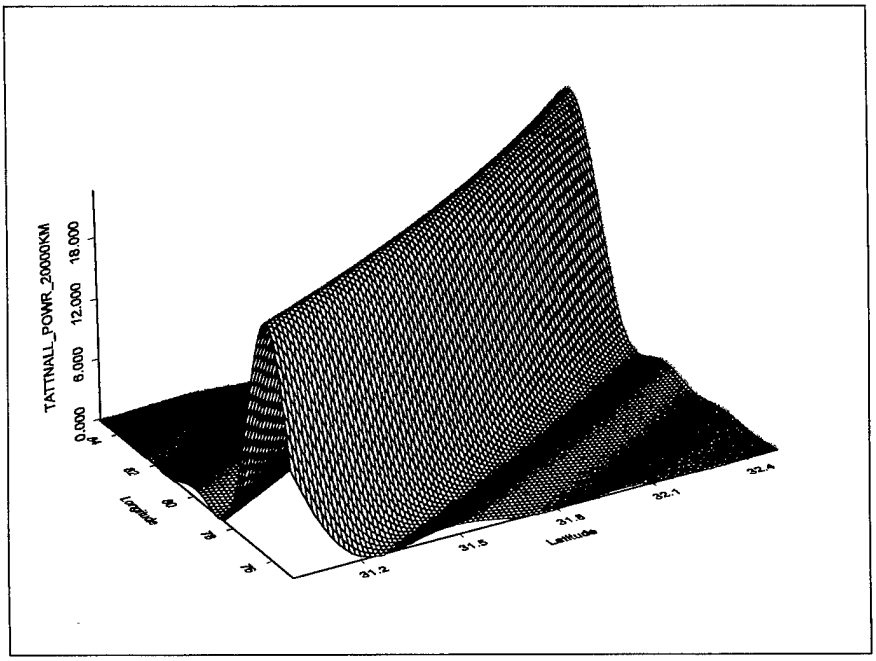

Figure 67—"Field" Intensity of the Tattnall Receiver Station at the Height of 20,000 km

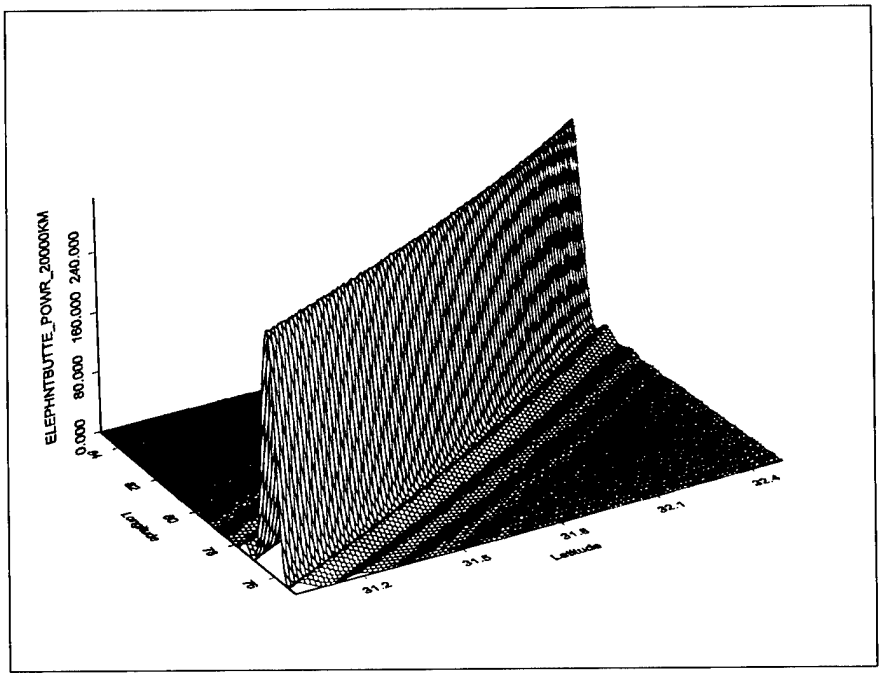

Figure 68—"Field" Intensity of the Elephant Butte Receiver Station at the Height of 20,000 km

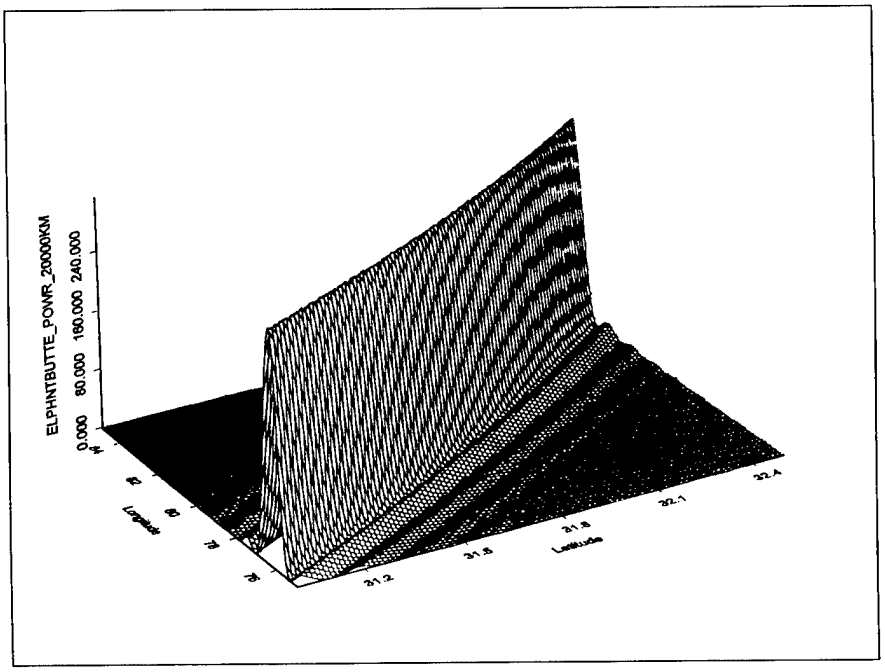

Figure 69—"Field" Intensity of the Jordan Lake Transmitter Station at the Height of 20,000 km

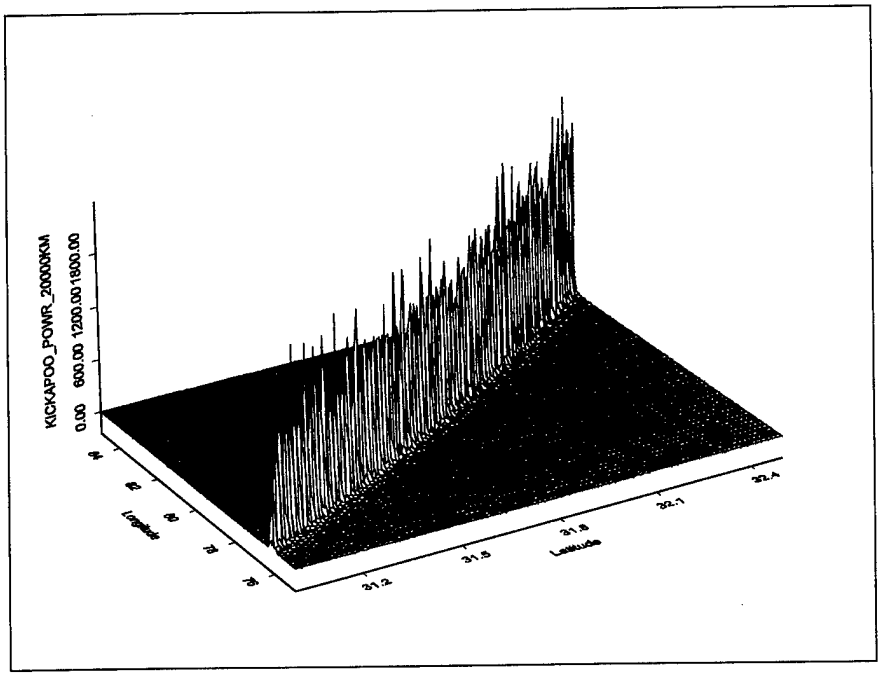

Figure 70—"Field" Intensity of the Kickapoo Complex at the Height of 20,000 km

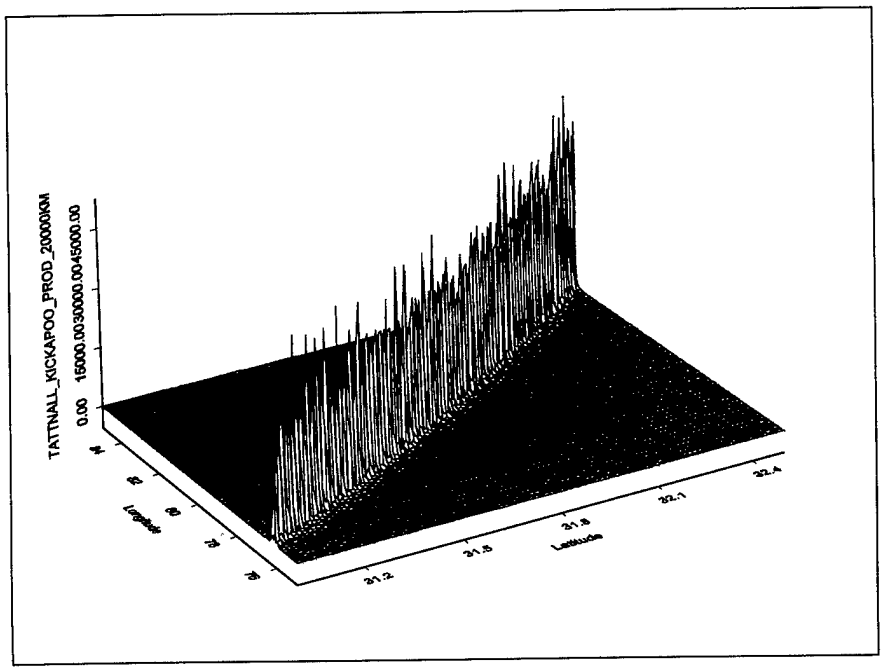

Figure 71—Product of the Intensities of the Kickapoo Complex and Tattnall Receiver Stations

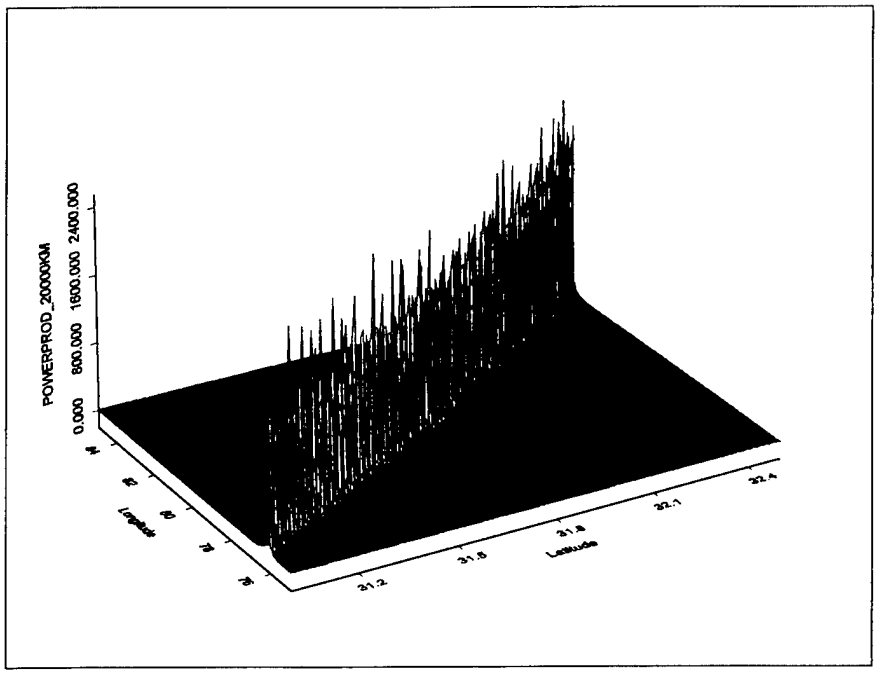

Figure 72—Combined Products of the Receiver and Transmitter Intensities

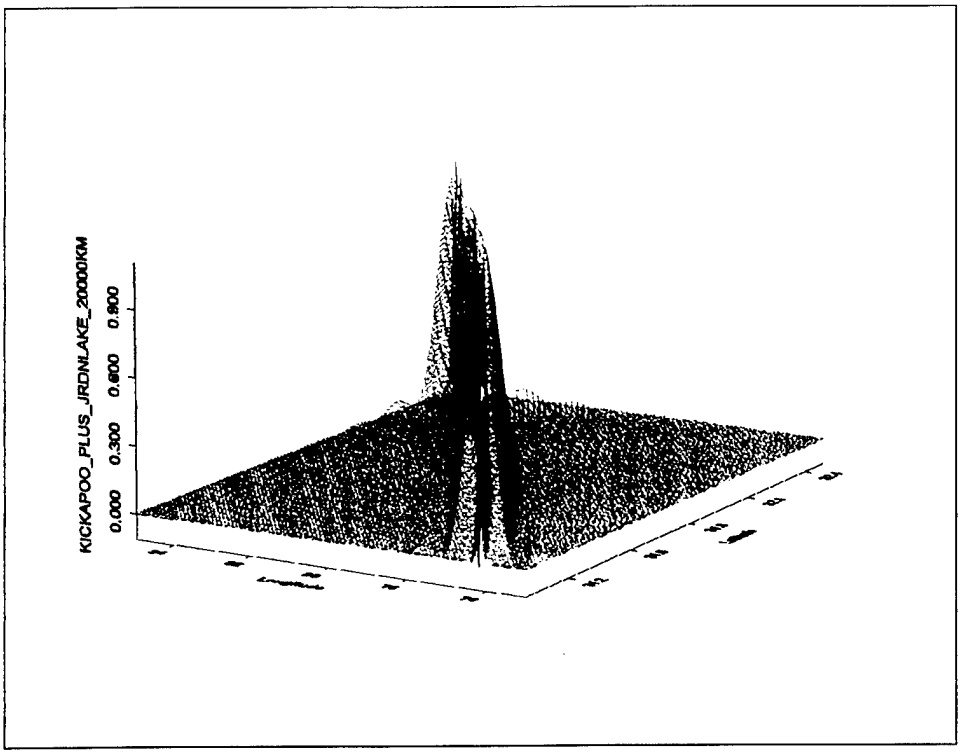

Figure 73—Jordan Lake (blue) and Lake Kickapoo (red)

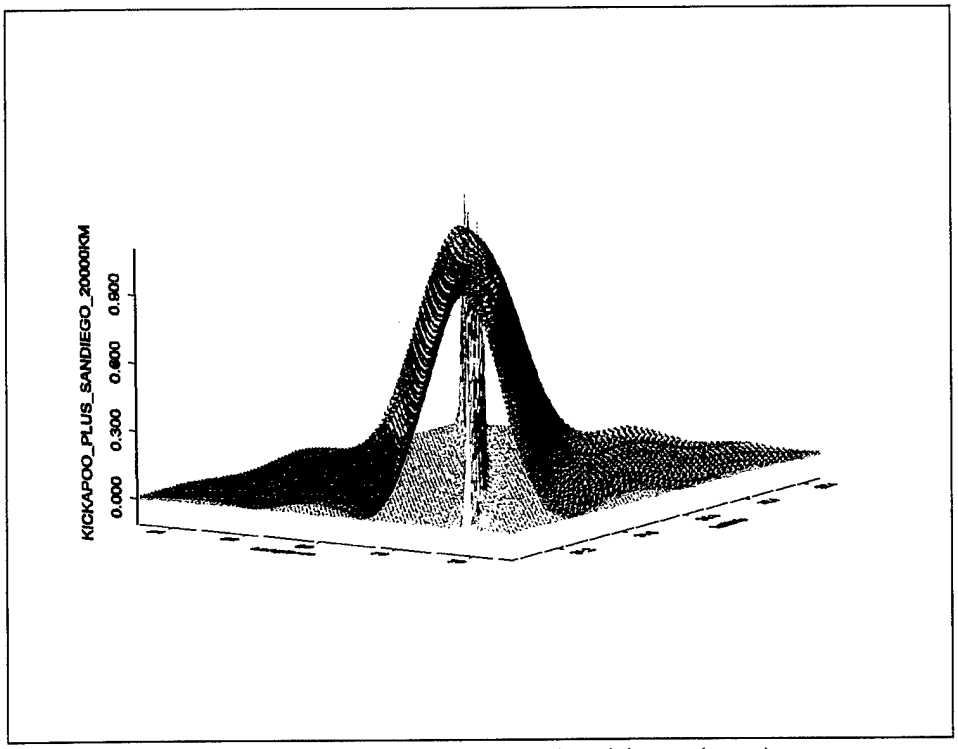

Figure 74—Tattnall (red) and Lake Kickapoo (green)

5.0 SUMMARY AND CONCLUSIONS

The goal of this report was to analyze the geometrical alignment of the existing Naval Space Surveillance Radar Fence. Secondary goals were to compute the parameters of a mean plane (which contains the mean great circle) that best fit the locations of the existing sites, compute the errors of each site from a mean plane, and investigate the effect of the alignment errors on performance. The methods used to reach these goals are described in the body of this report, along with several examples that illustrate the results. The choice of a mean plane was found to be subjective and may be based on many criteria. A couple of different examples were used in the report to illustrate the offsets of the sites from mean planes. Since the computer programs that were used to perform the analysis are part of the deliverables, the user may choose his own criteria to compute a mean plane at a future date. A description and a user's guide to these programs are included in Appendix A. A program description of the near-field model is presented in Appendix B.

The only significant misalignment of the sites from a mean plane was found to be due to a lateral offset rather than orientation. This offset causes the narrow dimension of the array factors to be displaced relative to each other. The displacement may be enough to cause a spatial overlap error between pairs of sites so that the volume of space illuminated by the transmitter does not completely intersect that captured by the receiver. This effect is most important with the site pairs having the longest arrays and narrowest array factors. The offset of the high-altitude receiver site at Hawkinsville relative to Lake Kickapoo was found to result in the largest mean loss of about 5 dB in the far field. The other site pairs resulted in losses of less than 1 dB. With this one exception, the overall alignment of the system was found to be quite good and sufficient for its intended mission.

The near-field results presented indicate that the current FENCE is aligned well as far as the overlap between the patterns of the constituent receiver and transmitter sites are concerned. The techniques employed by the authors are quite general. They could prove useful in any future studies regarding potential augmentations of the Space Surveillance System with new arrays in the same frequency band, or the creation of a new system with altogether different operational frequencies.

6.0 ACKNOWLEDGMENTS

The authors wish to thank the Naval Space Command for their support during this project. They also express their gratitude to Dr. Steven L. Berg, who generously provided a copy of his array-modeling computer code and helped with his time and effort to get the code incorporated into the current task.

7.0 REFERENCES

1. White, Haschal L.; Decker, B. Louis; and Kumar, Muneendra, "World Geodetic System 1984, A Modern and Accurate Global Reference Frame," *Proceedings of the 5th International Geodetic Symposium on Satellite Positioning*, Las Cruces, New Mexico, March 1989.

2. -----, *Space Surveillance Sensor Navy Fence*, Naval Space Command publication, Dahlgren, Virginia.

3. -----, Untitled Report containing descriptions and geodetic coordinates of selected monuments at each of the Naval Space Surveillance Field Stations, Defense Mapping Agency, Aerospace Center, St. Louis, Missouri, January 1993.

4. Kraus, John D., *Radio Astronomy*, McGraw-Hill Book Company, 1966, p. 164.

5. -----, *Space Surveillance Sensor Navy Fence*, Naval Space Command publication, Dahlgren, Virginia.

6. Berg, Steven L., *Theoretical Radiation Patterns of NAVSPASUR Transmitter Antennas*, Interferometrics Inc., Report, 30 November 1988.

7. Stutzman, Warren L. and Thiele, Gary A., *Antenna Theory And Design*, John Wiley & Sons, 1981, pp. 40-44.

APPENDIX A
PROGRAM DESCRIPTIONS

This appendix includes program descriptions and user guides for the following tasks:

1. Find an average plane given points and lines
2. Find the latitude of a point on a mean plane given its longitude and height
3. Find the look angles from an observer to a point in space
4. Compute the array factor using the look angles and a linear array model

All programs are run from the command line or the command line window in Windows. These programs were developed in C with a 16-bit compiler under Microsoft Windows NT 4.0™.

A.1 The Average Plane Program

The Average Plane Program uses least squares to compute the three direction cosines that define a plane. The direction cosines of the plane are the direction cosines of the normal line. Also computed are the directed perpendicular distances (in meters) of each input point from the fitted average plane. Three or more points and/or lines are expected as input values. Weights may be assigned to each point in order to emphasize some points relative to others in the fit.

This program is written to be run on a PC from the command prompt. A text editor utility is also required in order for the user to make changes to the configuration files.

The input points are placed in a Configuration File that is read by the program at each execution. The program prints to the screen the results of the computation, and a copy of this is written to a summary file. Another file, called the output file, contains the x, y, z points of a 10-m line perpendicular to the average plane. The midpoint of this line has as its x and y components the x and y components of the first point in the configuration file. This computed line may be used for input to other programs or can be deleted if this program is used alone.

The Configuration File

The form of the configuration file is described by the example that follows. This is an ASCII text file that must be edited offline in a text editor.

The first input line of the configuration file sets how much printout is desired. A 0 (zero) gives the least print. A value greater than 0 results in extensive printouts that are used for diagnostic purposes. The value must follow the colon, with a blank between.

The second input line allows the option to force the WGS84 origin to be on the average plane. Generally, this is not a good idea. A 0 (zero) indicates No, a 1 (one) indicates Yes. The value must follow the colon with a blank between.

The third input line indicates that the next line is the reference point. It may be any point and is used to fix the plane in space. Only one reference point is expected. The value may be any number and must follow the colon, with a blank between.

Following the indicator input line are the reference point coordinates. The line format begins with the name of the point, followed by a # separator. The (x, y, z) WGS84 coordinates (meters) follow the separator, with commas between. If there is a height offset between the monument and the actual point, this height follows last on the line.

The fourth input line indicates the number of single points N_p that will be used in this fit. The program expects to find the same number of input lines following, each input line gives the (x, y, z) WGS84 coordinates of each point. The value may be ≥ 0 and must follow the colon with a blank between.

If $N_p>0$, the next input line is the first point. The input line format begins with the name of the point, followed by a # separator. The (x, y, z) WGS84 coordinates (meters) follow the #, with commas between. If there is a height offset between the monument and the actual point, this height follows next. The last item on the line is the weight to be given to the point. Enter a value between zero and one, where one gives the most weight. The input weight values are normalized by the program and assigned values internally.

Following the N_p points is an input line that indicates the number of points to be derived from N_L lines. Since a line needs two endpoints, each two input lines in the configuration file indicates a single point—the midpoint of the line. Enter the number of input lines (must be even). The value may be zero and must follow the colon, with a blank between.

If $N_L>0$, the next input line is the first endpoint of the pair defining the first line. The format for each endpoint of a line is the same as described above for the points.

Following the input data is an input line asking for the output file name. The name is entered on the next line beginning in column 1.

Following the output file name is a the line asking for the summary file name. The name is entered on the next line beginning in column 1.

This ends the configuration file. The information entered on each line must fit within 80 columns.

Example Configuration File

```
Diagnostic Print Level (0..4): 0
Force Origin, Yes = 1, No = 0: 0
REFERENCE POINT: 1
KICKAPOO CENTER REF # -810636.2947, -5258907.7266, 3505495.6034, 1.5669
POINTS (Name # x,y,z,h,w), Number of points to follow: 3
KICKAPOO CENTER # -810636.2947, -5258907.7266, 3505495.6034, 1.5669, 1
```

```
JORDAN LAKE CENTER # 350280.345, -5363636.135, 3422238.494, 0, 1
GILA RIVER CENTER # -2006012.785, -4957401.988, 3464669.062, 0, 1
LINES (Name # x,y,z,h,w), Number of lines to follow: 12
TATTNALL TAT4-to-1 #    759866.207, -5357971.107, 3364441.155, 2.27, .01
TATTNALL TAT1 #    759905.856, -5357772.790, 3364745.940, 2.13
HAWKINSVILLE 2-to-1 # 607726.768, -5362947.729, 3387289.984, 0, .01
HAWKINSVILLE 1 # 607766.439, -5362749.426, 3387594.728, 0
SILVER LAKE 4-to-1 # -95423.787, -5344839.447, 3467465.560, 0, .01
SILVER LAKE 1 # -95384.141, -5344641.122, 3467770.271, 0
RED RIVER SW-to-NW # -330517.4052, -5324297.1376, 3484557.4828, 0, .01
RED RIVER NW # -330477.7586, -5324098.8137, 3484862.2415, 0
ELEPHANT BUTTE SW-to-NW # -1557953.6717, -5095819.1259, 3495960.5842, 0, .01
ELEPHANT BUTTE NW # -1557913.9684, -5095620.7774, 3496265.3240, 0
SAN DIEGO 4S-to-1N # -2440192.334, -4794858.212, 3414447.883, 0, .01
SAN DIEGO 1N # -2440139.418, -4794593.813, 3414854.245, 0
Output file name:
FITTX.OUT
Summary file name:
FITTX.SUM
```

The Screen Output and Summary File

The following information appears on the screen and in the summary file. The first output line shows the name of the summary file and is followed by a list of the points used to form the average plane. The weight column is derived from those supplied in the configuration file.

Following the list of points are the results of the fit. The direction cosines of the normal line are listed along with the estimated one standard deviation error on each, which is derived from the covariance matrix. Next, is the computed directed distance of the WGS84 origin from the average plane. The sign of the distance indicates the placement of the point relative to the plane. Starting at the point, if the direction toward the plane is in the same direction as the direction cosines, then the distance is positive. If the direction toward the plane is opposite to the direction cosines, the distance is negative. This same convention is used to find the distance of each input point from the plane. These distances follow. The average distance is also computed.

Finally, the endpoints of a 10-m perpendicular line, whose midpoint lies in the plane and whose x and y components are taken from the x and y components of the reference point, are listed. These are also put on the output file.

Example Summary File

```
Summary file = FITTX.SUM
Find the best fit plane to the following points.
```

	X	Y	Z	WT
0 KICKAPOO CENTER	-810636.4936	-5258909.0172	3505496.4695	1000.0
1 JORDAN LAKE CENTER	350280.3450	-5363636.1350	3422238.4940	1000.0
2 GILA RIVER CENTER	-2006012.7850	-4957401.9880	3464669.0620	1000.0
3 TATTNALL TAT4-to-1	759886.2934	-5357873.7948	3364594.7148	10.0
4 HAWKINSVILLE 2-to-1	607746.6035	-5362848.5775	3387442.3560	10.0

```
 5 SILVER LAKE 4-to-1
                          -95403.9640  -5344740.2845   3467617.9155      10.0
 6 RED RIVER SW-to-NW
                         -330497.5819  -5324197.9756   3484709.8621      10.0
 7 ELEPHANT BUTTE SW-to-NW
                        -1557933.8200  -5095719.9517   3496112.9541      10.0
 8 SAN DIEGO 4S-to-1N
                        -2440165.8760  -4794726.0125   3414651.0640      10.0
REFERENCE POINT (height included)
   KICKAPOO CENTER REF    -810636.4936 -5258909.0172  3505496.4695

Result:.................
Direction Cosines of Mean Plane
   l =   0.10873526 m =   0.54378339 n =   0.83215159
Standard Deviation of the Direction Cosines
   l =   0.00729146 m =   0.02595182 n =   0.01752638
Direction cosine difference: Line - Mean Plane
 3 l =  -0.00038529 m =  -0.00128774 n =   0.00089028
 4 l =  -0.00026791 m =  -0.00158883 n =   0.00107101
 5 l =  -0.00033085 m =  -0.00150158 n =   0.00102242
 6 l =  -0.00034083 m =  -0.00156272 n =   0.00106351
 7 l =  -0.00018692 m =  -0.00150102 n =   0.00100331
 8 l =  -0.00023087 m =  -0.00163261 n =   0.00109467

Distance of origin from plane d = -30747.5224 (meters)

Distance of SITE from the mean plane: Midpoint & h = 0 (meters).
KICKAPOO CENTER          d1 =      0.1944  d0 =     -0.3425 angle =   0.000000
JORDAN LAKE CENTER       d1 =     -0.2721  d0 =     -0.4571 angle =   0.000000
GILA RIVER CENTER        d1 =     -0.1815  d0 =     -0.7537 angle =   0.000000
TATTNALL TAT4-to-1       d1 =    296.0173  d0 =    295.9577 angle =   0.092375
HAWKINSVILLE 2-to-1      d1 =    531.4689  d0 =    531.3229 angle =   0.110852
SILVER LAKE 4-to-1       d1 =    423.5183  d0 =    423.4995 angle =   0.105796
RED RIVER SW-to-NW       d1 =    592.8263  d0 =    592.7217 angle =   0.110051
ELEPHANT BUTTE SW-to-NW  d1 =    326.7643  d0 =    324.2227 angle =   0.103998
SAN DIEGO 4S-to-1N       d1 =    369.6286  d0 =    369.3939 angle =   0.113397
Average distance from plane 282.2183 (m) Standard Dev =   231.1580

At the Reference site KICKAPOO CENTER REF
the azimuth and elevation angles of the normal to the mean plane are:
Azimuth =   1.41092447, Elevation =  -0.09950624 Degrees

Elevation, Azimuth, Pitch, and Yaw
 of each line with respect to the Mean Plane Normal (Deg)
 3 TATTNALL TAT4-to-1       -0.00773971,  1.40034159,  0.09176652, -0.01058289
 4 HAWKINSVILLE 2-to-1       0.01133851,  1.40961968,  0.11084475, -0.00130479
 5 SILVER LAKE 4-to-1        0.00614003,  1.40529283,  0.10564627, -0.00563165
 6 RED RIVER SW-to-NW        0.01039936,  1.40526134,  0.10990559, -0.00566314
 7 ELEPHANT BUTTE SW-to-NW   0.00446134,  1.41344050,  0.10396757,  0.00251603
 8 SAN DIEGO 4S-to-1N        0.01388444,  1.41209988,  0.11339068,  0.00117541

End points of a 10 (m) perpendicular line to mean plane,
where x and y of the midpoint are the same as KICKAPOO CENTER REF .
-810637.5810 -5258914.4550 3505488.3816
-810635.4063 -5258903.5793 3505505.0246
```

Command Line

The program is executed from the command prompt. The form is:

```
FITPLN filename.CFG
```

Filename.CFG is the configuration file name containing the positions of the points and lines as described above. Several different configuration files can be made ahead of time with a text editor. The executable and the configuration files are assumed to be in the current directory.

A.2 Latitude Computation Program

The Latitude Computation Program computes the three coefficients that define a plane from a list of one or more input point pairs. Each plane (defined from a pair of input points) is handled separately. The user enters a geodetic longitude and ellipsoid height (WGS84), and the program computes the corresponding latitude that intersects each of the planes.

This program is written to be run on a PC from the command prompt. A text editor utility is also required in order to make changes to the configuration file.

The input points are placed in a configuration file that is read by the program at each execution. The program prints to the screen the results of the computation, and a copy of this is written to a summary file that is saved.

The Configuration File

The form of the configuration file is described by the example that follows. This is a text file that must be edited offline in a text editor.

The first line sets how much printout is desired. A 0 (zero) gives the least print. A value greater than 0 results in extensive printouts that are used for diagnostic purposes. The value must follow the colon, with a blank between.

The second line indicates the number of single points N_L that will be used to define planes by computing their normal lines. Since a line needs two endpoints, each pair of input lines in the configuration file define a single plane through the midpoint of the line. Enter the number of lines (must be even). The value must follow the colon, with a blank between.

The next line is the endpoint of the first pair. The line format begins with the name of the point followed by a # separator. The x, y, z WGS84 coordinates (meters) follow the # with commas between. If there is a height offset between the monument and the actual point, this height follows the z component.

Following the points is a line that specifies how the user will enter the west longitudes. The program will prompt for decimal degrees (e.g., 98.3083333) or for degrees, minutes, and seconds (98 18 30). The solution for latitude will be in the same format. Enter a zero (0) for decimal degrees or a one (1) for degrees, minutes, and seconds.

Following the longitude format is a line asking for the summary file name. The name is entered on the next line beginning in column 1.

Example Configuration File

```
Diagnostic Print Level (0..4): 0
Position (Name # x y z), Number of lines to follow: 6
KICKAPOO SOUTH #  -810811.0344, -5259781.5064, 3504156.4003, 1.5669
KICKAPOO NORTH #  -810458.5260, -5258019.1344, 3506863.5535, 1.5669
TATTNALL TAT4 #    759866.207, -5357971.107, 3364441.155, 2.27
TATTNALL TAT1 #    759905.856, -5357772.790, 3364745.940, 2.13
SAN DIEGO 4S # -2440192.334, -4794858.212, 3414447.883, 0
SAN DIEGO 1N # -2440139.418, -4794593.813, 3414854.245, 0
Keyboard entries Decimal Degrees = 0, Deg Min Sec = 1: 1
Summary file name:
TLATPLN.SUM
```

The Screen Output and Summary File

The summary file lists the same information that is listed on the screen while the program executes. When the program is ready to compute a new latitude, it prompts the user to enter the longitude and ellipsoid height. To quit the program, enter Q at the prompt. The following is a listing of the summary file generated by the configuration file above and the information entered by the user.

```
Summary file = TLATPLN.SUM
Site coordinates  1:   -810811.2334 -5259782.7972  3504157.2660
Site coordinates  2:   -810458.7249 -5258020.4247  3506864.4199
Site coordinates  3:    759866.4772 -5357973.0121  3364442.3593
Site coordinates  4:    759906.1095 -5357774.5776  3364747.0702
Site coordinates  5:  -2440192.3340 -4794858.2120  3414447.8830
Site coordinates  6:  -2440139.4180 -4794593.8130  3414854.2450

Baseline  0:   352.5085 1762.3724 2707.1539 3249.4462
Baseline  1:    39.6323  198.4346  304.7108  365.7809
Baseline  2:    52.9160  264.3990  406.3620  487.6854
Direction cosines  0:   0.10848263  0.54236085  0.83311237
Direction cosines  1:   0.10834996  0.54249565  0.83304187
Direction cosines  2:   0.10850439  0.54215078  0.83324626
Baseline midpoints  0:   -810634.9791 -5258901.6110  3505510.8430
Baseline midpoints  1:    759886.2934 -5357873.7948  3364594.7148
Baseline midpoints  2:  -2440165.8760 -4794726.0125  3414651.0640
Distance of plane from origin  0:   19677.7248
Distance of plane from origin  1:   21441.3306
Distance of plane from origin  2:   18987.9492
Origin of great circle  0:   -2134.6914 -10672.4276 -16393.7560
Origin of great circle  1:   -2323.1674 -11631.8287 -17861.5261
Origin of great circle  2:   -2060.2758 -10294.3315 -15821.6376

Entered:  100.00000   0.00000   0.00000
West Long 100  0  0.000, Height =  300.00; Meets  0 at Latitude  33 34 24.309
West Long 100  0  0.000, Height =  300.00; Meets  1 at Latitude  33 33 54.037
West Long 100  0  0.000, Height =  300.00; Meets  2 at Latitude  33 33 56.387

Entered:  100.30000   0.00000   0.00000
West Long 100 18  0.000, Height =  300.00; Meets  0 at Latitude  33 34 34.441
West Long 100 18  0.000, Height =  300.00; Meets  1 at Latitude  33 34  4.030
West Long 100 18  0.000, Height =  300.00; Meets  2 at Latitude  33 34  6.573
```

```
Entered:  100.00000  18.00000   0.00000
West Long 100 18  0.000, Height =  300.00; Meets  0 at Latitude  33 34 34.441
West Long 100 18  0.000, Height =  300.00; Meets  1 at Latitude  33 34  4.030
West Long 100 18  0.000, Height =  300.00; Meets  2 at Latitude  33 34  6.573

Entered:  100.00000  18.00000  30.00000
West Long 100 18 30.000, Height =  300.00; Meets  0 at Latitude  33 34 34.686
West Long 100 18 30.000, Height =  300.00; Meets  1 at Latitude  33 34  4.270
West Long 100 18 30.000, Height =  300.00; Meets  2 at Latitude  33 34  6.818

Entered:  100.00000  18.50000   0.00000
West Long 100 18 30.000, Height =  300.00; Meets  0 at Latitude  33 34 34.686
West Long 100 18 30.000, Height =  300.00; Meets  1 at Latitude  33 34  4.270
West Long 100 18 30.000, Height =  300.00; Meets  2 at Latitude  33 34  6.818

Entered: -260.00000   0.00000   0.00000
West Long -260  0  0.000, Height =  300.00; Meets  0 at Latitude  33 34 24.309
West Long -260  0  0.000, Height =  300.00; Meets  1 at Latitude  33 33 54.037
West Long -260  0  0.000, Height =  300.00; Meets  2 at Latitude  33 33 56.387

Entered: -259.70000   0.00000   0.00000
West Long -259 42  0.000, Height =  300.00; Meets  0 at Latitude  33 34 34.441
West Long -259 42  0.000, Height =  300.00; Meets  1 at Latitude  33 34  4.030
West Long -259 42  0.000, Height =  300.00; Meets  2 at Latitude  33 34  6.573

Entered: -259.00000  42.00000  30.00000
West Long -259 42 30.000, Height =  300.00; Meets  0 at Latitude  33 34 34.195
West Long -259 42 30.000, Height =  300.00; Meets  1 at Latitude  33 34  3.788
West Long -259 42 30.000, Height =  300.00; Meets  2 at Latitude  33 34  6.325

Entered: -259.00000  41.00000  30.00000
West Long -259 41 30.000, Height =  300.00; Meets  0 at Latitude  33 34 34.686
West Long -259 41 30.000, Height =  300.00; Meets  1 at Latitude  33 34  4.270
West Long -259 41 30.000, Height =  300.00; Meets  2 at Latitude  33 34  6.818
```

Command Line

The program is executed from the command prompt. Type:

```
LATPLN filename.CFG
```

Filename.CFG is the configuration filename containing the positions of the points and lines as described above. Several different configuration files can be produced ahead of time with a text editor. The executable and the configuration files are assumed to be in the current directory.

A.3 The Look-Angle Program

The look angles are azimuth and elevation angles of a point in space as seen by an observer. The azimuth angle is generally measured in a local vertical coordinate system clockwise from north to the projection of the point on the east-north plane. The elevation is the angle from the plane to the point in space. This program computes a modified set of look angles, and a range, from an observer at the midpoint of a line defined by two endpoints to a point in space. This line, defined by its unit vector, in general is not aligned with any particular axis of the local vertical system.

The coordinate system defined by the line is related to the WGS84 geodetic system in the following way. The unit vector of the line is known from its endpoints. The geodetic coordinates of the midpoint can be used to compute the local vertical. The cross product of the line with the local vertical gives a perpendicular unit vector in the easterly direction. The normal to the plane containing the original line and the easterly unit vector forms a local array system in which the look angles of the point in space may be computed.

The Configuration File

The form of the configuration file is described by the example that follows. This is a text file that must be edited offline in a text editor.

The first line sets how much printout is desired. A 0 (zero) gives the least print. A value greater than 0 results in extensive printouts that are used for diagnostic purposes. The value must follow the colon with a blank between.

The positions of the point in space are selected by entering the limits of the grid and the radial shells. The look angles to every grid point on shells of different ellipsoid height are computed for the observer. The grid limits are entered following the print-level option.

The second line indicates that the west longitude limits and increment should be entered next. These are put on the following line in degrees with commas between. The first entry is the starting west longitude, the second entry is the stopping longitude, and the last is the increment. After the longitude limits are entered, the latitude limits are entered in the same type of format. Following the latitude are the ellipsoid height limits entered in meters.

Following the grid points are the positions of the observer. The observer is assumed to be at the midpoint of lines. The lines are specified by their endpoints. These lines may be the endpoints of arrays or normals to an average plane. Points are not satisfactory as input values, because the unit vector of lines are required to determine the modified look angles computed by this program.

The input line following the ellipsoid heights indicates the number of lines N_L that will be input. The program expects to find the same number of lines following. Each line gives the (x, y, z) WGS84 coordinates of an end point, and each pair defines an array line. The value must be greater than 0, even, and must follow the colon with a blank between.

The line format begins with the name of the point followed by a # separator. The (x, y, z) WGS84 coordinates (meters) follow the #, with commas between. If there is a height offset between the monument and the actual point, this height follows next.

Following the end point entries is a the line asking for the output file name. The name is entered on the next line beginning in column 1.

Following the output file name is a the line asking for the summary file name. The name is entered on the next line beginning in column 1. A sample configuration file follows.

Example Configuration File

```
Diagnostic Print Level (0..4): 0
Enter West Longitude Range (Deg) & Increment On Next Line:
98.7, 98.8, .01
Enter North Latitude Range (Deg) & Increment On Next Line:
33.45, 33.65, .01
Enter Ellipsoid Height Range (Meters) & Increment On Next Line:
10000000, 10000000, 5000
LINES (Name # x y z h), Number of lines to follow: 6
KICKAPOO SOUTH #  -810811.0344, -5259781.5064, 3504156.4003, 1.5669
KICKAPOO NORTH #  -810458.5260, -5258019.1344, 3506863.5535, 1.5669
RED RIVER SW # -330517.4052, -5324297.1376, 3484557.4828, 0
RED RIVER NW # -330477.7586, -5324098.8137, 3484862.2415, 0
ELEPHANT BUTTE SW # -1557953.6717, -5095819.1259, 3495960.5842, 0
ELEPHANT BUTTE NW # -1557913.9684, -5095620.7774, 3496265.3240, 0
Output file name:
LOOKLK.OUT
Summary file name:
LOOKLK.SUM
```

Summary and Output Files

The summary file provides a listing of the results from the program. The look angles are computed for each observer at each grid point specified. Some annotation is included to explain the columns of data. The output file contains the same information as the summary file but is not annotated. A short segment of a summary file for three observers (Kickapoo, Red River, and Elephant Butte) follows. The coordinates are for the midpoint of the line defined in the configuration file. The unit vectors listed include the local vertical (UP), the product of the line (NORH) crossed with the local vertical (EAST), and the normal (NORM) to the plane containing the line (NORH) and the east (EAST) unit vectors.

Following the observer locations are the geodetic coordinates of the points in space that constitute the grid. They are specified by ellipsoid height, geodetic longitude, and geodetic latitude. For each grid point, the corresponding look angles and range are listed for each observer. Also included are the vertical, west, and south vector components of the grid point with respect to the observer's coordinates.

```
Summary file = LOOKLK.SUM
 0 KICKAPOO SOUTH ..................    -810634.979  -5258901.611   3505510.843
 0 KICKAPOO SOUTH ..................  261.23709484   33.55412862       310.809
 0 WGS84 Unit vectors of Array plus Normal
to east cross north at the midpoint of the array.
UP    -0.12695967  -0.82363635   0.55272453
EAST   0.98595778  -0.16573269  -0.02049228
NORH   0.10848263   0.54236085   0.83311237
NORM  -0.12695974  -0.82363668   0.55272402
 1 RED RIVER SW ..................    -330497.582  -5324197.976   3484709.862
 1 RED RIVER SW ..................  266.44794374   33.33089360        56.624
 1 WGS84 Unit vectors of Array plus Normal
to east cross north at the midpoint of the array.
UP    -0.05176441  -0.83390613   0.54947340
EAST   0.99275901  -0.10269074  -0.06232305
NORH   0.10839443   0.54222067   0.83321509
NORM  -0.05177063  -0.83393726   0.54942556
```

```
 2 ELEPHANT BUTTE SW .................  -1557933.820  -5095719.952   3496112.954
 2 ELEPHANT BUTTE SW .................   252.99983664   33.44594365     1414.910
 2 WGS84 Unit vectors of Array plus Normal
to east cross north at the midpoint of the array.
UP    -0.24395903  -0.79794590   0.55115000
EAST   0.96369147  -0.26308208   0.04567898
NORH   0.10854834   0.54228238   0.83315490
NORM  -0.24395903  -0.79794589   0.55115003

>THE FOLLOWING LINES ARE WRAPPED TO FIT ONTO THE PAGES IN THIS REPORT.
 Ellipsoid        West             North                  0 KICKAPOO SOUTH
.................. 1  RED  RIVER  SW  .................. 2  ELEPHANT  BUTTE  SW
..................
 Height (m)  Longitude (deg) Latitude (deg)  Az (deg)    Elev (deg)   Range (m)
  Up (m)       West (m)       South (m)      Az (deg)    Elev (deg)   Range (m)
Up (m)       West (m)       South (m)      Az (deg)    Elev (deg)   Range (m)    Up
(m)       West (m)       South (m)
   10000000.0    98.700000    33.450000     151.79018     89.80927  9999710.740
9999655.333   -15735.434    29334.386     268.74940     82.96516 10029338.779
9953836.609  1228028.664    26808.640      90.81453     78.69393 10074609.939
9879101.029 -1974927.827    28077.843
   10000000.0    98.700000    33.460000     149.39553     89.82372  9999707.601
9999660.271   -15663.516    26480.841     268.88254     82.96509 10029339.320
9953835.565  1228100.522    23955.090      90.73178     78.69456 10074601.505
9879114.332 -1974856.771    25224.304
   10000000.0    98.700000    33.470000     146.57927     89.83780  9999704.779
9999664.710   -15591.598    23627.294     269.01568     82.96498 10029340.177
9953834.025  1228172.342    21101.537      90.64903     78.69516 10074593.384
9879127.139 -1974785.654    22370.762
   10000000.0    98.700000    33.480000     143.23727     89.85142  9999702.273
9999668.651   -15519.680    20773.744     269.14882     82.96483 10029341.348
9953831.988  1228244.125    18247.982      90.56627     78.69574 10074585.575
9879139.453 -1974714.478    19517.217
```

Command Line

The program is executed from the command prompt. Type:

```
LOOK filename.CFG
```

Filename.CFG is the configuration file name containing the geodetic coordinates for the grid positions and the array lines as described above. Several different configuration files can be produced ahead of time with a text editor. The executable and the configuration files are assumed to be in the current directory.

A.4 The Look-Angle and Beam Program

This program combines the results of the look-angle program with an idealized linear array definition to compute the array factor in geodetic coordinates. The array factor for a broadside linear array can be specified by the number of elements and their spacing in wavelengths. It is assumed that the elements are in phase and have a uniform amplitude distribution. Since the look angles are defined with respect to the array, and the array is specified by its unit vector in the WGS84 system, only the look angles and the array definition are required to compute the array factor at each grid point.

The Configuration File

The configuration file is a text file that needs to be edited before the program is executed. The configuration file for this program is similar to that used in the look-angle program. That description is repeated here.

The first line sets how much printout is desired. A 0 (zero) gives the least print. A value greater than 0 results in extensive printouts that are used for diagnostic purposes. The value must follow the colon, with a blank between.

The positions of the point in space are selected by entering the limits of the grid and the radial shells. The look angles to every grid point on shells of different ellipsoid height are computed for each observer. The grid limits are entered beginning on the second line.

The second line indicates that the west longitude limits and increment should be entered next. These are put on the following line in degrees with commas between. The first entry is the starting west longitude in degrees, the second entry is the longitude to stop, and the last is the increment. After the longitude limits are entered, the latitude limits are entered in the same type of format. Following the latitude are the ellipsoid height limits entered in meters.

Following the grid points are the positions of the observer. The observer is assumed to be at the midpoint of lines. The lines are specified by their end points. These lines may be the end points of arrays or normals to an average plane. Points are not satisfactory as input values, because the unit vector of lines are required to determine the modified look angles computed by this program.

The input line following the ellipsoid heights, indicates the number of lines N_L that will be input. The program expects to find the same number of lines following. Each line gives the (x, y, z) WGS84 coordinates of an end point and each pair defines an array line. The value must be greater than 0, even, and must follow the colon with a blank between.

The line format begins with the name of the point followed by a # separator. The (x, y, z) WGS84 coordinates (meters) follow the # with commas between. If there is a height offset between the monument and the actual point, this height follows next.

The next line calls for a flag to indicate whether the line, in the order just entered, is a transmitter or a receiver. A *T* indicates a transmitter, and an *R* indicates a receiver. This flag is used to model the element pattern. The transmitter elements are oriented differently from the receiver elements. One input line is used for each entry.

Next are entries that list the number of elements in each array. This number of elements is expected to be even. The elements are assumed to be equally spaced, in phase, with a uniform amplitude distribution. One input line is used for each entry.

Following the number of elements are their spacings in wavelengths. One input line is used for each entry.

Following the spacing entries is a the line asking for the output file name. The name is entered on the next line beginning in column 1.

Following the output file name is a the line asking for the summary file name. The name is entered on the next line beginning in column 1. A sample configuration file follows.

Example Configuration File

```
Diagnostic Print Level (0..4): 0
Enter West Longitude Range (Deg) & Increment On Next Line:
94., 108., .05
Enter North Latitude Range (Deg) & Increment On Next Line:
33.4, 33.7, .002
Enter Ellipsoid Height Range (Meters) & Increment On Next Line:
10000000, 10000000, 5000
LINES (Name # x y z h), Number of lines to follow: 6
KICKAPOO SOUTH #  -810811.0344, -5259781.5064, 3504156.4003, 1.5669
KICKAPOO NORTH #  -810458.5260, -5258019.1344, 3506863.5535, 1.5669
JORDAN LAKE SOUTH # 350263.444, -5363720.774, 3422108.469, 0
JORDAN LAKE NORTH # 350297.234, -5363551.515, 3422368.526, 0
GILA RIVER SOUTH # -2006039.531, -4957535.582, 3464463.859, 0
GILA RIVER NORTH # -2005986.057, -4957268.443, 3464874.298, 0
Enter T on the following lines if site is a transmitter:
T
T
T
Enter the number of elements per array on the following lines:
2556
256
404
Enter the element spacing (wavelength) on the following lines:
.92
.88
.94
Output file name:
LOOBTX.OUT
Summary file name:
LOOBTX.SUM
```

Summary and Output Files

The summary file provides a listing of the results from the program. The look angles are computed for each observer at each grid point specified. Some annotation is included to explain the columns of data. The output file contains the same information as the summary file but is not annotated. A short segment of a summary file for three observers (Kickapoo, Jordan Lake, and Gila River) follows. The coordinates are for the midpoint of the line defined in the configuration file.

Following the observer locations, are the geodetic coordinates of the points in space that constitute the grid. They are specified by ellipsoid height, geodetic longitude, and geodetic latitude. For each grid point, the corresponding look angles and range are listed for each observer. Following this is the array factor value (Power) in decibels. On the output file, these numbers are not annotated and can be imported to a plot program to graphically illustrate the array factor as a function—at each observation location—of the geodetic position of the grid points.

Example Summary File

```
>THE FOLLOWING LINES ARE WRAPPED TO FIT ONTO THE PAGES IN THIS REPORT.
Summary file = LOOBTX.SUM
  0 KICKAPOO SOUTH ..........................      -810634.979   -5258901.611
3505510.843
  1 JORDAN LAKE SOUTH .......................       350280.339   -5363636.145
3422238.498
  2 GILA RIVER SOUTH ........................     -2006012.794   -4957402.013
3464669.078
  Ellipsoid         West                North                    0 KICKAPOO SOUTH
..................... 1 JORDAN LAKE SOUTH ................... 2 GILA RIVER SOUTH
...................
 Height (m)  Longitude (deg) Latitude (deg)  Az (deg)    Elev (deg)    Range (m)
    Power       Az (deg)     Elev (deg)     Range (m)      Power       Az (deg)
Elev (deg)     Range (m)       Power
   10000000.0       94.0000       33.4000         89.493       83.494  10024829.68
    -5.2882       270.358        79.340  10067462.81       12.0066       89.847
   65.716  10352827.07       10.3696
   10000000.0       94.0000       33.4020         89.464       83.494  10024828.13
    -4.8756       270.376        79.339  10067465.95       11.9045       89.840
   65.717  10352820.85       10.0782
   10000000.0       94.0000       33.4040         89.435       83.494  10024826.60
    -6.0160       270.393        79.339  10067469.10       11.7969       89.832
   65.717  10352814.65        9.7678
   10000000.0       94.0000       33.4060         89.407       83.494  10024825.08
    -9.0135       270.411        79.339  10067472.27       11.6839       89.824
   65.717  10352808.46        9.4374
   10000000.0       94.0000       33.4080         89.378       83.495  10024823.58
   -15.7507       270.428        79.339  10067475.44       11.5652       89.817
   65.717  10352802.29        9.0859
   10000000.0       94.0000       33.4100         89.349       83.495  10024822.08
   -28.3510       270.446        79.338  10067478.63       11.4409       89.809
   65.717  10352796.12        8.7122
```

Command Line

The program is executed from the command prompt. Type:

```
LOOKB filename.CFG
```

Filename.CFG is the configuration file name containing the geodetic coordinates for the grid positions and the array lines as described above. Several different configuration files can be produced ahead of time with a text editor. The executable and the configuration files are assumed to be in the current directory.

APPENDIX B

FENCE ELECTROMAGNETIC FIELD ALIGNMENT PROGRAM

(DESCRIPTION AND OPERATION MANUAL)

This model is a UNIX-based program suite for the computation of the fields of the FENCE transmitter and receiver arrays, and the arrays' pairwise and total power products.

Diagram 1 below contains the directory structure for the program suite and will be referred to in the description of the code that follows.

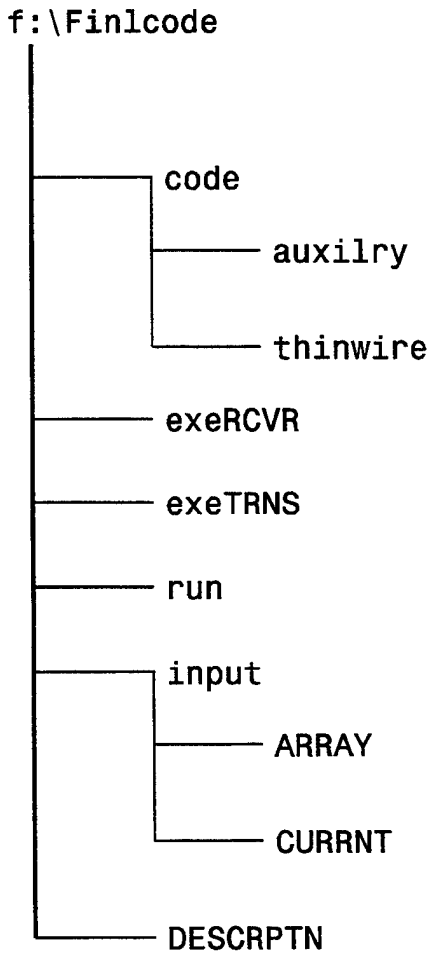

Diagram 1—Code Structure for the Near-Field Model

B.1 Code Components

I. Calculation of the Ground Screen Thinwire Current by Galerkin Method

Program THINWIRE has to be run in order to generate a file `thinwire.out`, which is used by the routine calculating the combined field of a transmitter element and the induced currents in the ground screen that lies beneath it. THINWIRE uses the piecewise Galerkin method of moments to calculate the complex current distribution in the wire-grid ground screen.

Referring to Diagram 1, the THINWIRE code, the corresponding JCL file, `THINWIRE.COM`, the executable, and the input and output files reside in the directory `f:\Finlcode\code\thinwire`. To run THINWIRE, one just needs to execute `THINWIRE.COM` once for all the runs with the given element—ground screen geometry. The files `thinwire.inp` and `thinwire.dat` should be used as given unless and until the ground screens or the transmitter elements are changed from their 1988 state.

II. Electromagnetic Field and Its Power Calculations

1. JCL File

The execution of this portion of the suit is handled by a UNIX JCL file `CODE.COM`, which resides at `f:\Finlcode\run`.

2. Computational Grid

The file `compgrid.inp` provides basic information on the computational grid, which is then used by the executable **COMPGRID** in order to generate the actual computational grid file `compgrid.dat`. The source file for the executable **COMPGRID** resides in the directory `f:\Finlcode\code\auxilry`. The files `compgrid.inp`, `compgrid.dat`, and COMPGRID reside in `f:\Finlcode\run`. The computational grid has geodetic coordinates.

3. Computations for Different Antenna Arrays

Once the computational grid is available, field computations are performed for all the points of the grid—one transmitter or receiver array at a time. This is repeated for all the chosen receiver and transmitter arrays. The receiver and transmitter arrays are assigned identification numbers within the file `antnas.dat`, which resides in the `f:\Finlcode\run` directory. The selection of a set of receiver arrays and transmitter arrays is performed by editing the file `antenhierarch.dat`, also residing in `f:\Finlcode\run`. The first column in that file contains the computational counter (always the natural sequence of integers 1,2, ...). The second column contains the array indices, designating the arrays for which the computations are to be performed.

4. Field Computations for a Given Array

Given array field computations are performed by executing either **nearfldRCVR** (for a receiver array) or **nearfldTRNS** (for a transmitter array). Both reside in `f:\Finlcode\run` and are products of the compilation using the Makefiles in `f:\Finlcode\exeRCVR` and `f:\Finlcode\exeTRNS`, respectively. The source code for these executables resides in the `f:\Finlcode\code` directory. The following steps are made in the matter of computation of the field for a given array:

A) *Convert a given geodetic coordinate of the computational point to its spherical coordinates associated with the array's phase center and its north-south axis (z-axis).* The reason for this conversion is that Berg's code, which performs the actual field computations, uses these spherical coordinates as an input. The operation is performed by the subroutine **coordtrnsf**, whose source code resides in `f:\Finlcode\code`. At the heart of all the orthogonal transformations used here is the multiplication of the coordinate vector pertaining to the current system by a matrix whose columns represent the coordinate vectors of the basis vectors of the current orthogonal system with respect to the new system. The following steps are performed in effecting the system of transformations from the initial geodetic coordinates of the observation point to the final local spherical coordinates:

a) Transform the geodetic coordinates of the point to the earth-centered xyz coordinates.
b) Find the coordinates of the point with respect to the system parallel to the earth-centered system but originating at the location of the array.
c) Find the earth-centered coordinates of the unit vectors of the east-north-up system associated with the phase center of the array.
d) Obtain the transition matrix from the earth-centered frame to the local frame with the unit vectors along xup, ywest, and zsouth.

e) Find the coordinates of the point in the xup-ywest-zsouth system.
f) Get the transition matrix associated with the yaw and sloping of the axis of the array.
g) Obtain the coordinates of the point in the tilted system.
h) Obtain the spherical coordinates of the point with respect to the tilted frame.

B) *Compute the field and its power at the given point using the Berg's code.* The actual subroutine that carries out the field computations is **array_sbr**, whose source code resides at `f:\Finlcode\code`. The following are several comments about the routines employed in this part of the code:

a) There is a far-field option that is triggered when the spherical coordinate range from the array to the observation point is set at 0.0. This causes no problems since, in the infinite range region, the electrical field range dependence is simply $\frac{e^{ikr}}{r}$ (r^{-2} for the power), which is incorporated into the computations at its last stage. Also, no true zero range computations are ever called for, which obviates the need for any further clarifications of the meaning of the expression r = 0.0.

b) The routines **elpos_rcvr** and **elpos_trns** supply information to the main program regarding the antenna element positioning on the arrays. The source code for both resides in `f:\Finlcode\code`. The necessary input for these routines comes from the file `antnas.dat`, which contains both the transmitter and receiver array coordinate and orientation information. This file resides in `f:\Finlcode\run`.

c) Subroutine **currnt** provides the amplitude and phase of the input current for each element in the array. There are four different **currnt** subroutines (**currnt_stnd**, **currnt_rbay**, **currnt_sbay**, and **currnt_rsby**) that are available here. The four choices offer random and systematic variation of currents and phases within and between the bays, which applies only to the Kickapoo complex. A more complete explanation of this issue is provided in the second paragraph on p. 23 of the Berg report. (See Reference 6 of this report.)

d) Subroutine **elffld** returns the far-electric-field values at a specified point in space for a particular element. For calculating transmitter patterns, one needs to use **elffld_trns.f** as the source code and for the receiver patterns - **ellfld_rcvr.f**. Both reside in `f:\Finlcode\code`.

e) The specific antenna array information is contained in various files of the directory `f:\Finlcode\input\ARRAY`.

C) *Use the computed powers for each of the transmitter and receiver arrays to form the products of powers.* The products are obtained by using the executables **pairpowerprod** and **powerprod** residing in `f:\Finlcode\run`. The former one is used to obtain various files containing power products for one receiver array /one transmitter array combinations. The latter is used to generate the products for the combined receiver/combined transmitter powers. The source codes for both reside in `f:\Finlcode\code\auxilry`.

B.2 Execution Sequence

The execution sequence can be followed by viewing the command file responsible for it. The file is CODE.COM, and it appears below. To help understand the roles played by the different files belonging to this suit, please see the table of the file dependencies following the command file.

```
#   CODE.COM

rm fort.*

# PREPARE A FILE WITH THE COORDINATES OF POINTS
vi COMPGRID.INP
compgrid

#
#PREPARE A FILE FOR THE TRANSMITTER POWERS AND ONE FOR THE RECEIVER POWERS
powerfilegen
#

#Assign the file with the computation points to unit 28.
ln -s COMPGRID.DAT fort.28
#

# Assign the unit numbers for the auxilliary files
ln -s ../code/thinwire/THINWIRE.OUT fort.4
ln -s ../input/CURRNT/CURRNT STND.INP fort.8
#
# Assign unit numbers to files with transmitter information
ln -s  ../input/ARRAY/ARRAY STE.INP fort.51
ln -s  ../input/ARRAY/ARRAY KB.INP fort.52
ln -s  ../input/ARRAY/ARRAY JL.INP fort.53
ln -s  ../input/ARRAY/ARRAY GR.INP fort.54
ln -s  ../input/ARRAY/ARRAY KC.INP fort.55
ln -s  ../input/ARRAY/ARRAY KN.INP fort.56
ln -s  ../input/ARRAY/ARRAY KS.INP fort.57
ln -s  ../input/ARRAY/ARRAY VTA.INP fort.58
#

# Assign unit numbers to files with receiver information
ln -s  ../input/ARRAY/ARRAY SRE.INP fort.11
ln -s  ../input/ARRAY/ARRAY 400.INP fort.12
ln -s  ../input/ARRAY/ARRAY 600.INP fort.13
ln -s  ../input/ARRAY/ARRAY 1200.INP fort.14
ln -s  ../input/ARRAY/ARRAY 2400.INP fort.15
#

# Assign unit number to file with antenna coordinates, angles, types
ln -s ANTNAS.DAT fort.2
#

# DO THE RECEIVERS
# ASSIGN THE RECEIVER POWER FILE
ln -s RECVRRPOWER.TXT fort.23
set count = 1
while ($count <=  86)
 echo ARRAY No $count
nearfldRCVR
 @ count++
end
```

```
echo "End of receiver calculatoins. Next go transmitters"
#

rm fort.23

# DO THE TRANSMITTERS
# ASSIGN THE TRANSMITTER POWER FILE
ln -s  TRANSMTRPOWER.TXT fort.23
set count = 1
while ($count <= 3)
 echo ARRAY No $count
nearfldTRNS
 @ count++
end
echo "End of the transmitter calculatoins."
#

# OBTAIN PRODUCTS OF RECVR AND TRANSMTR  POWERS FOR ALL TRANSMTR-RECVR PAIRS
#pairpowerprod

#CREATE PRODUCTS OF COMBINED RECEIVER AND COMBINED TRANSMITTER POWERS
powerprod
```

Table A-1—File Dependencies for the Field Power Products Code

File Name	File#	File Type	Directory	Purpose	Produced by(+)/Needed by (-) file #
CODE.COM	1	Macro	Run Directory	The command file in charge of the execution of the suite.	+Manually made
ANTENHIERARCH.DAT	2	Input Data File	Run Directory	Indicates the hierarchy of the field computations for the receiver and transmitter antennas.	+Manually made -26
ANTNAS.DAT	3	Input Data File	Run Directory	File with the antenna phase center coordinates, orientation, length (receivers only), site name, and number.	+Manually made -26, -37,-38, -41
COMPGRID.INP	4	Input Data File	Run Directory	Provides information for the creation of the Geodetic computational grid.	-6
Compgrid	5	Executable File	Run Directory	The executable that creates the Geodetic computational grid.	-1
compgrid.f	6	Source code file.	Code Directory	A source code file for the creation of the Geodetic computational grid.	-5
Powerfilegen	7	Executable File	Run Directory	The executable initializing the total receiver and total transmitter power files.	-1

Powerfilegen.f	8	Source code file.	Code Directory	A source code file for the initializing the total receiver and transmitter power files.	-7
COMPGRID.DAT	9	Input Data File	Run Directory	The file containing the Geodetic grid for the calculations.	-6, -8
THINWIRE.OUT	10	Input Data File	THINWIRE Directory	Contains ground screen complex current distribution obtained using Galerkin method.	-41
ARRAY STE.INP ARRAY KB.INP ARRAY JL.INP ARRAY GR.INP ARRAY KC.INP ARRAY KN.INP ARRAY KS.INP ARRAY VTA.INP	11 12 13 14 15 16 17 18	Input Data Files	ARRAY ------- - ------- - ------- ------- ------- ------- ------- -----	Contain geometric information on the configuration of the transmitter arrays in terms of the arrowhead transmitter elements. The arrays by the file number are: 11 – Single transmitter element; 12 – Single Kickapoo bay (144 elements); 13 – Jordan Lake array; 14 – Giva River array; 15 – Kickapoo Complex array; 16 – Kickapoo North array; 17 – Kickapoo South array; 18 - Variable Transmitter array.	+Manual -26, -38
ARRAY SRE.INP ARRAY 400.INP ARRAY 600.INP ARRAY 1200.INP ARRAY 2400.INP	19 20 21 22 23	Input Data Files	ARRAY ------- - ------- - ------- ------- --	Contain geometric information on the configuration of the receiver arrays in terms of the receiver elements. The arrays by the file number are: 19 – Single receiver element; 20 – 400 ft receiver array; 21 – 600 ft receiver array; 22 - 1200 ft receiver array; 23 – 2400 ft receiver array	+Manual -26, -37
RECVRPOWER.TXT	24	Output Data File	"run" directory	Contains combined receiver power information (incoherently added up receiver powers)	+ 26
TRANSMTRPOWER.TXT	25	Output Data File	"run" directory	Contains combined transmitter power information (incoherently added up receiver powers)	+26

nearfld.f	26	Source code file.	Code Directory	Main routine of the electrical field calculation program.	-27,-28
NearfldRCVR	27	Executable File	"run" directory	Executable for the computation of the EM field of a single receiver array	
NearfldTRNS	28	Executable File	"run" directory	Executable for the computation of the EM field of a single receiver array	
currnt_stnd.f currnt_rbay.f currnt_sbay.f currnt_rsby.f	29 30 31 32	Source code files	Code Directory	Contain information for random and systematic variations of currents and phases within arrays and -- for Kickapoo only -- between bays. Only one used per run per array.	
CURRNT_STND.INP CURRNT_RBAY.INP CURRNT_SBAY.INP CURRNT_RSBY.INP	33 34 35 36	Input Data Files	CURRNT Directory	Input to currnt_stnd.f Input to currnt_rbay.f Input to currnt_sbay.f Input to currnt_rsby.f	-29 -30 -31 -32
elpos rcvr.f	37	Source code file	Code Directory	Calculates element positions of specified linear receiver array and returns them to nearfldRCVR	-26, -27
elpos trns.f	38	Source code file	Code Directory	Calculates element positions of specified linear transmitter array and returns them to nearfldTRNS	-26, -28
array sbr.f	39	Source code file	Code Directory	calculates the electric field at a given point in space for a selected array	-26, -27, -28
elffld rcvr.f	40	Source code file	Code Directory	Returns far electric field at a specified point in space for a particular receiver element.	-26, -27
elffld trns.f	41	Source code file	Code Directory	Returns range independent far electric field for a specified direction of an arrowhead dipole with unit terminal current placed over a finite thin wire-grid ground screen.	-26, -28
Coordtrnsf.f	42	Source code file	Code Directory	Performs transformations taking Geodetic coordinates of a point for which field calculations are to be performed to each array's local spherical coordinates.	-26, -27, -28

Powerprod	43	Executable File	"run" directory	Executable for the computation of the products of receiver powers and transmitter powers.	-1
Powerprod.f	44	Source code file	Code Directory	Source code for "powerprod."	-43
EL-BUTTE-RCVRPWR.TXT HKNSVLLE-RCVRPWR.TXT RED-RIVR-RCVRPWR.TXT SAN-DIEGO-RCVRPWR.TXT SLVR-LAKE-RCVRPWR.TXT TATTNALL-RCVRPWR.TXT	45 46 47 48 49 50	Output Data Files	"run" directory	Elephant Butte Receiver Array Power File Hackinsville Receiver Array Power File Red River Receiver Array Power File San Diego Receiver Array Power File Silver Lake Receiver Array Power File Tattnall Receiver Array Power File	+27 +27 +27 +27 +27 +27
RECVRRPOWER.TXT	51	Output Data File	"run" directory	Combined Incoherent Receiver Power	+27
GILA-RIVR-TRNSPWR.TXT JRDN-LAKE-TRNSPWR.TXT KICKAPOO-TRNSPWR.TXT	52 53 54	Output Data Files	"run" directory	Gila River Transmitter Array Power File Jordan Lake Transmitter Array Power File Kickapoo Transmitter Array Power File	+28 +28 +28
TRANSMTRPOWER.TXT	55	Output Data Files	"run" directory	Combined Incoherent Transmitter Power	+28
POWERPROD.TXT	56	Output Data Files	"run" directory	Power Product Of All Receiver Arrays	+43
Pairpowerprod	57	Executable File	"run" directory	Executable for the computation of the pair-wise products of receiver powers and transmitter powers	-1
Pairpowerprod.f	58	Source code file	Code Directory	Source code for "powerprod"	-57
ELBUTTE_GILARIVR.TXT ELBUTTE_JORDANLAKE.TXT ELBUTTE_KICKAPOO.TXT HKNSVILLE_GILARIVR.TXT HKNSVILLE_JORDANLAKE.TXT HKNSVILLE_KICKAPOO.TXT REDRIVR_GILARIVR.TXT REDRIVR_JORDANLAKE.TXT REDRIVR_KICKAPOO.TXT SANDIEGO_GILARIVR.TXT SANDIEGO_JORDANLAKE.TXT SANDIEGO_KICKAPOO.TXT SLVRLAKE_GILARIVR.TXT SLVRLAKE_JORDANLAKE.TXT SLVRLAKE_KICKAPOO.TXT TATTNALLE_GILARIVR.TXT TATTNALLE_JORDANLAKE.TXT TATTNALLE_KICKAPOO.TXT	59 60 61 62 63 64 65 66 67 68 69 70 71 72 73 74 75 76	Output Data Files	"run" directory	Elephant Butte – Gila River Power Product File Elephant Butte – Jordan Lake Power Product File Elephant Butte – Kickapoo Power Product File Hawkinsville – Gila River Power Product File Hawkinsville – Jordan Lake Power Product File Hawkinsville – Kickapoo Power Product File Red River – Gila River Power Product File Red River – Jordan Lake Power Product File Red River – Kickapoo Power Product File San Diego – Gila River Power Product File San Diego – Jordan Lake Power	+57 +57 +57 +57 +57 +57 +57 +57 +57 +57 +57 +57 +57 +57 +57 +57 +57 +57

				Product File San Diego – Kickapoo Power Product File Silver Lake – Gila River Power Product File Silver Lake – Jordan Lake Power Product File Silver Lake – Kickapoo Power Product File Tattnalle – Gila River Power Product File Tattnalle – Jordan Lake Power Product File Tattnalle – Kickapoo Power Product File	

DISTRIBUTION

	Copies
DOD ACTIVITIES (CONUS)	
COMMANDER	
ATTN CARROLL HAYDEN N601	4
ALAN BAUER N601T	4
SAM ESTILL	2
ED LYDICK VN6323	2
PAUL SCHUMACHER VN63T	2
WILLIAM WALKER N60	1
PETER TRAAS	1
NAVAL SPACE COMMAND	
5280 FOURTH ST	
DAHLGREN VA 22448-5300	
COMMANDING OFFICER	
ATTN FRANCIS ALLSTON	1
SPAWARSYSCEN CHASN	
PO BOX 190022	
NORTH CHARLESTON SC 29419-9022	
COMMANDING OFFICER	
CSSDD NSWC	
6703 W HIGHWAY 98	
PANAMA CITY FL 32407-7001	1
ATTN RON BEARD	1
NAVAL RESEARCH LABORATORY	
4555 OVERLOOK AVENUE SW	
WASHINGTON DC 20375-5000	
DEFENSE TECH INFORMATION CTR	
8725 JOHN J KINGMAN RD	
SUITE 0944	
FORT BELVOIR VA 22060-6218	2

	Copies
NON-DOD ACTIVITIES (CONUS)	
THE CNA CORPORATION	
PO BOX 16268	
ALEXANDRIA VA 22302-0268	1
ATTN MICHAEL ALBIN CHIEF	1
ANGLO/AMERICAN ACQUISITIONS	
DIVISION	
LIBRARY OF CONGRESS	
101 INDEPENDENCE AVENUE SE	
WASHINGTON DC 20540-4170	
INTERNAL	
B60	3
T10	1
T12	1
T12 HERMANN	10
T12 ROGINSKY	10
T13	1